MECHANISMS OF STARCH-PROANTHOCYANIDIN INTERACTIONS AND IMPACT ON STARCH DIGESTIBILITY

A Dissertation

by

DERRICK BRIAN AMOAKO

Submitted to the Office of Graduate and Professional Studies of
Texas A&M University
in partial fulfillment of the requirements for the degree of

DOCTOR OF PHILOSOPHY

Chair of Committee,	Joseph M. Awika
Committee Members,	Stephen T. Talcott
	Nancy Turner
	Carmen Gomes
Head of Department,	Boon Chew

December 2017

Major Subject: Food Science and Technology

ABSTRACT

Excess calorie intake is a growing global problem, and can be managed by impacting satiety and the rate of starch digestion in the small intestine. Proanthocyanidins (PA) are known to interact with amylose in cooked starch to increase resistant starch (RS). There is therefore an opportunity to utilize PA to directly reduce starch digestibility. The aim of this study was to investigate the effect of complexing partially gelatinized starch with PA on *in-vitro* starch digestibility, as well as to evaluate the interaction mechanisms involved in the complex formation. We also investigated potential intra-granular cross-linking of starch by PA.

Starch-PA complexes were formed by incubating PA extract with normal and waxy maize starch in 30% (30E) and 50% (50E) ethanol solutions at 70 °C / 20 min. The complexes were reacted with 6M urea and 15% aqueous dioxane to evaluate the contribution of H-bonding and hydrophobic interactions to starch-PA complexes, respectively. Treatments were analyzed for *in-vitro* digestibility and starch physicochemical properties. Cross-linked starches were formed with PA and phosphoryl chloride ($POCl_3$), and the effect on starch pasting properties evaluated.

In the 30E treatments, PA significantly increased crystallinity, pasting temperature, peak viscosity, and slow digesting starch (SDS) (from 100 to 274 mg/g) in normal starch. PA doubled RS to approximately 300 mg/g in both waxy and normal

starches. In 50E treatments, PA made both maize starches behave like raw potato starch (>90% RS).

In 30E treatments, urea reduced RS by 39% and increased rapidly digestible starch (RDS) by 92% in normal maize-PA complexes, while freeing ~100% of PA bound in complex, suggesting H-bonds stabilize starch-PA complex in gelatinized starch. In 50E, dioxane released more PA (39-42%) bound in the complex than urea (25-31%). Furthermore, restricting H-bond formation during starch-PA complexation with deuterated solvents, did not significantly affect starch digestibility, suggesting hydrophobic interactions stabilize starch-PA complexes in intact starch granules. PA formed V-type complexes with amylose. PA acted synergistically with $POCl_3$ to form heat resistant cross-linked starch.

Our findings suggest PA can be used as ingredients to reduce the caloric impact of starch in foods, and improve the functionality of cross-linked starches.

DEDICATION

To my Lord and Savior Jesus Christ, in You, I live, move, and have my being. To my mum (Esther Amoako) and dad (Collins Kojo Agyei Amoako), thanks for all your support and love. To my sisters Lina and Joyceline Amoako, thanks for encouraging me and having confidence in my abilities.

ACKNOWLEDGEMENTS

I would like express my sincere gratitude to my committee chair, Dr. Joseph M. Awika, for his mentorship and training. I owe the biggest part of my training and achievements to him. Thank you so much for all the times you encouraged and pushed me beyond my comfort zone. It has been worth the journey!

Many thanks also to my committee members, Dr. Stephen T. Talcott, Dr. Nancy Turner, Dr. Ximena Quintero-Fuentes, and Dr. Carmen Gomes, for their guidance and support throughout the course of this research. Thanks for the constructive criticisms, and guidance to think outside the box. I'm a better-rounded food scientist because of their inputs.

Thanks to my colleagues and the department faculty and staff for making my time at Texas A&M University a great experience. Special thanks to my Cereal Quality Lab (CQL) colleagues; Audrey Girard, Julia Brantsen, Shreeya Ravisankar, Tadesse Tefera, Taehoon Kim and Fariha Irshad. You guys have been more than family to me! You supported and rooted for me in my ups and downs, and I cannot thank you enough.

A big thank you to Dr. Youjon Deng and his students Chu-Chun Hsu and Bidemi Fashina, for opening their labs to me and assisting me to run my X-ray Diffraction Analysis.

I would also like to thank Dr. Elena Castell and Paulo Fortes Da Silva for training and helping me run my Differential Scanning Calorimetry (DSC) analysis.

Big thank you to Dr. George Amponsah-Annor for the research collaboration and running all the gel permeation chromatography as well as HPAEC-PAD analyses for me. You've been of tremendous help.

I would also like to acknowledge the use of the TAMU Materials Characterization Facility for my FE-SEM analysis.

Finally, thanks to my mother and father for their encouragement and to my girlfriend (Ashley Ofori) for her support and love.

All in all, Glory be to God the Father, the Son and the Holy Spirit for driving my purpose and academic journey. You are my EVERYTHING.

CONTRIBUTORS AND FUNDING SOURCES

Contributors

This work was supervised by a thesis committee consisting of Dr. Joseph Awika, Dr. Stephen T. Talcott, Dr. Nancy Turner, Dr. Ximena Quintero-Fuentes and Dr. Carmen Gomes.

The methodology and part of data presented in section 4.2.5, 4.2.6 and 4.3.3 were provided by Dr. George Amponsah Annor of the Department of Food Science and Nutrition, University of Minnesota (Twin Cities).

All work for the thesis was completed independently by the student.

Funding Sources

Graduate study and research was partially supported by Texas A&M Borlaug International Scholars Program.

This work was also partially supported by USDA National Institute for Food and Agriculture Hatch Project No. 1003810.

TABLE OF CONTENTS

Page

LIST OF FIGURES

Page

LIST OF TABLES

Page

1. INTRODUCTION

The rising prevalence of chronic diseases related to excess caloric intake – such as diabetes and obesity – is one of the most critical public health problems facing both developed and developing countries. Carbohydrates are implicated in the excess calorie intake due to their large proportion of human diets. Carbohydrates are the major source of metabolic energy in foods, accounting for approximately 52% of calories derived from food in the US, and up to 80% in developing countries [1,2]. The prominent role of carbohydrates in the diet implies that strategies that can reduce carbohydrate digestibility would greatly benefit efforts to reduce caloric intake. Among the dietary carbohydrates, starch contributes most of the calories and has therefore become a prime target for favorably altering caloric profile of foods.

Starch is nutritionally classified as rapidly digestible starch (RDS), slowly digestible starch (SDS), and resistant starch (RS) [3]. The nutritional quality of starch is thus related to its digestion rate. The RDS and SDS fractions together represent the starch that is likely to be digested completely in the human small intestine, though the SDS fraction will take a much longer time period [3,4]. RDS contributes to a rapid peak in blood glucose level after digestion, while SDS results in a much slower postprandial glucose response, so SDS is thought to help improve satiety [5,6]. The RS fraction escapes enzyme hydrolysis in the small intestine and is fermented in the large bowel by colon bacteria. RS and SDS therefore offer advantages for the manipulation of

postprandial blood glucose levels [5,6]. Increasing SDS and RS in starchy foods is therefore of great interest to the food industry.

Polyphenols comprise a diverse group of secondary plant metabolites that perform various roles in plants, including structure, cell signaling, and natural defense, among others [7,8]. Many reports have elucidated polyphenols as potential regulators of glucose uptake and metabolism [9,10]. Evidence however suggests that, interaction of large molecular weight (MW) polyphenols with starch has more practical impact on starch digestibility profile than their monomeric counterparts [11-14]. Of particular interest is proanthocyanidins (PA) (also called condensed tannins, CT); which are capable of binding to starch to reduce its digestibility. Barros et al. [15] showed that, high MW PA from sorghum interact with amylose to form RS in completely gelatinized and dispersed starch (no intact granules); interaction of the PA with amylopectin did not form RS [16]. They explained that the steric compatibility of the amylose and PA structures affords a more efficient interaction between the two molecules, likely via H-bonds and hydrophobic interactions due to the close proximity and abundance of hydroxyl groups in PA and amylose. Other authors have found limited impact of PA on resistant starch formation in heterogeneous food matrix [17-19], but reported significant increase in SDS [19] and reduced estimated glycemic index [17].

Thus, there is opportunity to utilize PA to directly reduce starch digestibility. However, given that starch is only partially gelatinized in most starchy foods – e.g., cookies – 2-11%, crackers – 3%, bread – 33-71%, cereal flakes – 24-27% [20,21], and

granule integrity is largely retained, it is not clear how the observations described above would translate into a typical food system.

Available evidence suggests that PA-starch interactions may involve extensive hydrogen-bonding, along with hydrophobic interactions, as was demonstrated for other carbohydrates [22,23]. There are, however, no studies that have demonstrated the involvement of specific interactions in stabilizing starch-PA complexes. Knowledge of specific interactions involved can lead to opportunities to optimize the interactions to develop novel starch processing methods to form less digestible starches.

In a recent study, Barros et al. et al. [15] showed that PA significantly increased peak time and peak viscosity in gelatinized normal starch; citing the interaction of PA with starch to be responsible. Indeed, this increase in peak time and peak viscosity observed is typical of minimally cross-linked starch (containing a high proportion of monostarch phosphate) [24]. We therefore hypothesize that PA may be useful for cross-linking starches. An understanding of the crosslinking mechanism between PA and starch can be useful to PA application as a cross-linking agent (or in combination with commercial cross-linking agents) for cleaner food labels. PA may also offer added health benefits as a cross-linking agent considering its health implications in human diet.

The overall objective of this study was to investigate the mechanisms of interactions of proanthocyanidins with starch and their effects on *in-vitro* starch digestibility. The specific objectives were:

1. To investigate how the degree of starch swelling and gelatinization affects starch-proanthocyanidin interactions, and the effect of these interactions on starch properties and digestibility.
2. To evaluate mechanisms of starch-proanthocyanidins interactions.
3. To investigate potential intragranular cross-linking of starch with proanthocyanidins.

2. LITERATURE REVIEW

2.1 Prevalence of obesity and diabetes

Of the many socio-economic problems facing the world today, health conditions related to excess calorie intake (such as obesity and diabetes), remain top of the agenda of most developed countries. Obesity is a health disorder involving excessive body fat often resulting from taking in more calories than are utilized during exercise and normal daily activities, and typified by a BMI (Body Mass Index) ≥ 30 [25]. Obesity is of particular concern because it is currently the fifth leading risk factor for global mortality, with 2.8 million deaths each year [26]. Obesity is also known to increase the risk of a number of other health conditions including hypertension, adverse lipid concentrations, and type 2 diabetes [27]. Diabetes on the other hand, describes a group of glucose metabolism disorders, which produces high blood glucose in persons, either because insulin production is inadequate, or because the body's cells do not respond properly to insulin, or both. It is a major cause of heart disease, blindness and kidney failure; and thus contribute substantially to death resulting from such conditions [28].

Here in the US, more than one-third (34.9% or 78.6 million) of adults are obese, and the estimated annual medical cost of obesity in the U.S. is $147 billion to nearly 210 billion [29]; the medical cost for each obese person is about $1,429 higher than for a normal weight individual [27,30]. About 9.3% (29.1 million) of the US population have diabetes, and it is estimated that one in every three Americans will develop diabetes in their lifetime if current trends continue [31]. Considering the socio-economic impact of

diabetes and obesity on the population, their prevention and treatment is central to achieving a healthy and productive citizenry.

Efforts that have been made over the years to manage obesity prevalence include education of the public on obesity and behavioral/lifestyle changes that would result in decreased risk, use of weight-loss drugs, recommendation/counselling for dietary changes towards low-calorie foods, and in certain cases surgical procedures, though this is typically reserved for morbidly obese individuals [32]. Of these prevention and treatment methods, lifestyle changes have proven to be the best way to prevent and treat obesity and related diseases; though this is difficult to achieve in individuals who are less self-motivated. Diet based interventions are also inexpensive and useful alternatives to aid in weight loss and weight management [33]. Thus, regular physical activities [34] and diets with less fat [35], sugar [36] and more fiber, fruits, vegetables and whole grains [37] are key to successfully limiting the onset and development of obesity and diabetes. Though use of drugs to treat obesity promises easy, quick results; that may not help individuals to achieve long-term weight management and may produce undesirable side effects [38,39].

2.2 Carbohydrates and their role in obesity and diabetes

Food carbohydrates constitute a diverse group of food nutrients, which occur naturally in fruits, vegetables, milk, nuts, grains and legumes [40]. They are also often isolated and used as ingredients in many other processed foods and beverages. Nearly all carbohydrates are obtained from plant sources, and are nutritionally classified as sugars

(fructose, glucose, sucrose, etc.), starch and non-starch polysaccharides (NSPs). Sugars are the simplest form of carbohydrates; while starch comprises large complex polymers of glucose. Sugars and starches are together classified as available carbohydrates, because they can be easily metabolized by human digestive enzymes and utilized by the body [40]. Starch is composed entirely of glucose monomers linked by α-glycosidic bonds; and can be hydrolyzed by human digestive enzymes [41]. NSPs on the other hand are complex carbohydrates composed of different kinds of monomers, which are linked predominantly by β-glycosidic bonds. β-glycosidic bonds cannot be broken down by human digestive enzymes in the upper GIT (gastrointestinal tract); so NSPs are fermented by colon bacteria [40].

Food carbohydrates are major dietary sources of metabolic energy, and contribute 45-55% of calories derived from food in the US, and up to 80% in the poorest regions of the world [1,2]. Lack of available carbohydrates in the human diet is associated with under-nutrition and other related conditions prevalent in the poor areas of the world [42]. An excess intake of available carbohydrates on the other hand, is linked with obesity, diabetes and metabolic syndrome – common conditions facing the developed world [42]. Considering the fact that carbohydrates contribute the majority of the daily calorie requirements, they have become good targets to limit calorie intake in order to reduce the prevalence of obesity and diabetes.

2.3 Carbohydrate digestion and glucose metabolism

Starch and sucrose are the most important dietary carbohydrates in the human diet. Their digestion takes place in the upper gastrointestinal tract, where they are broken down by hydrolytic enzymes into monosaccharides (primarily glucose). α-Amylase and α-glucosidases are the key hydrolyzing enzymes for dietary carbohydrates. After carbohydrate breakdown, the liberated glucose is absorbed across the intestinal brush border via specific glucose transporters. Inhibition of carbohydrate digestive enzymes or glucose transporters would reduce the rate of glucose release and absorption in the small intestine respectively, and consequently suppress postprandial hyperglycemia [10]. Absorbed glucose translates into elevated blood glucose concentration which triggers insulin secretion from the β-cells (located in the pancreas) to control the uptake of glucose into peripheral tissues (including muscles) to fuel body functions. When blood glucose level falls below normal (90 mg/dL), the hormone glucagon is secreted from the pancreatic α-cells which promotes liver glycogen break down to release enough glucose into circulation [43,44].

2.4 Starch properties

Starch is a polymeric carbohydrate widely distributed in plants; cereals, tubers, legumes, fruits and vegetables. In nature, it is found in the endosperm of grains/seeds as discrete molecules called granules. Depending on the botanical source, starch granules may appear in different shapes; polygonal (rice), oval (potato), bimodal (wheat), spherical (maize). Sizes may also range from about 1 μm (rice) to 100 μm (in potatoes)

[45]. Starch granules are composed of glucose polymers; amylose and amylopectin. Amylose consists of glucose molecules linked by mostly α-1,4 glycosidic bonds into a linear polymer (helical structure), whereas amylopectin glucose molecules are linked by α-1,4 and α-1,6 glycosidic to form a highly branched polymer. Some amylose molecules may contain a few branch points [46]. These two starch polymers are densely packed into amorphous and crystalline regions in the starch granule, which gives starch a semi-crystalline structure observed as a 'maltese cross' or birefringence under plain polarized light. Starch granules also contain other minor components such as lipids, proteins, and phosphates [47].

The crystalline structure of starch displays a characteristic X-ray diffraction pattern depending on its botanical origin and composition [48]. A-type crystalline form is mainly found in cereal starches and the B-type is observed in tubers and starches with high amylose [48].

Starch begins to lose its crystalline structure when cooked at high temperatures (> ~ 65 °C) in excess water [49]. During heating of starch in excess water, starch granules absorb water, swell, and eventually rupture, leading to an irreversible disruption of order in the crystalline and amorphous regions, a process referred to as starch gelatinization [49]. Gelatinization releases amylose into solution. When gelatinized starch is cooled, amylose tends to reassociate to restore partial crystallinity in the amorphous region; a process described as retrogradation [49].

2.4.1 Resistant starch

Resistant Starch (RS) is the fraction of dietary starch, which escapes digestion in the small intestine [50]. It is measured chemically as the difference between total starch (TS), and the sum of rapidly digestible starch (RDS) and slowly digestible starch (SDS); RS = TS – (RDS + SDS). RS is often classified into four types, namely, RS1, RS2, RS3, and RS4, based on the extent of digestibility of the starch, structural properties, and their method of preparation [50]. RS1 is starch that is in a physically inaccessible form such as partly milled grains and seeds and in some very dense types of processed starchy foods [50]. RS2 represents starch in granular form, which is resistant to enzyme digestion. Granular starch is relatively dehydrated, and tightly packed in a radial pattern giving it a compact structure that limits the accessibility of digestive enzymes. An example is ungelatinized or raw starch foods like banana.

RS3 is the most resistant starch fraction and is comprised mainly of retrograded amylose formed during cooling of gelatinized starch. This type of RS is formed from complete hydration of starch granules, followed by amylose leaching from the granules into solution, and subsequent cooling which results in reassociation of the polymer chains as double helices stabilized by hydrogen bonds. RS3 also retains the characteristic A- or B- crystalline structure of its native starch [51]. Chemically RS3 is measured as the fraction, which resists both dispersion by boiling and enzyme digestion [50]. RS3 is entirely resistant to digestion by pancreatic amylases, though resistance is reduced by processing. RS4 is the RS where novel chemical bonds other than α-(1-4) or α-(1-6) are

formed. This includes most modified starches obtained by various types of chemical treatments.

2.4.2 Cross-linked starch

Native starch has limited application / functionality in food [52]. Its lack of stability under harsh conditions of temperature, shear, pH and refrigeration during processing makes it less functional [52]. For example, under cooking temperatures, native starches produce weak-bodied, cohesive, rubbery pastes and undesirable gels when the pastes are cooled [53]. Starch is thus modified via a variety of processes to improve its functionality and application in food.

Native starch is modified by altering its physical and chemical properties to tailor it to specific food applications [54]. Native starch modification may consist of low levels of substitution of –OH groups of the starch with functional molecules (esterification, etherification, phosphorylation / cross-linking), hydrolysis of starch with enzymes to form smaller or desirable molecular weight forms, and heat/moisture treatment (pre-gelatinization, annealing, etc.) [53,55].

Cross-linking of starch is one of the commonest starch modification processes utilized to increase starch functionality and application. The process involves mixing native starch granules in an aqueous system at high pH (~9-12) with phosphorylation reagents capable of forming intermolecular bridges with at least two hydroxyl groups of the starch [56]. Phosphorous oxychloride ($POCl_3$) [57] and sodium trimetaphosphate (STMP) [58] are the common reagents used to form distarch phosphates (crosslinks) in

starch. Cross-linking starch adds covalent bonds at random locations in the starch granule, which stabilizes the granules and strengthens the starch [59,60]. Other phosphorylating reagents such as monosodium orthophosphate (SOP) and sodium tripolyphosphate (STPP) are used to form monostarch phosphates (MSP) by esterification with native starch [24]. Distarch phosphate (DSP) / cross-linked starch is more resistant to acid, heat, and shearing than native starch, which makes it suitable for applications as thickeners, stabilizers, and texture improvers [61,62]. Monostarch phosphate on the other hand exhibit increased paste clarity, viscosity and water binding capacity [24,63].

Factors such as type and concentration of cross-linking reagent used, pH, reaction time, temperature and presence of catalyst (sodium sulfate) all influence the degree of crosslinking and the type of starch phosphate formed [54]. Low concentrations of cross-linking reagent (0.001 - 0.5% w/w of starch) results in minimal cross-linking and a high ratio of MSP : DSP formed [52,64]. Higher concentrations in the range of > 0.5 however form a high proportion of DSP.

2.5 Rising interest in polyphenols

In the last few decades, researchers and food manufacturers have turned tremendous attention to polyphenols due to their well-known antioxidant properties, abundance in our diet, and their probable role in the prevention of various degenerative diseases such as cancer, diabetes, cardiovascular and neurodegenerative diseases [65]. Polyphenols are derived from dietary sources (fruits, vegetables, cereals, chocolate,

legumes, and plant-derived beverages such as fruit juices, tea, coffee, and red wine). They comprise a variety of compounds such as phenolic acids, flavonoids, coumarins, quinones, tannins, lignans and stilbenes [66]. It is estimated that ~1 g of polyphenols is consumed daily, and plasma concentrations are typically less than 1 mM after the consumption of 10–100 mg of a single phenolic compound [67]. Considering the fact that these polyphenols are largely distributed in our diets, and co-exist with other food nutrients in the same food matrix, their interaction and impact on food quality is a relevant area of research.

2.6 Polyphenol interaction with macronutrients in food

It is now well understood that polyphenols interact extensively with proteins, carbohydrates and fatty acids in a food matrix. Thus, the co-existence of polyphenols and macronutrients in the same food matrix is considered a viable opportunity for molecular interactions between them.

Proteins have the highest affinity for polyphenols among macronutrients. This is largely due to the fact that polyphenols can act as polydentate ligands on the protein surface through their hydroxyl groups and aromatic rings, as well as, long chain polymers to achieve higher binding efficiency [68,69]. Polymeric proanthocyanidins (PA) are known to interact with proteins [70] and digestive enzymes to reduce protein digestibility [14,71]. Hydrophobic interactions and hydrogen bonding dominate protein-PA interactions, and the products of such interactions are generally non-digestible or only poorly digestible, and have been implicated in reduced feed efficiency of, for

example, high tannin sorghums [72]. Other food models describing flavonoid-protein interactions [14,73,74] also show effective binding of proteins by flavonoids in food matrices to form stable complexes.

The interaction of polyphenols with carbohydrates in food has received increased interest in the past few years, due to increasing evidence of the impact of these interactions on the nutritional quality of carbohydrates [11,15,18,71,75] as well as emerging applications as functional ingredients and in novel food products [9,76,77]. The versatile structure of carbohydrate molecules allow them to interact with polyphenols via a variety of mechanisms; dominated by non-covalent interactions [76]. Carbohydrate-polyphenol interactions have been reported in molecules such as starch [15], pectin [23], cellulose [75], cyclodextrin [78] and dietary fiber [79-81].

Of carbohydrate-polyphenol interactions, starch-polyphenol interactions are by far more interesting with regards to health. Starch-polyphenol interactions have been shown to limit glucose release from starch *in-vitro* [15]. This implies that starch-polyphenol interactions can be utilized as a potentially viable strategy to reduce starch digestibility in foods to benefit efforts to reduce excess caloric intake, and by extension contribute to reducing the increasing burden of obesity and associated health conditions.

Polyphenol-lipid interactions in food have been much less researched compared to proteins and carbohydrates. The most notable functional effect of polyphenol-lipid interactions in food is the antioxidant action of flavonoids in fruit and vegetable oils [82,83]. The structure of flavonoids, allows it to bind with lipids to reduce the occurrence of auto-oxidation, as described by Das and Pereira [84] in palm oils.

2.7 Impact of polyphenol-starch interaction on dietary glucose availability (*in-vitro* evidence)

A large body of evidence supports the fact that starch-polyphenol interactions affect the nutritional quality of starch. It is of a general consensus that starch-polyphenol interactions alter the susceptibility of starch polymers to enzyme hydrolysis through (1) polyphenol interference with digestive enzymes (α-amylase and α-glucosidase) in the upper gut and glucose transporter at the intestinal brush border [10,76,85], and / or (2) non-covalent interactions between polyphenols and starch, which result in structural changes in starch molecule making the starch resistant to enzyme hydrolysis [76].

Research demonstrating the impact of polyphenol-starch interactions on glucose availability have been largely based on *in-vitro* evidence. It is clear that the impact of these interactions on glucose availability is influenced by factors such as starch type, type of extracts or polyphenols used, enzyme type and unit of activity, as well as the presence of other ingredients in the food model / matrix used – whether homogenous or heterogeneous [15,18,19].

2.7.1 Type of extracts / polyphenols

A variety of plant extracts are known to possess the ability to inhibit starch hydrolyzing enzymes *in-vitro* [86]. These extracts contain different types and distribution of polyphenols, which inhibit starch digestion to different degrees. Generally, higher amounts of phenolic extracts have greater inhibitory action [12,13,18]. Phenolic content levels in the range of about 0.40-1 mg GAE (gallic acid equivalent) /g

[87,88] are typically reported to significantly inhibit starch hydrolyzing enzymes, though levels as low as 4.5 μg GAE/mL [13] are reported to inhibit α-amylase.

Of the eleven berries studied by Grussu et al. [13] raspberry and rowanberry extracts possessed the highest α-amylase inhibition (IC50 of 21.0 and 4.5 μg GAE/mL, respectively) when two levels of the berry extracts (50 and 100 μg of GAE/mL) were applied to a potato starch substrate. The authors [13] further substantiated that, red and yellow raspberry extracts, had similar inhibitory action on α-amylase (IC50 of 13.5 and 16.5 μg GAE/mL, respectively), though they possessed different distribution of major polyphenols. Red raspberry polyphenols were dominated by anthocyanins, while yellow raspberry was dominated by ellagitannins, flavonols, hydroxycinnamate derivatives. Indeed, the anthocyanins and ellagitannins in raspberries were not crucial for α-amylase inhibition, but proanthocyanidins were identified to play a more key role in α-amylase inhibition. Other studies [11,15,16] have also confirmed that polyphenol type and molecular distribution impacts their inhibitory action. The inhibitory action of 6 groups of flavonoids (0.50 mM) against porcine pancreatic α-amylase was reported by Tadera et al. [87] in the following order; flavonol > flavone > anthocyanidin > isoflavone > flavanone = flavan-3-ol. A different order was reported [87] for α-glucosidase inhibition; flavonol > flavone ≥ flavan-3-ol ≥ anthocyanidin > flavanone = isoflavone.

It appears that crude plant extracts have greater inhibition potential than purified forms of the major polyphenols present. McCue and Shetty [89] compared the effects of crude oregano extracts (100 mg) with same amount of the purified form of the major phenolic compound (rosmarinic acid) and found that the crude extract had higher

amylase inhibition properties. Synergistic mechanisms may be the likely reasons for this observation in crude extracts. In another study [13], seven fractions (20 μg GAE/mL per fraction) of the major components of rowanberry extract were found to inhibit α-amylase much less (0-20%) than the unfractionated extract (100% inhibition). The fraction rich in proanthocyanidins (PA) was however as effective (~90% inhibition) as the whole rowanberry extract. It is possible that proanthocyanidins (PA) are an exception to this rule, considering the fact that some other studies [16,18] have reported a greater decrease in starch hydrolysis in assays utilizing purified PA than in crude PA extract.

Within the same group of polyphenols, polymeric forms are known to demonstrate higher enzyme inhibition than monomeric or low molecular weight forms. Indeed, high molecular weight PA have been demonstrated in many studies [11-14] to be more effective at inhibiting starch hydrolyzing enzymes in many applications compared to low molecular weight forms. Mkandawire et al. [18] demonstrated how differences in PA molecular weight impact α-amylase activity by comparing PA extracts from two sorghum varieties; Shanqui Red Y1 (with a high proportion of oligomers and polymers) and Shanqui Red Y2 (with a high proportion of monomers and dimers). They found that an extract (0.3–1.3 mg CE/mL) from Shanqui Red Y1 displayed a greater ability to reduce amylase activity compared to Shanqui Red Y2. Indeed, no decrease in α-amylase activity was observed with the Shanqui Red Y2 extract at the lower concentrations tested (0.3 – 1.1 mg CE/mL); as much as 1.3 mg CE/mL was required to cause a significant decrease.

Goncalves et al. [12] demonstrated a greater ability of high molecular weight procyanidins to inhibit α-amylase activity than low molecular weight forms by showing that the inhibition factor (I.F - a measure of the ability of procyanidins to inhibit α-amylase activity) of procyanidins fraction III (average MW = 2052) was significantly higher than fraction II (average MW = 1513) and I (average MW = 949); corresponding to I.F=0.38 for fraction I, I.F=0.80 for fraction II, and I.F=0.97 for fraction III. Among tea polyphenols, Guzar et al. [90] showed that catechin polymers (such as theaflavins and thearubigins) in black tea were more effective at reducing starch hydrolysis during RVA cooking of starch (wheat, potato, corn, rice) in the presence of pancreatin, compared to green tea, which is dominated by monomeric catechins such as epicatechins and epigallocatechins. The authors; however, found that freeze dried starch products prepared by cooking starches with each tea-extract, possessed similar hydrolysis kinetics (except for potato starch); suggesting that monomeric compounds (in green tea) may also be effective at reducing starch digestibility, though their interaction with starch probably occurs during the cooling phase of RVA cooking when the starch gel network is set. This study also points to the fact that starch interaction with monomeric compounds follows a different mechanism than polymeric phenolic compounds, and monomeric forms could be potentially utilized similarly as polymeric compounds to reduce starch digestibility when mechanisms of interactions are better understood. It must however be noted that, Barros et al. [15,16] showed that high MW PA from sorghum reduced starch digestibility in both completely gelatinized high amylose maize and normal maize starch; while monomeric catechins had no significant effect. More so,

the high MW PA reduced starch digestibility in high amylose maize starch to a greater extent than in normal maize starch, suggesting that specific interactions between starch and proanthocyanidins are influenced by the nature and abundance of amylose.

2.7.2 Type of starch system: homogeneous vs. complex / heterogeneous systems

Starch type/ botanical source as well as the nature of the food system (simple or complex) used in an assay, have different impacts on the interactions, which occur between polyphenols and starch polymers, and their ultimate susceptibility to enzyme hydrolysis. It is clear that since the botanical source of starch impacts the starch granule size and surface morphology, as well as the distribution and size of amylose and amylopectin molecules, polyphenol interactions with starch follow a different mechanism for a given starch type, and by extension, its potential to inhibit starch hydrolysis.

By cooking different starches (wheat, potato, corn and rice starches) with black tea extracts (high in polymerized catechins) in the absence and presence of pancreatin, Guzar et al. [90] demonstrated that black tea extracts (20 mg ferulic acid equivalent) interacted differently with each starch (3 g), and reduced starch hydrolysis to different extents. It is interesting to note that, the highest reduction in starch hydrolysis (estimate obtained by measuring peak viscosity) occurred in potato starch. This was attributed to its longer external and internal starch polymer chains compared with the other starches, which allows it to easily associate with catechin polymer chains from black tea, thereby limiting starch availability for enzyme hydrolysis. In this same study, wheat (% amylose

– 34%) and corn (% amylose – 22%) starch produced greater enzyme inhibition, 91.5% and 100% respectively, compared to rice (% amylose – 9%). Apparently, the starch hydrolysis inhibiting effect of tea catechins is dependent on starch structure, specifically the amylose content.

Thus, amylose interaction with catechin polymers is preferred, which results in reduced starch hydrolysis by enzymes. Barros et al. [16] confirmed this observation by showing that increasing the proportion of PA in sorghum extracts enhanced interactions between amylose in cooked maize starch (250 mg/mL in distilled water) and sorghum extracts (100 mg extract/ g starch) to limit starch hydrolysis. Monomeric catechins on the other hand seemed to interact better with branched chain amylopectin to limit starch digestibility [16]. Liu et al. [91] showed that waxy maize (200 mg) cooked with tea polyphenols (10% w/w, based on starch) produced a more attenuated starch digestion (RDS = 8% decrease, SDS = 62% increase, RS= 26% increase) than corresponding normal maize starch (RDS = 5% increase SDS = 5% decrease, RS= 36% increase) compared to controls. Barros et al. [16] reported 186% increase in RS for normal maize cooked similarly as above with purified PA extract (10% w/w, based on starch) from sorghum; RS increased from 2.9% to 8.3%). Indeed, amylose seems to possess a preferred interaction with PA, while branched chain amylopectin interacts better with monomeric catechin and epigallocatechin.

In complex systems in which starch co-exists with other food ingredients in a matrix, starch interactions with polyphenols occur via more complex mechanisms, and its impact on starch digestibility is often limited. This is because other food ingredients

(particularly proteins) can interfere with starch-polyphenol interactions due to their higher affinity for polyphenols than starch. In a bid to compare the impact of polyphenols on starch digestibility between a simple starch matrix and sorghum flour (a more complex matrix), Mkandiwire et al. [18] measured the starch digestibility profile of normal corn starch (treated with sorghum extract) with whole grain sorghum flour (with an equivalent amount of starch). The authors found that normal starch cooked with 12.5% PA (w/w of starch; closest to actual levels in sorghum flour used) possessed a more desirable digestibility profile (RDS=63% SDS=10% RS=26%) compared to sorghum flour (RDS=80% SDS=15% RS=6%); alluding to the fact that other components in the flour matrix limited the role of starch-PA interactions in reducing starch hydrolysis.

Though the above study by Mkandiwire et al. [18] supports the reported limited polyphenol-starch interactions in heterogeneous systems, a direct comparison is difficult. Utilizing sorghum starch (instead of maize starch) and sorghum flour from endosperm only (instead of whole grain), and cooking them with equivalent amounts of PA extracts (from the same sorghum variety) may have allowed an easier and more direct comparison. Dunn et al. [19] also found that significant sorghum proanthocyanidin-wheat gluten interactions occurred during dough (25% sorghum bran substitution /g of flour) mixing that limited starch-proanthocyanidin interactions. Interestingly, they found that the PA-gluten interactions resulted in a 73% increase in SDS compared to monomeric forms, but no increase in RS in tortilla matrix. This implies that gluten-polyphenol interactions may have precluded RS formation.

Other food models describing flavonoid-protein interactions [14,73,74] have shown effective binding of proteins by flavonoids in food matrices to form stable complexes, precluding the availability of flavonoids for starch interaction. Though, there is little data describing polyphenol-fatty acid interactions, it is well understood that fatty acids (including palmitic and linoleic acid) can complex with amylose on the surface of starch granules [92-94], which can potentially impact the interaction of starch and polyphenols.

While studies utilizing heterogeneous/complex starch systems have practical implications for direct applications in food products, mechanisms of starch-polyphenol interactions are difficult to understand from such systems. Homogeneous matrices on the other hand offer simple systems for investigating mechanisms of starch-polyphenol interactions that could allow for better application of these interactions to improve food quality. More in-depth investigations are needed to fully describe the interaction mechanisms between starch and polyphenols, and how they can be directly applied to developing novel low calorie food products.

2.8 Proanthocyanidins interaction with starch

Proanthocyanidins (PA) are tannins of the ‘condensed type’, composed of oligomers or polymers of flavonoids (flavan-3-ols and flavan-3,4-diols), or a mixture of the two, linked by 4-8 or 4-6 C-C bonds, and may contain from 2 to 50 or greater flavonoid units [95] (Figure 1). Proanthocyanidins are widely distributed in fruits

(grapes and apples), vegetables, legumes, cocoa, red wine, and certain grains, such as sorghum and finger millets [96,97].

The structure of PA polymers gives them a conformational flexibility to interact with other food molecules, such as proteins [98-100] and amylose [15] through their hydroxyl groups and aromatic rings. Beyond the well documented impact of PA on digestive enzymes and transporter proteins [10,12], it is of particular interest to food scientists to establish whether PA interactions with starch can produce complexes that resist or reduce rate of enzyme hydrolysis.

Lemlioglu-Austin et al. [17] reported that a tannin sorghum extract was more effective at reducing starch digestibility when cooked with normal and high amylose maize starch, and produced lower estimated glycemic index, EGI (48 – 49) and higher resistant starch, RS, (15 – 58%) compared to non-PA treatments (EGI, 67 – 90; RS, 0 – 51%). Barros et al. [15,16] showed that the high MW PA from sorghum interact with amylose to increase RS formation in completely gelatinized starch. They [15,16] explained that, sorghum PA possess a ‘linear’ structure (Figure 1), which may be responsible for their ‘unhindered’ interaction with linear amylose molecules.

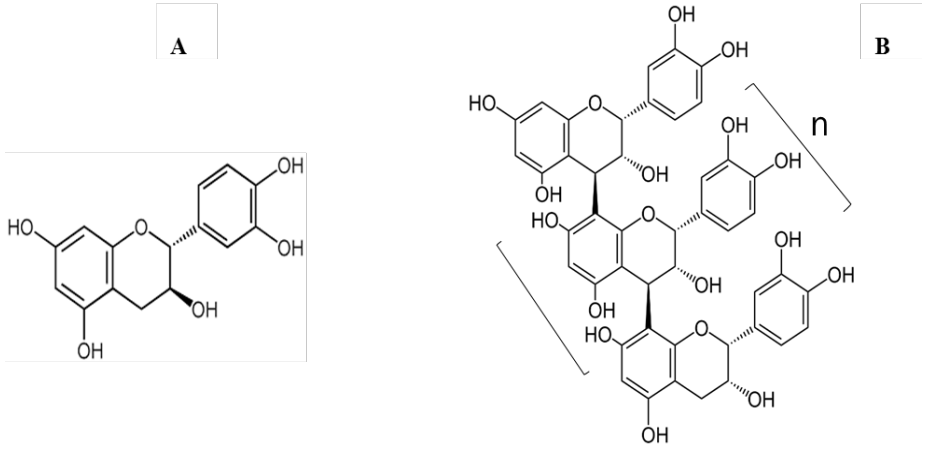

Figure 1 Chemical structure of A: catechin unit; B: polyflavan-3-ol (trimer).

Barros et al. [15,16] showed that sorghum PA significantly increased RS in starches that contain amylose, but not in waxy starch or isolated amylopectin. Monomeric sorghum polyphenols at equivalent levels had no effect [15].

Thus, it is apparent that specific amylose-PA binding forms non-digestible complexes. For example, at 25.8 mg PA/g starch, a 66.5% amylose maize starch increased in RS by 155 mg/g, whereas a 23.9% amylose (normal) starch increased in RS by 70 mg/g, and waxy starch (0.36% amylose) had no increase in RS [16]. Furthermore, debranching the normal starch with isoamylase before reacting with the PA produced a modest increase in net RS by 86 mg/g [15]. This suggests that the branching in amylopectin sterically interferes with its ability to complex with PA, and that the freed linear amylopectin branch fragments also interact with PA, but to a lesser extent than the longer amylose polymers. Also higher MW PA led to higher RS formation [16]. Under similar conditions, monomeric polyphenols (including catechin) had insignificant effect

on starch digestibility. These findings reveal that it is possible to form non-digestible complexes between PA and amylose, but not amylopectin.

2.9 Nature of non-covalent interactions that impact starch digestion

Starch is made up of polymer chains of glucose (straight chain amylose and branched chain amylopectin) arranged into a semi-crystalline structure. These polymers have several hydroxyl groups, and loose helical amylose chains have a hydrophobic interior, which allow them to interact with polyphenols via a variety of mechanisms. Non-covalent interactions between starch and polyphenols in food systems consist of hydrophobic interactions, hydrogen bonds, electrostatic, and ionic forces [9]. They are, however, largely driven by hydrophobic and hydrogen bond interactions. It is important to note that formation of non-covalent interactions between starch and polyphenols impacts both the functional and nutritional properties of starch [15].

Chai et al. [101] and Wu et al. [102] showed that tea polyphenols formed complexes with starch stabilized largely by hydrogen bonding. Barros et al. [15] also observed textural changes (increase in RVA peak viscosity) in starch treated with sorghum PA, explaining that the PA acted as plasticizers by simply utilizing their hydroxyl groups to form hydrogen bonds with amylose chains. Like other carbohydrates [23,103], it is likely that amylose interactions with PA involves extensive hydrogen bonding due to the steric ‘compatibility’ of the linear amylose chains with the PA (abundant –OH groups in close proximity). Additionally, hydrophobic interactions (possibly partial inclusion of one of the aromatic rings into the hydrophobic interior of

the amylose [104]) that stabilize the complex are likely. It will be interesting to establish how these amylose-tannin complexes affect the rate of glucose release from starch *in vivo*, and the fate of the non-digested complexes in the colon, including interaction with colon microbiota.

Monomeric polyphenols have also been shown to interact with starch and other carbohydrates [91,105]. Liu et al. [91] suggested the possible formation of inclusion complexes between tea catechins with amylose, when they observed moderate reduction of the postprandial glycemic response to starch co-cooked with 10% tea polyphenols (dry weight of starch). Tea catechins are sterically bulky and dominantly made up of highly hydrophilic epigallocatechin-3-gallate (EGCG) [91]; it is therefore not likely that the hydrophobic core of an amylose coil would include these molecules. Even if this occurred, such interactions appear to be rather modest. A more likely interaction mechanism would be a weak partial inclusion of the B-ring of the EGCG into the amylose core, anchored/stabilized by hydrogen bonding through the D-ring galloyl ester hydroxyl groups on the outside [86].

2.10 Impact of polyphenol-starch interaction on dietary glucose availability (*in-vivo* and clinical evidence)

Clinical studies involving human subjects are considered more reliable for evaluating the glycemic-controlling effects of polyphenols; however, few papers describe such properties. In a mouse model study reported by Liu et al. [91], tea polyphenols (10%, based on starch dry weight) were cooked together with various maize

starches varying in amylose content and fed to mice. The tea polyphenols moderately decreased (not significantly) the blood glucose concentration from consumption of waxy and normal starch, but increased blood glucose concentration and delayed blood glucose peaking in the high amylose starch. A similar phenomenon was observed by Chai et al. [101]; utilizing a mouse model, they showed that a slow digestion property with an extended and moderate glycemic response was achieved by feeding mice a high amylose maize starch (1.5 g) co-cooked with tea polyphenols (150 mg). Though the results of these studies highlight the potential of utilizing tea polyphenols for producing low calorie starch products, it must be noted that the levels used are too high for practical applications. For example a cup of tea contains approximately 80−105 mg of tea polyphenols [106].

Hogan et al. [107] also showed that oral intake of the red grape pomace extract (400 mg/kg body weight) after approximately 30 minutes of administering a potato starch suspension (2 g/kg bw) significantly suppressed the postprandial hyperglycemia by 35% in streptozocin-induced diabetic mice. The observations were attributed to bioactive compounds in the red grape pomace extract inhibiting the α-glucosidase action at the brush border of the small intestine.

In a clinical study by Coe et al. [108], 9 female subjects consumed polyphenol rich baobab extract as an aqueous drink at two dose levels (a low-dose: 18.5 g; and a high-dose: 37 g) together with white bread (~120 g), and glycemic response, satiety, and postprandial energy expenditure were measured. It was found that both dose levels resulted in significant reduction in glycemic response (Glycemic response area under the

curve, GR $AUC_{0\text{-}120\ min}$: 18.5 g dose = 142.6 and 37 g dose = 135.8) compared to a control (GR $AUC_{0\text{-}120\ min}$ = 175.3); although there was no significant effect on satiety or on energy expenditure. The reduction in sugar release after consumption of baobab fruit extract was attributed to the polyphenols in the extract.

It is important that more clinical studies be conducted to establish the physiological impacts of polyphenols on glucose metabolism from starch. It is evident however, that the combination of polyphenols with specific starches could be employed to successfully manipulate available glucose and postprandial glycemic response in humans.

3. POLYMERIC TANNINS SIGNIFICANTLY ALTER PROPERTIES AND *IN-VITRO* DIGESTIBILITY OF PARTIALLY GELATINIZED INTACT STARCH GRANULES*

3.1 Introduction

The rising prevalence of chronic diseases related to excess caloric intake – such as diabetes and obesity – is one of the most critical public health problems facing both developed and developing countries. Strategies that lower caloric impact of foods without negatively affecting their sensory properties are necessary. Carbohydrates are the major source of metabolic energy in foods, accounting for approximately 52% of calories derived from food in the US, and up to 80% in the developing countries [1,2]. Among the dietary carbohydrates, starch contributes most of the calories and is thus a prime target for favorably altering caloric profile of foods.

Starch is nutritionally classified as rapidly digestible starch (RDS), slowly digestible starch (SDS), and resistant starch (RS) [3,4]. RDS leads to rapid spike in blood glucose level after ingestion, whereas the SDS results in a slower sustained postprandial glucose response and is thus thought to help improve satiety [5,6].

*Reprinted from Food chemistry, 208, Amoako, D.B. and Awika, J.M., Polymeric tannins significantly alter properties and in vitro digestibility of partially gelatinized intact starch granule, 10-17, 2016, with permission from Elsevier.

The RS fraction escapes enzyme hydrolysis in the small intestine and functions as dietary fiber. Increasing SDS and RS in starchy foods is therefore of great interest to the food industry. Interest in polyphenols as potential regulators of glucose uptake and metabolism has grown [9,10]. However, evidence suggests that direct interaction of monomeric polyphenols with starch, has limited practical impact on starch digestibility profile [91].On the other hand, Barros et al. [16,109] recently showed that the high molecular weight proanthocyanidins, PA, (condensed tannins) from sorghum interact with amylose to form RS in completely gelatinized and dispersed starch (no intact granules); interaction of the tannins with amylopectin did not form RS. The evidence suggests that the structure of amylose affords a more efficient interaction with the high MW tannins, suggesting the interactions involve extensive hydrogen-bonding, along with hydrophobic interactions, as was demonstrated for other carbohydrates [22,110], and well documented for proteins [98].

Thus, there is opportunity to utilize the tannins to directly reduce starch digestibility. However, given that starch is only partially gelatinized in most starchy foods (e.g., cookies – 2-11%, crackers – 3%, bread – 33-71%, cereal flakes – 24-27% [20,21], and granule integrity is largely retained, it is not clear how above observations would translate into a typical food system.

Dunn et al. [19] reported that tortilla (in which starch is partially gelatinized) processed from wheat flour with added high tannin sorghum bran (rich in high MW PA), increased SDS from 13 to 21% (compared to control and non-tannin brans) without an increase in RS formation. Extensive interaction of PA with gluten proteins during the

dough mixing stage was observed; thus, it was not clear whether the protein-PA interactions influenced the observed changes in starch digestibility. Other authors also found limited impact of PA on RS formation in heterogeneous food matrix [17,18], but significant increase in SDS and reduced glycemic index [17]. This study thus investigates how the degree of starch swelling and gelatinization affects tannin-starch interactions, and the effect of the interactions on starch properties and *in-vitro* digestibility.

3.2 Materials and methods

3.2.1 Sorghum phenolic extracts

Two sorghum varieties grown in College Station, TX were chosen based on their different polyphenol concentration and profiles. High tannin sorghum (high in polymeric tannins) and a white pericarp sorghum (with no tannins) were used. Sorghum brans were obtained by decorticating 1 kg batches in a PRL mini-dehuller (Nutama Machine Company, Saskatoon, Canada) and were separated with a KICE grain cleaner (model 6DT4-1, KICE Industries Inc., Wichita, KS). The brans (approximately 10% yield) were milled to pass through a 0.5 mm screen using a UDY cyclone mill (model 3010−030, UDY Corporation, Fort Collins, CO). They were kept at −20 °C until used. Brans (100 g) were extracted in 70% acetone (400 mL) and stirred for 2 h. The mixture was then filtered, and the residue re-extracted twice for one hour each time. The acetone was

immediately removed from the combined supernatant under vacuum at 40 °C and stored at −20 °C until used. Portions of the aqueous extracts were also freeze-dried.

3.2.2 Starch and reagents

Normal (amylose content = 23.9%) and waxy (amylose content = 0.36%) maize starches were obtained from National Starch Food Innovation (Bridgewater, NJ). All solvents (HPLC or analytical grade) and reagents were obtained from Sigma (St. Louis, MO). Porcine pancreas α-amylase (EC 3.2.1.1) was also purchased from Sigma–Aldrich Chemical Co., Ltd (St. Louis, MO), while D-Glucose (GOPOD format) assay was purchased from Megazyme (Ireland).

3.2.3 Preparation of phenolic-extract-treated starch products

Tannin extract (2.5 g total solids; 111.08 ± 30.29 mg PA per gram of extract) from high-tannin sorghum was incubated separately with normal and waxy maize starch (25 g), in 30% and 50% aqueous ethanol solutions (v/v) at 70 °C for 20 minutes. Ethanol solution and tannin extract made up a total volume of 75 mL. Ethanol competes with starch for water, and was therefore included in the treatments to control starch swelling and gelatinization. It also increases the solubility of PA, which can facilitate PA-starch interactions. Samples were then centrifuged to remove the supernatant, and the sediments collected was oven dried at 40 °C overnight to remove residual ethanol and water. The sediments were then gently dispersed with pestle and mortar to obtain

powdered samples, which were stored at 4 °C until use. Two other treatments were included, replacing the tannin extract with non-tannin extract from white sorghum (2.5 g total solids) for comparison, and cellulose powder (2.5 g) as a control treatment.

3.2.4 Phenolic extract characterization

Phenol content of the sorghum extracts was estimated according to the Folin−Ciocalteu method described by Kaluza et al. [112]. An Agilent 1200 HPLC system with a diode array detector was used to profile phenolic compounds present in the extracts as previously described by Awika et al. [113] with modifications. A reversed phase 150 × 2.00 mm, 5 μm, C-18 column (Phenomenex, Torrance, CA) was used. The freeze dried phenolic extracts were dissolved in methanol, filtered, and then injected in the column. HPLC conditions were as follows: injection volume, 1.0 μL; flow rate, 0.25 mL/min. The mobile phase consisted of (A) 1% formic acid in water and (B) 1% formic acid in acetonitrile. The 33 min elution gradient for (B) was as follows: 0−3 min, 10% isocratic; 3-10 min, 20%; 10−20 min, 40% isocratic; 20−23 min, 60% isocratic; 23−27 min, 60% isocratic; 27−29 min, 10%; 29−33 min, 10% isocratic.

The tannin extract was also profiled for PA content and MW distribution by the normal-phase HPLC-FLD method of Langer et al. [114] using conditions described by Barros et al. [15] Catechin and procyanidin B1, and C1 were used to quantify monomers, dimers, and trimers, respectively. Quantitative data for PA with a DP greater than or

equal to four were based on procyanidin C1 (DP 3) peak response as previously described by Ojwang et al. [115].

3.2.5 Quantifying proportion of proanthocyanidins that reacted with starch

The normal-phase HPLC-FLD method described above was used to profile and quantify PA in both supernatant collected after incubating the starch with tannin extract, as well as the methanolic extract (400 mg starch: 1.2 mL MeOH) of the final dried tannin-treated starches. Samples were filtered (0.45 μm, nylon) and then injected (10 μL) into HPLC. Proportion of PA that reacted with starch (mg PA/g of starch) was calculated as: Total mg PA in starting extract – (mg PA in methanolic extract + mg PA in supernatant after starch-PA incubation)

3.2.6 Starch swelling properties

Solubility (%S) and swelling power (SP) were determined for starch treatments following a method described by Kibar et al. (2010), with some modifications. Starch suspension (1:15 w/v) was incubated for 30 min at room temperature (25 °C) with horizontal shaking in a reciprocating shaker set at low speed. The suspension was then centrifuged at 8,000 × *g* for 20 min, and the supernatant decanted into previously tared aluminum tin. The tin was dried for 24 h at 105 °C, and the soluble solids weighed and used to measure %S. The sediment left after decanting was weighed and used to calculate the SP. Calculations were done as follows:

%S = [(mass of solubles) / (mass of dry starch)] x 100

SP = (mass of sediment) / [(mass of dry starch) x (1 - (%S / 100))]

3.2.7 Thermal properties of starch samples

Differential Scanning Calorimetry (DSC) measurements were done using a Perkin-Elmer DSC-6 (Boston, USA). The calorimeter was calibrated with indium, and the DSC runs were operated under ultra-high purity nitrogen (30 mL/min) using a sealed empty aluminum pan as reference. Starch samples (3 mg, db) were each weighed into an aluminum pan, and distilled water added to get to 12 mg total weight (1:3 starch: water ratio, w/w). The pan was then hermetically sealed and equilibrated at room temperature overnight to allow adequate starch hydration. Samples were heated from 20 °C to 95 °C at a rate of 10 °C/min at a heat flow rate of 20 mW/g. The raw data was processed with Pyris 5 software (Perkin-Elmer) to obtain the onset (T_o), peak (T_p), and conclusion (T_c) temperatures and gelatinization enthalpies (ΔH). The degree of gelatinization (DG) of each starch treatment sample was determined by comparing the gelatinization enthalpy of the treatment sample (ΔH_s) to its native form (ΔH_n) [116]; $DG = 1 - (\Delta H_s / \Delta H_n)$

3.2.8 Starch pasting properties

A Rapid Visco Analyzer (RVA) was used to record starch pasting properties of the treatments, as detailed by Barros et al. [15]. Distilled water was added to each of the prepared samples (3.0 g, dry basis) in the RVA canister to obtain a total constant sample weight of 28 g. An RVA model 4 (Newport Scientific PTY Ltd., Warriewood, Australia) was used. Initial sample equilibration at 50 °C for 1 min followed by a linear temperature increase from 50−95 °C in 7.5 min, and then a holding step at 95 °C for 5 min, cooling to 50 °C within 7.5 min, and another holding step at 50 °C for 2 min, for a total of 23 min.

3.2.9 Starch crystallinity

Starch crystallinity determination was carried out using a method described by Mutungi et al. [117] with some modifications. A Bruker D8 Advanced X-ray diffractometer was used. Samples were scanned with Cu Kα radiation (λ = 0.154 nm), and reflections were detected in the angular range 2θ = 2–32° with a step interval of 0.05°. Scanning duration at each step was 5 s. The X-ray generator operating conditions were 35 kV and 45 mA. Raw waxy and normal corn starch samples were also scanned for comparison. All samples were conditioned at room temperature (25 °C) for 48 h before scanning. Percent crystallinity was calculated using DIFFRAC^{plus} TOPAS software following recommendations by Lopez-Rubio et al. [48].

3.2.10 In-vitro *starch digestibility*

In-vitro digestibility of samples was measured as previously described by Englyst et al. [118]. In summary, the starch treatments (400 mg) were digested by α-amylase (300 U/mg, A3176 Sigma-Aldrich, St. Louis, MO) and amyloglucosidase (95 U/mL, Cat. No. E-AMGDF, Megazyme International) mixture. Glucose released after 20 and 120 min was determined by reacting an aliquot with glucose oxidase reagent (K-GLUC GOPOD format assay kit, Megazyme, Ireland) and the absorbance at 510 nm read on a UV−vis spectrophotometer (Shimadzu Scientific Instruments) using a glucose standard assay kit (K-GLUC GOPOD format assay kit, Megazyme, Ireland). The content of the hydrolyzed starch was calculated by multiplying a factor of 0.9 with the glucose content. The percentage of SDS (%) in the products was obtained by the following equation: SDS% = [(G120 – G20) X 0.9/ TS] X 100; where, G_{20} and G_{120} are glucose content released after 20 and 120 min, respectively; and TS is the weight of starch in sample used for each test. Results were expressed on db.

3.2.11 Statistical analysis

Data were analyzed using a one-way analysis of variance (ANOVA) to determine significant differences among them. Tukey's HSD ($P \leq 0.05$) was used to separate means. The software used was SAS version 9.4 for windows. All tests were replicated at least twice.

3.3 Results and discussion

3.3.1 Phenolic profile of the sorghum extracts

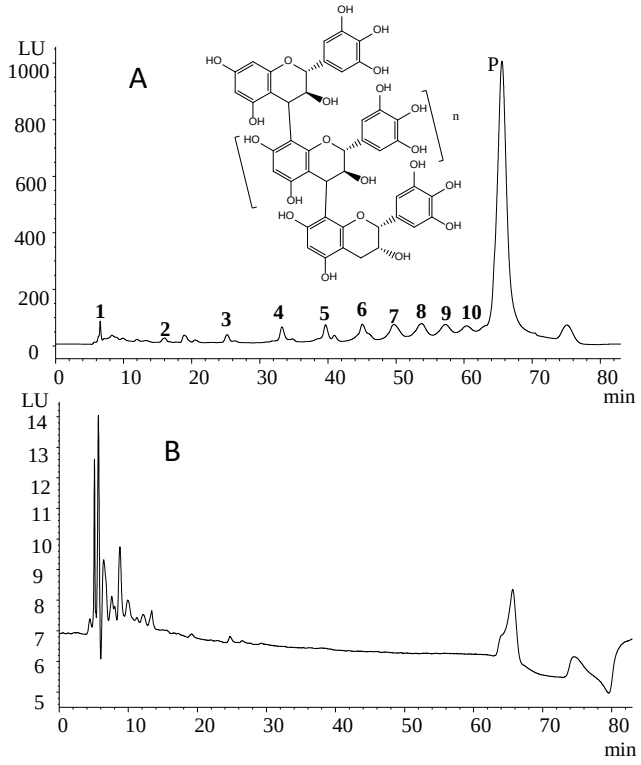

Figure 2 Normal phase HPLC-FLD of sorghum proanthocyanidin (tannin) profile of high-tannin sorghum used in the study (A), and profile obtained from methanolic extract of dried tannin-reacted normal starch from 30% ethanol treatment (B). Numbers on peaks denote degree of polymerization (DP). P = polymers with DP > 10. Figure 2 A insert represents generic structure of sorghum proanthocyanidin polymer.

Phenol content (mg GAE/g) of the sorghum phenolic extracts were 255.3 ± 0.7 (tannin) and 23.6 ± 0.3 (white, non-tannin). Phenolic acid acyl-glycerides were identified as the major monomeric polyphenols in both sorghum extracts, similar to previous observation [119] (data not shown). The tannin sorghum extract contained 111 ± 3.0 mg PA per g. More than 99% of this was made up of polymeric tannins (DP > 3) (Figure 2). The PA profile is consistent with that reported previously by Barros et al. [15].

3.3.2 Starch swelling and gelatinization properties

Starches treated with tannin extract in 30% ethanol (30E) had higher amounts of tannins (average 6.2 mg PA/g starch) interacting with starch compared to 50% ethanol (50E) treatments (average 3.5 mg PA/g of starch) (Table 1). This is likely due to greater extent of swelling of 30E starches compared to the 50E starches (Table 2). When the starch swells substantially, pores on the granule surface become easy channels for tannins to migrate into the interior of the granule to interact with starch polymers. The tannins that interacted with starch were essentially unextractable in methanol (Figure 2). As expected, the 30E starches were also more gelatinized (67.2-97%) compared to 50E starches (1.3-45.3%) (Table 3).

Table 1 Amount of proanthocyanidins (tannins) that reacted with starch in aqueous ethanol solutions.

Treatment	[a]Amount of tannins bound to starch (mg PA/g starch)	Proportion of added tannins that reacted with starch (%)
30% Ethanol		
Normal starch	6.47 ± 0.62[a]	5.82
Waxy starch	5.94 ± 0.80[ab]	5.35
50% Ethanol		
Normal starch	3.47 ± 0.70[b]	3.12
Waxy starch	3.44 ± 0.45[b]	3.10

[a] Calculated as mg PA in starting extract – (mg PA in methanolic extract + mg PA in supernatant after starch-PA incubation). PA; proanthocyanidins. Means followed by the same letter are not significantly different ($P \leq 0.05$).

The 30E starches had lower melting/gelatinization enthalpies (ΔH) and narrower melting temperature range ($T_c - T_o$), than the 50E treatments. This confirms that the 30E starches underwent a higher degree of gelatinization. The 30E starches exhibited higher DSC onset (T_o) and peak (T_p) temperatures than the 50E starches (Table 3). The higher T_o and T_p is an indication of greater resistance of the starch to gelatinization; which may have resulted from a modification/ rearrangement of the internal amorphous structure of the starch into a more rigid form, more resistant to gelatinization; a phenomenon common in heat treated starches [120,121]. Mutungi et al. [117] explain that, different combinations of thermal treatments induce ordering effects in starch granule structure

that result in new products of different crystalline orientations, some of which have high resistance to gelatinization.

Table 2 Swelling properties of maize starches treated in ethanol solutions with sorghum phenolic extracts.

Starch treatment	Normal starch (23.9% amylose)		Waxy starch (0.36% amylose)	
	Solubility (%)	Swelling power (%)	Solubility (%)	Swelling power (%)
Native starch[A]	0.02 ± 0.00^{e}	1.94 ± 0.04^{c}	0.11 ± 0.10^{c}	2.11 ± 0.01^{e}
30% Aqueous ethanol				
Control Starch	2.07 ± 0.10^{bc}	4.70 ± 0.05^{a}	6.19 ± 0.86^{a}	5.05 ± 0.13^{c}
Starch + cellulose	1.7 ± 0.17^{c}	4.72 ± 0.13^{a}	4.06 ± 0.59^{b}	6.66 ± 0.15^{a}
Starch + non-tannin extract	4.97 ± 0.09^{a}	4.87 ± 0.01^{a}	7.46 ± 0.14^{a}	5.44 ± 0.09^{b}
Starch + tannin extract	0.31 ± 0.01^{e}	4.09 ± 0.06^{b}	3.01 ± 0.06^{b}	4.21 ± 0.01^{d}
50% Aqueous ethanol				
Control Starch	0.34 ± 0.03^{e}	2.06 ± 0.06^{c}	0.28 ± 0.00^{c}	2.26 ± 0.05^{e}
Starch + cellulose	0.28 ± 0.08^{e}	2.09 ± 0.02^{c}	0.47 ± 0.01^{c}	2.27 ± 0.02^{e}
Starch + non-tannin sorghum extract	2.54 ± 0.26^{b}	2.01 ± 0.07^{c}	2.88 ± 0.13^{b}	2.22 ± 0.06^{e}
Starch + tannin extract	0.89 ± 0.18^{d}	2.10 ± 0.01^{c}	1.24 ± 0.00^{c}	2.18 ± 0.00^{e}

Starch treatments were heated at 70ºC/20 min in specified solutions, rinsed and dried before analysis. [A]Native starch = starch not subjected to the thermal treatment. Means followed by the same letter within column are not significantly different ($P \leq 0.05$).

Table 3 Thermal properties of starch treated in aqueous ethanol solutions with sorghum phenolic extracts.

Sample	T_o °C	T_p (°C)	T_c (°C)	$T_c - T_o$ (°C)	ΔH (J/g dry starch)	Degree of Gelatinization (%)[C]
Normal Maize Starch						
NS[A]	66.0 ± 0.1[b]	71.9 ± 0.2[c]	78.3 ± 0.3[bc]	12.3 ± 0.4[a]	12.2 ± 1.1[a]	0.0[e]
30% Aqueous ethanol						
Cellulose	73.2 ± 0.5[a]	76.4 ± 0.1[a]	80.1 ± 0.6[a]	6.9 ± 0.3[cd]	0.4 ± 0.1[e]	97.1 ± 0.6[a]
White[B]	73.4 ± 0.0[a]	76.6 ± 0.1[a]	80.1 ± 0.0[a]	6.7 ± 0.0[d]	1.6 ± 0.2[d]	87.2 ± 1.3[b]
Tannin[B]	72.4 ± 0.0[a]	74.9 ± 0.2[b]	78.8 ± 0.1[b]	6.4 ± 0.1[d]	1.5 ± 0.0[d]	87.8 ± 0.3[b]
50% Aqueous ethanol						
Cellulose	65.6 ± 0.9[b]	69.9 ± 0.9[d]	74.7 ± 0.2[e]	9.1 ± 0.7[cb]	4.7 ± 2.6[c]	45.0 ± 1.6[c]
White[B]	67.0 ± 0.8[b]	72.1 ± 0.2[c]	77.4 ± 0.9[d]	10.4 ± 1.4[ab]	9.1 ± 0.8[b]	29.7 ± 1.2[d]
Tannin[B]	66.8 ± 0.3[b]	72.1 ± 0.3[c]	77.7 ± 0.0[dc]	10.9 ± 0.3[ab]	12.0 ± 0.1[a]	1.3 ± 1.0[e]
Waxy Maize Starch						
NS[A]	66.2 ± 0.4[c]	72.3 ± 0.2[d]	79.1 ± 0.1[b]	12.9 ± 0.4[ab]	15.3 ± 1.0[a]	0.0[f]
30% Aqueous ethanol						
Cellulose	74.8 ± 0.4[a]	77.5 ± 0.3[a]	81.2 ± 0.3[a]	6.4 ± 0.2[d]	1.5 ± 0.1[f]	90.5 ± 0.8[a]
White[B]	73.9 ± 0.4[ab]	77.3 ± 0.4[a]	82.0 ± 0.3[a]	8.2 ± 0.2[c]	5.0 ± 0.5[d]	67.2 ± 3.1[c]
Tannin[B]	72.7 ± 0.6[b]	75.9 ± 0.5[b]	79.9 ± 0.2[b]	7.2 ± 0.4[cd]	3.0 ± 0.3[e]	80.4 ± 1.7[b]

Table 3 Continued

50% Aqueous ethanol						
Cellulose	66.7 ± 0.4^{c}	73.3 ± 0.7^{cd}	79.9 ± 0.1^{b}	13.2 ± 0.3^{ab}	11.1 ± 0.7^{c}	30.0 ± 0.5^{d}
White[B]	67.2 ± 0.2^{c}	73.6 ± 0.1^{c}	79.6 ± 0.5^{b}	12.4 ± 0.3^{b}	14.3 ± 0.9^{b}	10.3 ± 0.4^{e}
Tannin[B]	66.1 ± 0.5^{c}	72.4 ± 0.0^{d}	79.6 ± 0.4^{b}	13.5 ± 0.2^{a}	10.9 ± 0.1^{c}	28.6 ± 0.4^{d}

Starch treatments were heated at 70°C/20 min in specified solutions, rinsed and dried before analysis. [A]Native starch not subjected to the thermal treatment. [B]Sorghum extracts (White = non-tannin extract). T_o, onset temperature; T_p, peak temperature; T_c, Conclusion temperature; $T_c - T_o$, melting temperature range; ΔH, melting enthalpy change. [C]Degree of gelatinization calculated as: $[1 - (\Delta H_{sample} / \Delta H_{native\ starch})] \times 100$. Means followed by the same letter within column and starch type are not significantly different ($P \leq 0.05$).

An interesting observation was that in the 30E treatments, both sorghum extracts had similar effect on the extent of normal starch gelatinization (Table 3). However, in the 50E treatment, the tannin extract completely inhibited gelatinization of the normal starch, and had a melting enthalpy similar to raw starch (Table 3). On the contrary, in waxy starch, the 50E tannin treatment had similar degree of gelatinization as the cellulose control (almost 30%) and higher than the white sorghum treatment (10%).

The high MW tannins are relatively hydrophobic, and are thus more soluble in 50% ethanol compared to 30% ethanol. Thus, besides inhibiting starch swelling to a higher degree than in 30E, the 50E treatment would likely allow tannins to solubilize more freely and thus interact better with starch molecules. The fact that there was such a sharp contrast in behavior of normal vs waxy starch in presence of tannins in 50E treatment despite similar tannin inclusion (approx. 3.5 mg/g starch) (Table 1) suggests different chemical interactions are involved. The data suggests strong specific interaction of the tannins with the normal starch, but not waxy starch, in the 50E, which supports the specificity of amylose-tannin interactions hypothesis [15].

Amylose structure is more likely to allow for a high degree of hydrogen bonding and hydrophobic interactions with tannins, compared to the highly branched amylopectin, which is sterically unfavorable for such interactions. Thus, it is plausible that tannins acted as cross-linkers of amylose polymers near the granule surface in the 50E treatments. The fact that the non-tannin waxy starch treatments had lower degree of gelatinization compared to the tannin and cellulose control may be due to the highly

branched amylopectin undergoing a less-hindered interaction with monomeric phenolic compounds, especially in their amorphous regions. This would conceivable strengthen the amorphous regions (reduce mobility) and make them more resistant to gelatinization. Chai et al. [101] reported that relatively high levels of monomeric tea polyphenols at 100 mg/g starch slightly (though not significantly) reduced postprandial glycemic response to waxy starch, but significantly increased the response in a high amylose starch.

3.3.3 Starch pasting properties

In general, the pasting temperatures and peak times were higher for the 30E normal starches than their control, whereas the 50E normal starches were generally similar to the control (Table 4). This suggests a higher degree of crystallinity of the 30E normal starches, likely due to reassociation of amylose polymers in the granule, which agrees with the DSC data (Table 3). For the waxy starches, there were no clear differences between the 30E and 50E treatments, and both groups were similar to control (Table 4). This is likely because the lack of amylose in the waxy starch limits available regions of starch polymers that can reassociate after hydrothermal treatment. By contrast, the 30E normal starch tannin treatment had a markedly higher pasting temperature compared to all other normal starch treatments and control (Table 4). A possible explanation is that the 30E treatment resulted in enough starch swelling to allow the tannin polymers to migrate into the granule interior and partially cross-link the amylose polymers inside the granule thus making the granule more resistant to swelling.

The interaction of tannins with the 50E normal starch likely occurred mostly close to the surface, thus did not have as much impact on pasting temperature. Within the waxy starch treatments, the non-tannin extract treatments tended to have higher pasting temperatures than comparable tannin and cellulose treatments, which may be due to the association of monomeric phenolics with amylopectin discussed in Section 3.3.2 above.

Table 4 Pasting properties of maize starches treated in ethanol solutions with sorghum phenolic extracts.

Treatment	Pasting properties				
	Peak time (min)	Pasting temp. (°C)	Peak viscosity (cP)	Final viscosity (cP)	Breakdown (cP)
Normal Maize starch					
NS[A]	8.3[e]	72.5[d]	4370[a]	4411[a]	1822[a]
30% Aqueous ethanol					
Cellulose	10.2[a]	75.7[b]	3086[c]	3981[bcd]	606[d]
White[B]	9.9[b]	74.2[bc]	3020[c]	3741[d]	706[d]
Tannin[B]	9.6[c]	84.8[a]	3220[bc]	4032[bc]	884[c]
50% Aqueous ethanol					
Cellulose	8.5[e]	72.5[d]	3329[bc]	3767[cd]	1102[b]
White[B]	8.3[e]	72.8[cd]	3543[b]	3863[cd]	1228[b]
Tannin[B]	8.7[d]	74.0[cd]	4300[a]	4150[ab]	1833[a]
Waxy Maize Starch					
NS[A]	5.7[b]	69.5b[c]	4826.0[c]	2216[a]	3109[c]
30% Aqueous ethanol					
Cellulose	5.7[b]	50.0[d]	3697[g]	1595[e]	1863[e]
White[B]	6.1[a]	71.4[a]	4252[f]	1830[d]	2660[d]
Tannin[B]	6.0[ab]	68.9[c]	5571[a]	1772[d]	4034[a]
50% Aqueous ethanol					
Cellulose	5.8[ab]	70.1[abc]	4506[e]	1983[c]	2913[c]
White[B]	5.9[ab]	70.8[ab]	4675[d]	2193[ab]	2910[c]
Tannin[B]	5.8[ab]	70.1[abc]	5157[b]	2078[bc]	3504[b]

Starch treatments were heated at 70°C/20 min in specified solutions, rinsed and dried before analysis. [A]Native starch not subjected to the thermal treatment. [B]Sorghum extracts (White = non-tannin extract). Means followed by the same letter within column and starch type are not significantly different ($P \leq 0.05$).

The peak viscosity for the heat-treated starches were generally lower than corresponding untreated starches (Table 4), which indicates the heat treatments reduced swelling capacity of the starches. However, the tannin treatments consistently had higher peak viscosities than comparable treatments for both normal and waxy starches, and actually produced higher peak viscosities than untreated waxy maize starch (Table 4). A similar phenomenon was reported for sorghum starch in presence of tannins [122]. This suggests cross-linking and/or granule stabilizing effect of the polymeric tannin. The similarity of pasting properties of the tannin treated 50E normal starch to non-treated starch also agreed with the DSC data (Table 3), which showed that the 50E normal tannin treatment behaved similar to the raw starch.

3.3.4 Starch crystallinity

All treatments retained the typical A-type polymorph diffraction patterns of their native/raw starches (data not shown), which indicates no inclusion complexes between amylose and polyphenols were formed. The monomeric polyphenols are too hydrophilic to interact with amylose polymers in this manner, whereas the polymeric tannins are too bulky. This may suggest that the interaction of tannins with starch is most strongly influenced by hydrogen-bonding, with the close proximity of hydroxyl groups in the polymeric tannins ensuring stronger interactions with amylose. However, formation of inclusion complexes have been reported between amylose and the monomeric flavonoid, genistein [123], though such complexes are likely weak due to flavonoid bulk [104] and

limited hydrogen bonding sites. Clear evidence with other carbohydrates consistently demonstrate that the carbohydrate polymers with hydrophobic regions bind much more strongly to polymeric tannins than carbohydrates with similar structures but no hydrophobic regions [22]. This indicates that hydrophobic interactions likely play an important role in stabilizing amylose-tannin complexes as well.

The X-ray crystallinity of the starch treatments present some interesting results (Table 5). The 50E treatments generally had higher crystallinity than raw starches and 30E treatments. This observation was expected, considering the fact that starch gelatinization results in loss of starch crystallinity. Also, the limited moisture in the 50E treatments restricted starch swelling while allowing for some internal molecular rearrangement/association within the granule during the heat treatment, which may explain their higher crystallinity than raw starches. Heat treatment of starches can result in the rearrangement of starch molecules, which can effect double helical chains shifting within the crystallites, resulting in a more ordered, hence more crystalline structure [117,124]. Wongsagonsup [121] made similar observations in temperature cycled (TC) normal maize starch.

The 30E normal starch tannin treatment was a lot more crystalline (51.4%) than comparable non-tannin extract and cellulose treatments (16.0 – 22.8%), which explains its much higher pasting temperature than the other treatments (Table 4). The fact that such a difference was not observed in the 30E waxy treatments confirms that specific tannin-amylose interactions are responsible for the apparent anomalous observations.

Thus tannin-amylose interactions appear to be relatively specific with consistent effect on starch properties. Also, worth noting, was the fact that the 50E waxy non-tannin extract treatment had a slightly (but significantly) higher crystallinity than comparable tannin and cellulose treatments (Table 5), which also confirms the RVA data.

Table 5 X-Ray diffraction crystallinity (%) of maize starches treated in ethanol solutions with sorghum phenolic extracts.

Starch treatment	% Crystallinity (A-Type polymorph)[a]	
	Normal starch	Waxy starch
Native starch[A]	27.63 ± 1.62[bc]	45.82 ± 0.71[c]
30% Aqueous ethanol		
Cellulose	22.83 ± 2.65[dc]	24.35 ± 0.28[e]
Non-tannin extract	15.97 ± 1.08[d]	26.86 ± 2.68[de]
Tannin extract	51.36 ± 2.22[a]	29.25 ± 0.93[d]
50% Aqueous ethanol		
Cellulose	33.67 ± 0.25[b]	52.26 ± 0.21[b]
Non-tannin extract	46.13 ± 0.32[a]	63.32 ± 0.51[a]
Tannin extract	45.12 ± 2.58[a]	56.43 ± 0.23[b]

Starch treatments were heated at 70ºC/20 min in specified solutions, rinsed and dried before analysis. [a]Percent crystallinity was calculated using DIFFRAC^{plus} TOPAS software following recommendations by Lopez-Rubio [48]. [A]Native starch not subjected to the thermal treatment. Means followed by the same letter within column are not significantly different ($P \leq 0.05$).

3.3.5 In-vitro starch digestibility

Of particular interest is how the observed effects of tannins on physical properties of starch affect starch digestibility. This would provide insight on how starch-tannin interactions can be utilized to produce nutritionally desirable starches. The tannins had marked effect on starch digestibility compared to other treatments (Figure 3). In the 30E starches, tannins reduced RDS in normal starch (from 735 mg/g to 397 mg/g); representing a 46% decrease (Figure 3). The white sorghum extract had no effect on RDS (was similar to cellulose). The tannin treated normal 30E starch also had much higher SDS (274 mg/g) and RS (299 mg/g) compared to non-tannin treatments, which were similar (SDS average = 96.7 mg/g, RS average = 148 mg/g). Thus, the tannin-starch interactions produced a net SDS and RS increase of 177 and 151 mg/g, respectively, in the normal 30E maize starch. This indicates that the tannins formed non-digestible and slow-digesting complexes with starch. The effects are especially remarkable given there was only 6.5 mg tannins/g of starch in the complexes (Table 1). Barros et al. [16] observed up to a maximum 86 mg RS/g starch when completely gelatinized and dispersed normal maize starch was reacted with approx. 24 mg tannins/g starch. The complete disruption of granule integrity may be a factor in their lower values. However, they used an aqueous matrix for reacting starch with tannins; this likely limited starch-tannin interaction due to tannins readily precipitating in water.

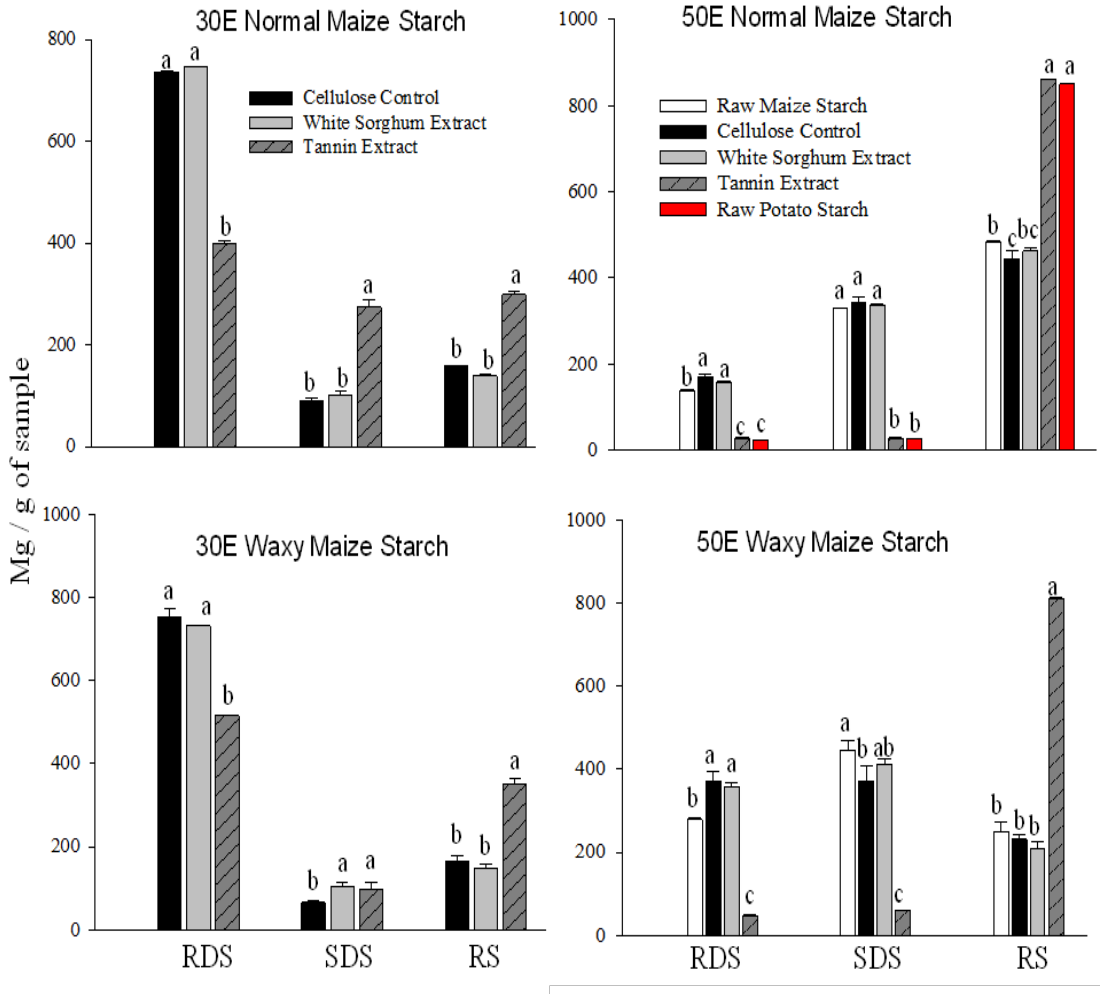

Figure 3 Effect of starch-tannin interactions on digestibility of partially gelatinized normal and waxy maize starches treated in 30% (30E) and 50% (50E) aqueous ethanol solution. Samples were incubated in respective solutions at 70ºC/20 min. RDS, SDS, and RS represent rapidly digesting, slow digesting, and resistant starch, respectively. Raw starch denotes native starch not subjected to the solvent/heat treatments. Native (untreated) raw potato starch digestibility included for comparison; the potato starch was digested under similar conditions as the maize starches. Error bars indicate ± standard deviation. Same letters within starch digestibility types are not significantly different (P ≤ 0.05).

In the waxy 30E starch, tannins had a smaller but still substantial reduction in RDS, from 754 mg/g to 516 mg/g, representing a 31.6% reduction. The change in RDS was mostly explained by a concomitant increase in RS; the tannin effect on the SDS (98 mg/g vs. control cellulose 65 mg/g) was small and similar to the non-tannin extract (105 mg/g) (Figure 3). The observation was somewhat unexpected, because Barros et al. [15,16] reported that tannin interaction with amylopectin did not produce any change in RS in fully gelatinized waxy starch and isolated amylopectin. Thus, it appears from our data that starch gelatinization and granule integrity have a marked effect on the ability of tannins to interact with starch in a way that impedes enzyme digestion. This is highly relevant because starch granule integrity is largely retained in most starchy foods. We theorize that the effect of the tannins on RS formation in waxy maize starch may be due to formation of sufficient hydrogen bonding to partially block enzyme access to the starch hydrolysis sites. The non-tannin extract had no effect on RS formation in the 30E waxy maize starch, further highlighting limited impact of monomeric polyphenols on starch digestibility [16]. However, it produced a slight, but significant increase in SDS compared to cellulose control, supporting the theory that the monomeric polyphenols interacted mainly with the amorphous regions of amylopectin, which are usually more readily hydrolyzed by α-amylases.

Based on the degree of gelatinization and starch properties, we expected the 50E treatments to have significantly different starch digestibility profiles compared to the 30E treatments. In the 50E samples, the cellulose and white sorghum treatments had digestibility profiles near identical to raw starches (Figure 3), indicating the starches did

not swell enough to enhance their digestibility during the heat treatment. Interestingly, both normal and waxy 50E starches were almost non-digestible when reacted with tannins (both had approx. 90% RS) (Figure 3). This was remarkable, given the low level of tannins that reacted with these starches (3.4 mg/g starch, Table 1). In fact, the 50E tannin treatments had much lower digestibility than corresponding raw normal and waxy maize starches; and behaved more like raw potato starch (Figure 3).

Considering the fact that the 50E starches underwent minimal swelling/gelatinization (Table 2), interactions between tannins and starch likely occurred largely close to the granule surface. The interactions would most likely be concentrated in/near granule pores, where enzymes initially access starch. This would in turn essentially block the pores, making enzyme access difficult. Raw cereal starches are susceptible to enzyme hydrolysis due to the presence of these surface pores. By blocking these pores, tannins made the maize starches behave like native raw potato starch, in which the lack of surface pores on granules gives it a low digestibility (RS > 90%) [125].

3.4 Conclusion

Our findings clearly demonstrate that polymeric tannins, even at relatively low levels, interact with starch in a way that alter starch properties, and dramatically affect starch digestibility profile. The degree of granule swelling and gelatinization has a big impact on the starch-tannin interactions. Obviously, the interactions are enhanced in amylose-containing starch, due to the more likely strong amylose-tannin interaction

through extensive hydrogen bonding and hydrophobic interactions. It appears that conditions that allow for complete solubilization of tannins (i.e., take advantage of their partition coefficient) can significantly improve the efficiency of their interactions with starch. This study provides a compelling evidence for the potential of natural high molecular weight polyphenols as new ingredients to produce nutritionally beneficial starches. The fate of the tannin-starch complexes *in vivo* and interaction with gut microbiota will be of particular interest.

4. CHARACTERIZING INTERACTIONS INVOLVED IN STABILIZING STARCH-PROANTHOCYANIDIN COMPLEXES

4.1 Introduction

Proanthocyanidins (PA) are capable of binding strongly to food macro-polymers, especially proteins (including digestive enzymes), significantly altering their properties. PA can also bind to starch [15,16], cell wall material [23] and other polysaccharides [75] via non-covalent interactions. A plethora of studies [15,16,111] have shown that high molecular weight PA interact with starch polymers to reduce their digestibility. Barros et al. [15] showed that the high molecular weight PA from sorghum interact with amylose to form resistant starch (RS) in completely gelatinized and dispersed starch (no intact granules). More recently, Amoako and Awika [86] showed that polymeric PA significantly increased crystallinity, pasting temperature, peak viscosity, and slow digesting starch (from 100 to 274 mg/g) in normal, but not waxy starch, suggesting intragranular cross-linking with amylose. Other authors have found limited impact of PA on RS formation in heterogeneous food matrix [17-19], but report significant increase in SDS [19] and reduced glycemic index [17].

Reduced starch digestibility as a result of starch-PA interactions is of particular interest. This is because starch is the major dietary contributor (about two thirds) of calories from carbohydrates, and this implies that strategies that can reduce starch digestibility in foods would greatly benefit efforts to reduce excess caloric intake, and by extension contribute to reducing the burden of obesity and associated health conditions.

It is, however, not clear what specific types of interactions are involved in the formation of these indigestible starch-PA complexes. Available evidence suggests that these interactions may involve extensive hydrogen-bonding, along with hydrophobic interactions, as was demonstrated for other carbohydrates [22,23]. Amoako and Awika [111] and Barros et al. [15] have also suggested the likely involvement of H-bonds in stabilizing starch-PA complexes due to the close proximity and abundance of hydroxyl groups in PA and amylose. There are, however, no studies that have demonstrated the involvement of specific interactions in stabilizing starch-PA complexes.

Indeed, knowledge of specific interactions involved can lead to opportunities to optimize the interactions to develop novel starch processing methods to form less digestible starches. This study is aimed at investigating the specific types of interactions involved in the formation of starch-tannin complexes, and how the interactions impact the levels of slowly digestible starch (SDS) and resistant starch (RS) formed.

4.2 Materials and methods

4.2.1 Proanthocyanidin extraction, purification, and characterization

Proanthocyanidin extract was obtained from high tannin sorghum, as previously described by Amoako and Awika [111]. A portion of this PA extract was purified using the method described by Awika et al. [126] with some modifications. In brief, a sample of the high tannin sorghum extract was dissolved in ethanol (1:3 v/v) and 10 mL of the solution was applied to a Sephadex LH-20 column. The column was washed with 50 mL

of 50% methanol in water to remove low MW phenols, and the PA was recovered with 80 mL of aqueous acetone (70% v/v). The eluents were evaporated to dryness under vacuum at 45 °C in a Rotovapor R-100 (Buchi, USA), and the residue freeze-dried and stored at -20 °C until use.

The PA extract as well as the purified PA extract were profiled for PA content and MW distribution by the normal-phase HPLC-FLD method of Langer et al. [114] using conditions described by Barros et al. [109]. Catechin and procyanidin B1, and C1 were used to quantify monomers, dimers, and trimers, respectively. Quantitative data for PA with a DP greater than or equal to four were based on procyanidin C1 (DP 3) peak response, as previously described by Ojwang et al. [115].

4.2.2 Starch and reagents

Normal (amylose content = 23.9%) and waxy (amylose content = 0.36%) maize starches were obtained from Ingredion Incorporated (Westchester, IL). Potato amylose (95% amylose) and corn amylopectin (>99.9% amylopectin) were obtained from Sigma (St. Louis, MO). All solvents (HPLC or analytical grade) and reagents were obtained from Sigma (St. Louis, MO). Porcine pancreas α-amylase (EC 3.2.1.1) was also purchased from Sigma–Aldrich Chemical Co., Ltd (St. Louis, MO), while D-Glucose (GOPOD format) assay was purchased from Megazyme (Ireland).

4.2.3 Preparation of proanthocyanidins treated starch products

PA treated starch products and their controls were prepared as previously described by Amoako and Awika [86]. PA extract (2.5 g total solids; 121 ± 12 mg PA per gram of extract) from high-tannin sorghum was incubated separately with normal and waxy maize starch (25 g), in 30% and 50% aqueous ethanol solutions (v/v) at 70 °C for 20 min. Samples were then centrifuged (15,000 x *g*, 8 min) to remove the supernatant, and the sediments collected were oven dried at 40 °C overnight to remove residual ethanol and water. The sediments were then gently dispersed with pestle and mortar to obtain powdered samples, which were stored at 4 °C until use. Another treatment was included, replacing the PA extract with cellulose powder (2.5 g) as a control treatment.

4.2.4 Field emission scanning electron microscope (FE-SEM) and scanning electron microscope (SEM) imaging

FE-SEM and SEM imaging was used to observe the effect of starch-PA interactions on the physical structure of enzyme degraded granules. FE-SEM and SEM images of PA treated normal starch and their controls were taken before and after *in-vitro* digestion (described in section 4.2.9).

After the *in-vitro* digestion, the samples were dissolved in 20 mL of 66% ethanol to deactivate the enzyme, and subsequently centrifuged (15,000 x *g*, 8 min) to obtain

sediments. Sediments were then washed twice with 20 mL of water to remove residual enzyme and oven dried overnight at room temperature.

For FE-SEM imaging, dry starch samples were each sprinkled on double-sided adhesive carbon tape mounted on a stainless-steel stub, and coated with a mixture of platinum (80%) and palladium (20%) to a thickness of ~ 5 nm using a sputter coater, 208 HR (Cressington, USA). Coated samples were then observed in a JSM-7500F FE-SEM (JEOL, Japan) at an accelerating voltage of 10 kV. Granule structure observations were made using a secondary electron (SE) detector at magnification range (2000 – 6500 X) and resolution of 1 – 10 µm. Representative starch micro images were taken using an automatic image capture software (PC-SEM).

For SEM, starch samples were each sprinkled on double-sided adhesive tape mounted on an aluminum stub, and coated with a thin gold film using sputter coater Emitech K550X (Quorum Technologies Ltd., UK). Gold coated samples were then observed in a Vega2 microscope (Tescan, Czech Republic) at an accelerating potential of 10 kV. Granule structure observations were made using a secondary electron detector "SE" and an "In Lens" detector, and photographs of starch micro images were taken using an automatic image capture software.

4.2.5 Gel permeation chromatography (GPC)

In order to describe the type of starch polymers and molecular weight sizes, which form indigestible complexes with PA, PA treated normal starch and their controls

were enzyme hydrolyzed and the starch residues remaining were analyzed for molecular weight distribution using gel-permeation chromatography, as described below.

In the enzyme hydrolysis process, each starch sample (0.4 – 1 g) was dissolved in 10 mL of 2 M sodium acetate buffer (pH = 5.9), followed by the addition of 10 mL enzyme mixture of α-amylase (300 U/mg, A3176 Sigma-Aldrich, St. Louis, MO) and amyloglucosidase (95 U/mL, Cat. No. E-AMGDF, Megazyme International). The solution was then incubated at 37 °C for 20 min. At the end of the enzyme hydrolysis, samples were placed in a boiling water bath for 10 min to inactivate the enzymes. The solution was then freeze-dried to obtain partially digested starch powder, and stored at -20 °C until use. Another treatment in which the starch samples were enzyme hydrolyzed for 120 min was included to compare the effect of long digestion time.

The partially hydrolyzed starch samples above were analyzed for their starch molecular size distribution using a GPC method described by Annor et al. [127]. Fifty microliters of 5 M NaOH was added to each starch sample (4 mg) and the sample diluted to 1.5 mL with deionized water. One milliliter of the sample was then applied to a column (1 × 90 cm) of Sepharose CL-6B gel (GE Healthcare, Uppsala, Sweden), and eluted with 0.5 M NaOH at 1 mL/min. Fractions collected (1 mL) were analyzed for carbohydrate content using phenol–sulfuric acid reagent as described by Dubois et al. [128]. A graph of percent (%) carbohydrates against fraction number was then plotted to obtain chromatograms.

The GPC column was calibrated with glucose, maltose, malto-heptaose (Sigma-Aldrich, St. Louis, MO, USA), and larger α-glucans (using debranched waxy barley starch, DWBS). The DWBS was previously analyzed by high-performance anion-exchange chromatography with pulsed amperometric detection (HPAEC-PAD) method described below [129]. A standard curve for the GPC column was obtained by comparing the elution of dextrins from debranched WBS with HPAEC analysis on a weight basis, and the standard curve was extended linearly past the last clearly resolved DP-peak of 60 by HPAEC analysis to cover the remaining volume of the GPC column [129].

4.2.6 Anion-exchange chromatography-pulsed amperometric detection (HPAEC-PAD)

The low molecular weight sugars and oligomers in the partially hydrolyzed starch samples above were analyzed by HPAEC-PAD, as described by Wikman et al. [130]. Fifty microliters of 5M NaOH was added to 4 mg of each starch sample (partially enzyme hydrolyzed starch samples above) and then diluted to 1.5 mL with deionized water. The samples were then filtered and injected (25 μL) onto a CarboPac PA-100 column and eluted at 1 mL/min flow rate. The mobile phase consisted of eluent A (150 mM NaOH) and eluent B (150 mM NaOH containing 1M NaOAc). The 110 min elution gradient for (B) was as follows: 0–9 min from 7 to 18%; 9–18 min from 18 to 22%; and 18–110 min from 22 to 50%. The PAD response was adjusted to carbohydrate contents, as described by Koch et al. [131]. DWBS was used as standard to assign DP for linear

dextrins, and it was assumed that branched dextrins of certain DP was eluted in front of linear dextrins of corresponding DP [132]. Dextrins with DP > 35, which are not resolved as peaks were quantitatively approximated by a continuous area division of the chromatograms [130].

4.2.7 The role of hydrogen bonds and hydrophobic interactions in stabilizing starch-proanthocyanidins complexes

To determine the relative contribution of H-bonding and hydrophobic interactions in the formation of starch-PA complexes, samples of the starch-PA complexes prepared previously were each incubated separately with urea and 1,4-dioxane, which disrupts H-bonds and hydrophobic interactions, respectively; to release the PA from the complexes.

Each sample (400 mg) was incubated with 5 mL of 2-6 M urea and 10–15% 1,4-dioxane at room temperature with horizontal shaking in a reciprocating shaker set at low speed (160 cycles / min). The sediments were rinsed three times (by gentle vortexing), each time with 5 mL of water, to remove residual solvents. The sediments were subjected to *in-vitro* digestion. The supernatants collected after the solvent incubation and water rinses were combined and profiled for PA content and MW distribution using normal-phase HPLC-FLD described in section 4.2.1.

Urea is a chaotropic agent; its structure consists of an amide with two $–NH_2$ groups joined by a carbonyl (C=O) functional group. This structure allows it to act as

both a proton donor and acceptor, enabling it to participate in the formation of strong hydrogen bonds [133,134]. It is also an effective solvent for dissociating H-bonds between complexed molecules. 1,4-Dioxane on the other hand possesses a heterocyclic structure that allows it to disrupt hydrophobic interactions between molecules.

To further elucidate the relative contribution of H-bonding in starch-PA complexation, starch samples were treated with purified PA extracts in deuterated solvents that limit H-bonding between starch and PA.

In this procedure, 1 g of purified PA extract was incubated separately with 25 g of normal maize starch, waxy maize starch, potato amylose and corn amylopectin in 30% and 50% solutions of deuterated ethanol (C_2H_5OD) in deuterated water (D_2O) at 70 °C for 20 min. The deuterated ethanol solution made up a total volume of 75 mL. Samples were then centrifuged (15,000 x *g*, 8 min), the supernatants collected, and the sediments oven dried at 40 °C overnight to remove residual solution. The sediments were gently dispersed with pestle and mortar to obtain powdered samples, which were stored at 4 °C until use. For the control set, the deuterated water (D_2O) and ethanol (C_2H_5OD) were replaced with regular water and ethanol respectively. Another sample set in which PA is excluded from the reaction was prepared. Dry powders of all sets of starch samples were also analyzed for starch properties (swelling, pasting, crystallinity) described in section 4.2.8 below.

The deuterium in deuterated water and ethanol causes more restricted atomic vibrations in their molecular structure (compared to the H), which reduce the negative

effect of its van der Waals repulsive core in the molecules, thereby increasing its overall hydrogen bond energy and strength [135,136]. Thus, deuterium is able to form H-bonds, which are about 20% stronger than that formed by H [137]. In our experiment, the deuterium from the ethanol and water will exchange D for H with accessible hydroxyl groups on the starch and PA molecules and strengthen starch-starch and PA-PA bonding, thereby limiting H-bond formation between PA and starch [137].

4.2.8 Amylose – iodine complexation

To better understand the nature of hydrophobic interactions between amylose and PA, PA-treated amylose samples and controls were each complexed with iodine, and UV-VIS spectra was obtained to observe the change in maximum wavelength. Iodine forms an inclusion complex with amylose by occupying the hydrophobic amylose helical core. The availability of the free space in the hydrophobic core is confirmed by the successful formation of an amylose-iodine inclusion complex observed at a peak maximum of 625 nm on a UV-VIS spectrum. Peak maxima of amylose-iodine inclusion complex will be affected by the extent of helix occupation by PA.

Amylose-iodine complexation was carried out using a procedure previously described by Baks et al. [116] with some modifications. Amylose samples (0.02 g) were each dissolved in 25 ml of 0.15 M KOH and the solution was mixed for 30 min. The resulting solution was then centrifuged (16,600 x *g*, 10 min) to remove the insoluble part of the sample. An aliquot of the supernatant (1 mL) was taken and neutralized with 9 mL

of 0.017 M HCl. Subsequently, 0.1 ml iodine reagent (5 g iodine and 10 g potassium iodide in 100 ml water) was added to form a complex with the amylose present in the sample. The final solution was then scanned from 250 to 800 nm using a UV-VIS spectrophotometer (UV-2450, Shimadzu, Japan).

4.2.9 Starch physicochemical properties

Starch solubility (%S) and swelling power (SP), pasting behavior, and crystallinity were analyzed following procedures and methods previously described by Amoako and Awika [86].

4.2.10 Starch thermal properties

The thermal properties were measured using a Differential Scanning Calorimeter (TA Instruments DSC Q2000, New Castle, USA). The calorimeter was calibrated with indium, and the DSC runs were operated under ultra-high purity nitrogen (30 mL/min) using a sealed empty aluminum pan as reference. Samples of interest (3 mg, db) were each weighed into an aluminum pan, and distilled water added to get to 12 mg total weight (1:3 starch:water ratio, w/w). The pan was then hermetically sealed and equilibrated at room temperature for at least two hours to allow adequate starch hydration. Samples were then heated from 40 °C to 180 °C at a rate of 10 °C/min. The raw data was processed with DSC software (TA Instruments) to obtain onset (T_o), peak (T_p), and conclusion (T_c) temperatures and gelatinization enthalpies (ΔH).

4.2.11 In-vitro *starch digestibility*

In-vitro digestibility of samples was measured, as previously described by Englyst et al. (2000). In summary, the starch treatments (400 mg) were digested by α-amylase (300 U/mg, A3176 Sigma-Aldrich, St. Louis, MO) and amyloglucosidase (95 U/mL, Cat. No. E-AMGDF, Megazyme International) mixture. Glucose released after 20 and 120 min was determined by reacting an aliquot with glucose oxidase reagent (K-GLUC GOPOD format assay kit, Megazyme, Ireland) and the absorbance at 510 nm was read on a UV−vis spectrophotometer (Shimadzu Scientific Instruments) using a glucose standard assay kit (K-GLUC GOPOD format assay kit, Megazyme, Ireland). The content of the hydrolyzed starch was calculated by multiplying a factor of 0.9 by the glucose content. The percentage of SDS (%) in the products was obtained by the following equation: SDS% = [(G120 – G20) X 0.9/ TS] X 100; where, G_{20} and G_{120} are glucose content released after 20 and 120 min, respectively; and TS is the weight of starch in the sample used for each test. Results were expressed on db.

4.2.12 Statistical analysis

Data was analyzed using a one-way analysis of variance (ANOVA) to determine significant differences among treatments. Tukey's HSD ($P \leq 0.05$) was used to separate means. The statistical software SAS version 9.4 for windows was used. All tests were replicated at least twice.

4.3 Results and discussion

4.3.1 Phenolic profile of proanthocyanidins extract and purified proanthocyandins extract

The sorghum PA extract contained 121 ± 12 mg PA per g. More than 99% of this was made up of polymeric PA (DP > 3) (Figure 2). Purified PA extract contained 251.4 ± 2.5 mg PA / g of extract. The PA profile is consistent with that reported previously by Barros et al. [15,16].

4.3.2 Changes in starch granules morphology after in-vitro digestion

As previously discussed (section 3.3.5), treatment of starch with PA forms complexes that limit the action of digestive enzymes. Treatment of normal starch with PA extract in 30E solution increased SDS from 96.7 mg/g to 274 mg/g and RS from 148 mg/g to 299 mg/g. PA treated 50E normal starch was almost non-digestible with approximately 90% RS (Figure 3). These digestibility profiles were confirmed by the morphological features of starch granules observed (via FE-SEM and SEM imaging) after *in-vitro* digestion.

Comparison of FE-SEM images of starch treatments (post *in-vitro* digestion) shows clear differences between PA treated starches and controls (Figure 4 and Figure 5). Starches treated with PA did not show marked differences in their granule appearance before and after *in-vitro* digestion, showing few visible signs of enzyme

degradation. Control samples however showed more pronounced signs of enzyme action. Control starches treated in 30E solutions showed signs that enzyme action had occurred from within the granule (Figure 4); whereas 50E samples showed enzyme action occurred primarily from the exterior, seen as crevices and pits on the granule surface.

Considering the fact that starches treated in 30E solutions underwent near complete gelatinization, their granules showed visible signs of granule rupturing (Figure 4). On the other hand, 50E treatment starches showed minimal or no signs of rupturing because of their limited gelatinization (Figure 5). The difference in degree of starch gelatinization influenced the enzyme degradation pattern of 30E and 50E control starches. In 50E PA treatments; it appears the PA blocked the granule surface pores (where enzyme action on non-gelatinized starch is initiated) to limit enzyme access to the starch granules. The resulting pits formed after enzyme hydrolysis, thus appeared much smaller and less visible. These observations suggest PA interaction with gelatinized starch likely limits enzyme degradation within granule, whereas interactions with intact starch granules block enzyme at the granule surface.

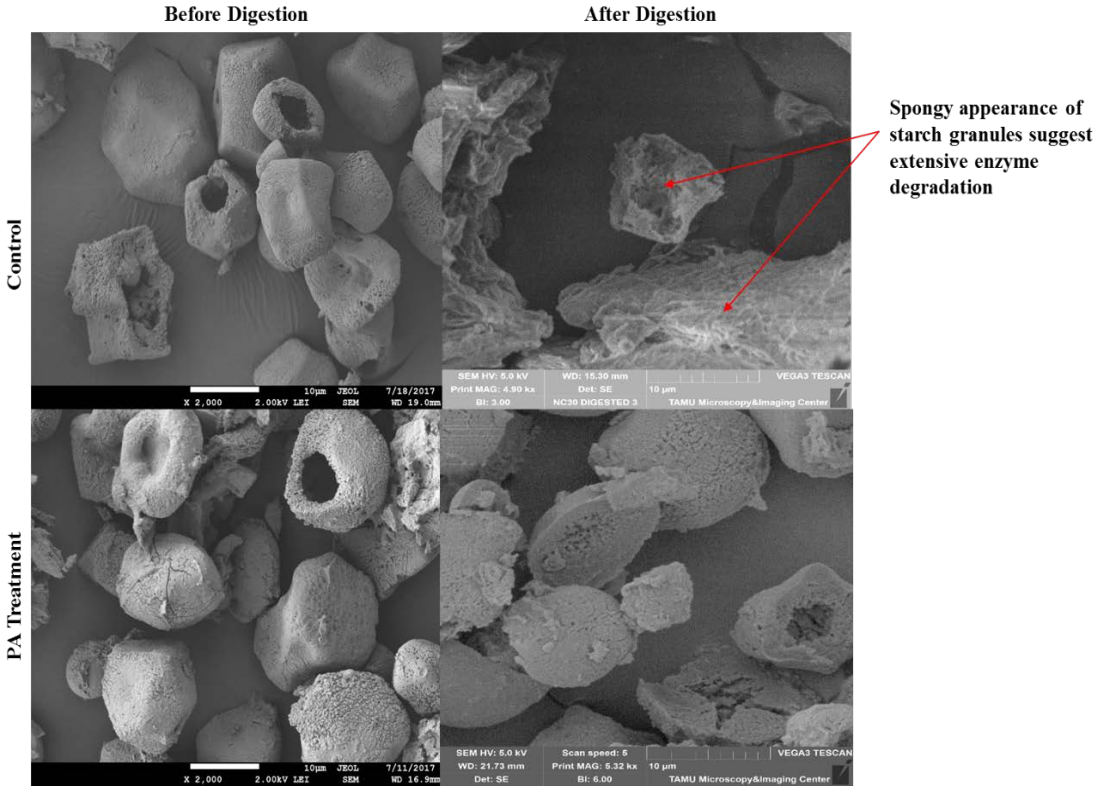

Figure 4 Field emission scanning electron microscopy (FE-SEM) and scanning electron microscopy (SEM) images of normal starch treated with proanthocyanidins extract in 30% ethanol solution, and their controls, before and after in-vitro digestion for 2 h. Starch products were previously prepared by incubating normal maize starch with proanthocyanidins extract in 30% (30E) aqueous ethanol solution at 70 °C / 20 min.

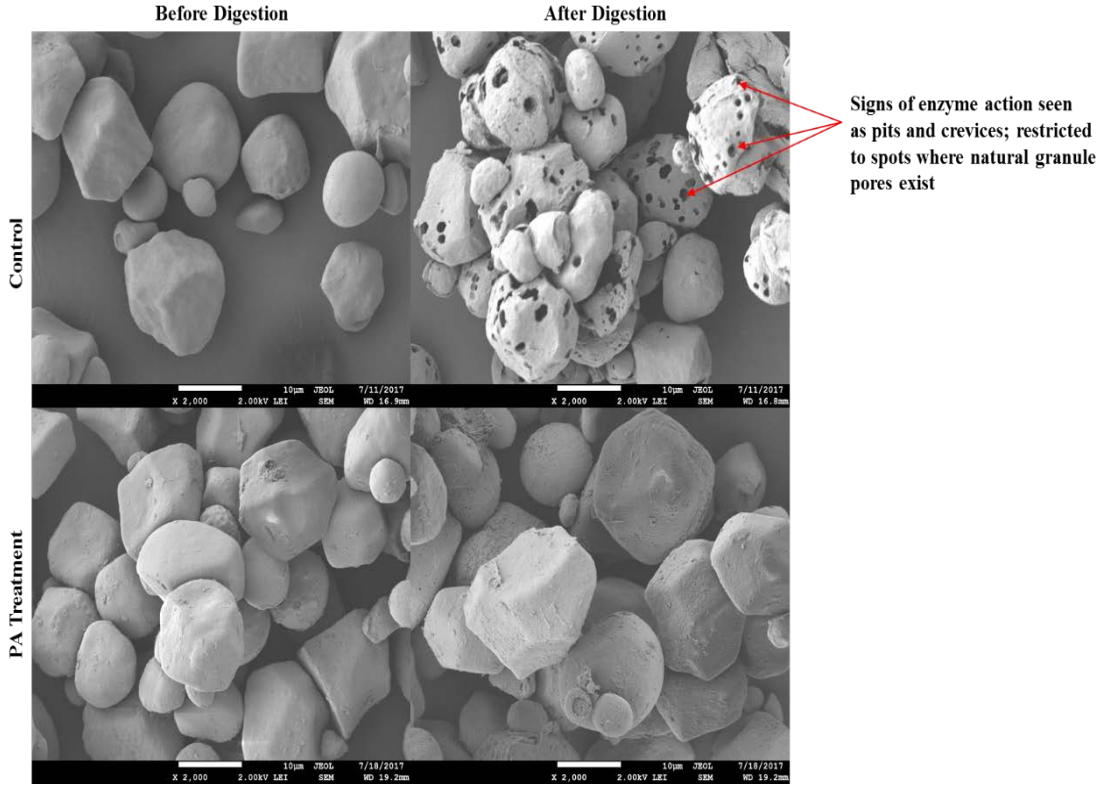

Figure 5 Field emission scanning electron microscopy (FE-SEM) images of normal starch treated with proanthocyanidins extract in 50% ethanol solution, and their controls, before and after in-vitro digestion for 2 h. Starch products were previously prepared by incubating normal maize starch with proanthocyanidins extract in 50% (50E) aqueous ethanol solution at 70 °C / 20 min.

4.3.3 Molecular size distribution of partially hydrolyzed starch samples

Figure 6 and Figure 7 show the molecular weight (MW) distribution of PA-treated normal starches, digested for 20 min (short digestion time) and 120 min (long digestion time), compared to their controls. Before enzyme digestion, PA treated starch and controls (non-PA treatment) possessed similar MW distribution (Table 6).

In 30E control samples, 20 min digestion resulted in a drastic reduction in the proportion of large MW starch (DP $\sim \geq 78.8 \times 10^4$), from 82% to 4%, with a concomitant increase in proportion of low MW starch (DP $\sim \leq 0.6 \times 10^4$) from 6% to 90% (Table 6). Corresponding 30E PA-treated starch, showed a less drastic reduction in proportion of large MW starch (91% to 34%) and smaller increase in low MW starch proportion (0% to 54%), compared to control. Thus, PA formed complexes with large MW starch molecules and limited the hydrolysis of the starch into sugars and low MW dextrins. This observation confirms what was previously observed in Chapter 3, section 3.3.5, in which *in-vitro* digestion of control starch resulted in the formation of higher levels of RDS (starch hydrolyzed to glucose after 20 min of digestion) compared to PA-treated starch.

Changes in the MW profile of 30E starch treatments digested for 120 min were similar to 20 min digestion, though changes were more drastic at 120 min. After 120 min of digestion, control samples had no large and medium MW starch left; all starch molecules (100%) were of low MW sizes (DP $\sim \leq 0.6 \times 10^4$) (Table 6). In corresponding PA-treated starch however, the proportion of low and medium MW starch after 120 min of digestion, were 16% and 18%, respectively.

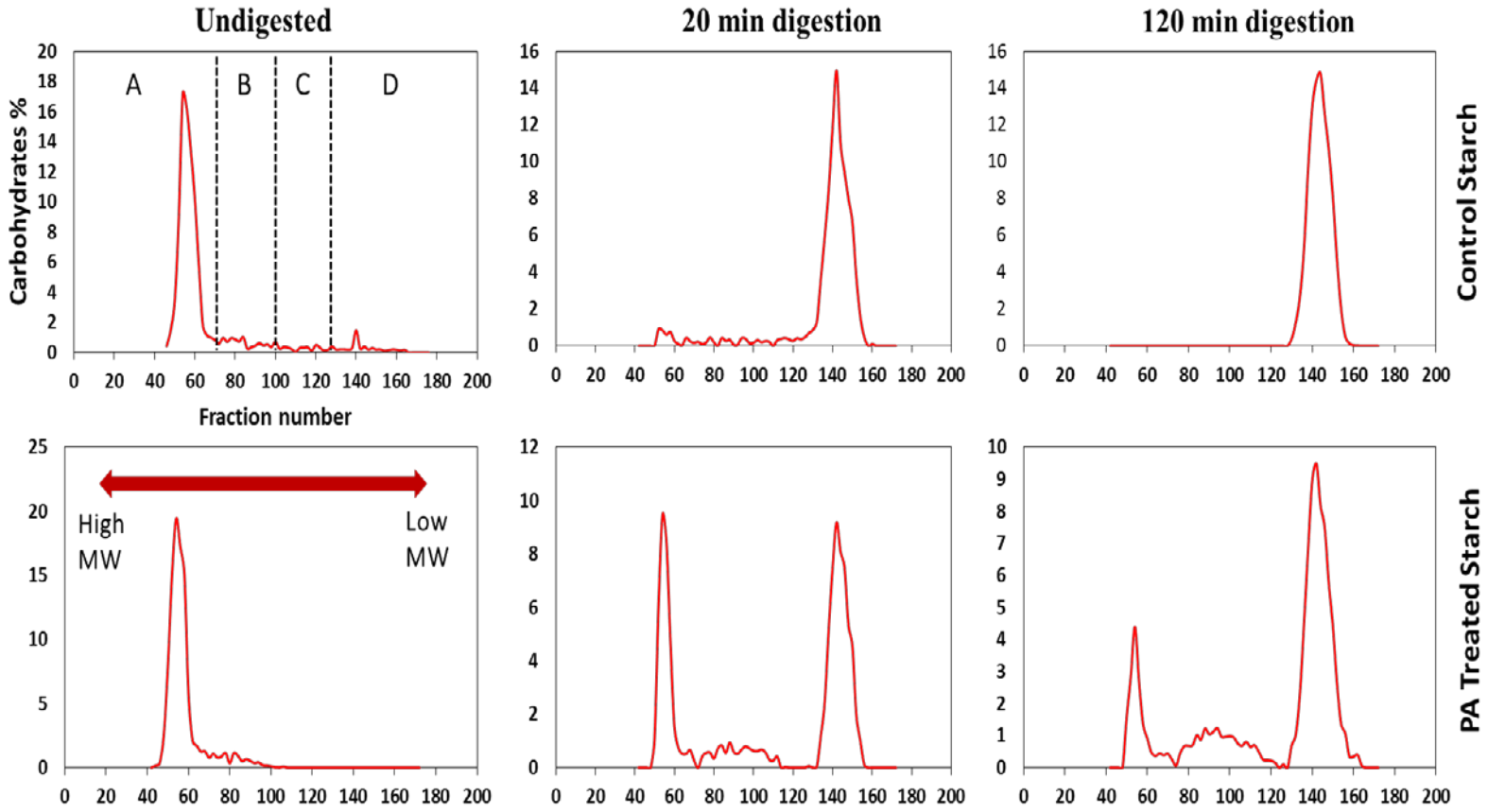

Figure 6 Molecular weight distribution of normal starch-proanthocyanidins complex prepared in 30% ethanol and their controls, before and after 20 min and 120 min of *in-vitro* digestion. Starch products were previously prepared by incubating normal maize starch with proanthocyanidins extract in 30% (30E) aqueous ethanol solution at 70 °C / 20 min. Regions labels A, B, C and D represent degree of polymerization (DP) ranges of > 78.8 X 10^4, 21.2 – 2.3 X 10^4, 2.3 – 0.6 X 10^4, and <0.6 X 10^4 respectively.

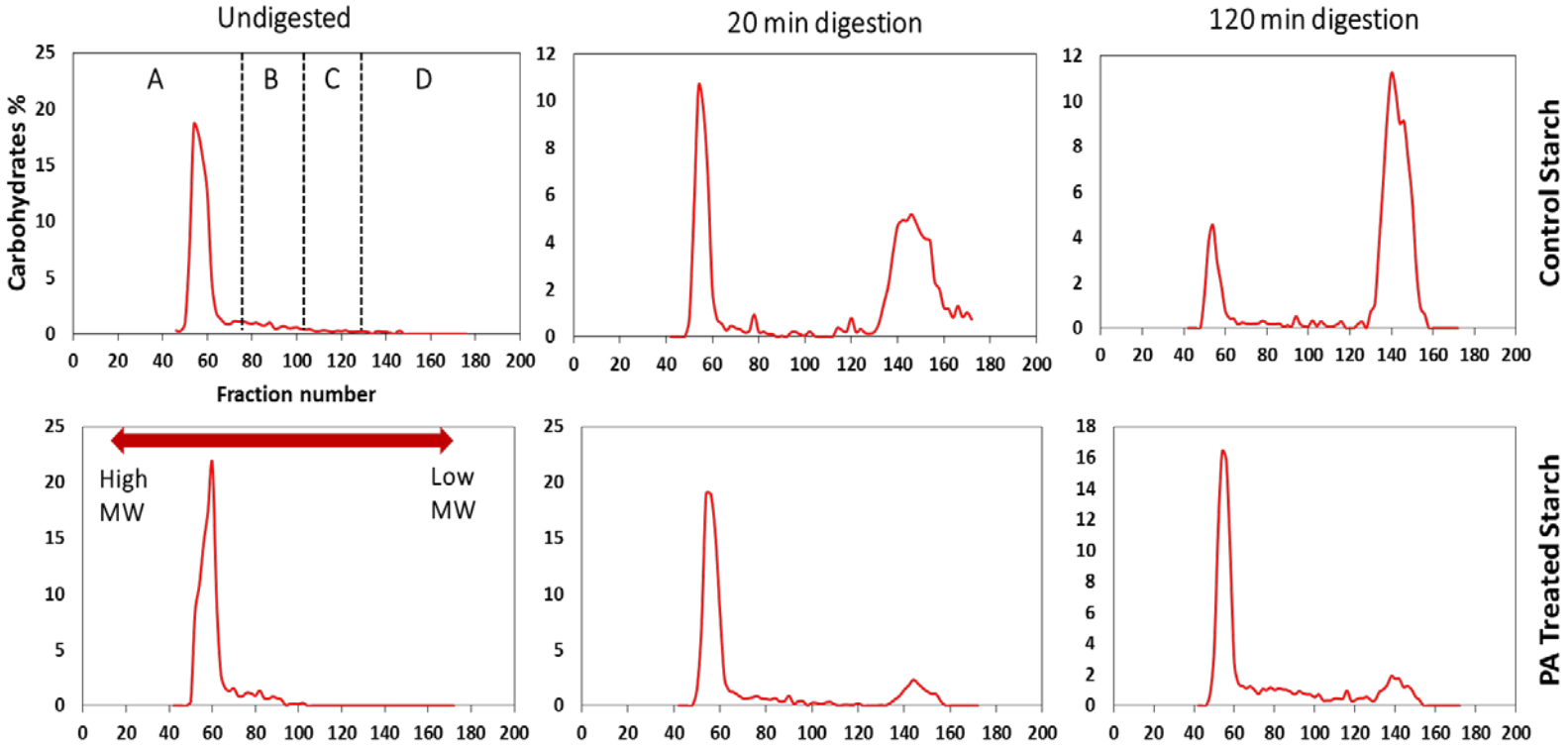

Figure 7 Molecular weight distribution of normal starch-proanthocyanidins complex prepared in 50% ethanol and their controls, before and after 20 min and 120 min of *in-vitro* digestion. Starch products were previously prepared by incubating normal maize starch with proanthocyanidins extract in 50% (50E) aqueous ethanol solution at 70 °C / 20 min. Regions labels A, B, C and D represent degree of polymerization (DP) ranges of > 78.8 X 10^4, 21.2 – 2.3 X 10^4, 2.3 – 0.6 X 10^4, and <0.6 X 10^4 respectively.

Table 6 Relative molar composition (%) of proanthocyanidins-treated starch and controls before and after *in-vitro* digestion.

Treatment	Relative molar composition (%)		
	High molecular weight (DP~ ≥ 78.8 x 10^4)	Medium molecular weight (DP~ 21.2 – 0.6 x 10^4)	Low molecular weight (DP~ ≤ 0.6 x 10^4)
Undigested			
30% ethanol treatment			
Non-PA control	82^{b}	12^{c}	6^{g}
PA treatment	91^{a}	9^{cd}	0^{h}
50% ethanol treatment			
Non-PA control	84^{b}	14^{bc}	2^{h}
PA treatment	90^{a}	10^{d}	0^{h}
20 min digestion			
30% ethanol treatment			
Non-PA control	4^{g}	6^{e}	90^{b}
PA treatment	34^{e}	12^{d}	54^{e}
50% ethanol treatment			
Non-PA control	38^{e}	4^{e}	58^{d}
PA treatment	77^{c}	8^{de}	15^{f}
120 min digestion			
30% ethanol treatment			
Non-PA control	0^{g}	0^{f}	100^{a}
PA treatment	16^{f}	18^{a}	66^{d}
50% ethanol treatment			
Non-PA control	17^{f}	4^{e}	79^{c}
PA treatment	67^{d}	17^{a}	16^{f}

This observation is supported by data previously described in Chapter 3, section 3.3.5, in which ~85% of the control starch was hydrolyzed into glucose after 120 min of digestion (RDS + SDS), while only ~67% of PA-treated starch was hydrolyzed.

In PA-treated 50E starch, the proportion of medium and high MW starch retained after 20 min of digestion (medium MW = 8%, large MW = 77%) were significantly higher than control (medium MW = 4%, large MW = 38%). This difference in MW profile between PA-treated starch and control was also observed in starches digested for 120 min. After 120 min of digestion, 50E PA-treated starch contained 67% of large MW starch, 17% medium MW starch, and 16% of low MW starch. Corresponding control sample contained 17% of large MW starch, 4% medium MW starch, and 79% of low MW starch.

50E PA-treated starch retained most of the large MW starch ($DP\sim \geq 78.8 \times 10^4$) after 20 min and 120 min of digestion (20 mins = 77%, 120 min = 67%) compared to 30E PA-treated starch (20 mins = 34%, 120 min = 31%). This significant retention of large MW starch in PA-treated 50E starch, suggests that PA interaction with minimally gelatinized starch severely restricted starch hydrolysis. This observation is confirmed by FE-SEM / SEM images, where granules of PA-treated 50E starch looked intact after 120 min of *in-vitro* digestion (Figure 5) whereas 30E treatment showed signs of significant granule degradation (Figure 4). Other confirmatory evidence, is the higher level of RS (860 mg / g of starch) present in 50E PA-treated starch compared to 30E PA-treated starch (299 mg / g of starch) (Figure 3).

4.3.4 Effect of hydrophobic and hydrogen bond disruptors on proanthocyanidins release from starch-proanthocyanidins complexes

In gelatinized starch (30E treatments), disruption of H-bonds in normal starch–PA complexes with urea released virtually all of the PA bound in the complex (Table 7). For corresponding 30E waxy starch treatment, urea released (~90%) of PA bound in the complex. The significant levels of PA released into solution after H-bond disruption suggest H-bonds play a major role in stabilizing starch-PA complexes in gelatinized starch. Other studies have shown that washing PA-cell wall complexes with 8 M urea resulted in total re-extraction of the PA; and the authors concluded that the adsorption mechanism was H-bond dominated [103,138].

In slightly gelatinized starch (50E treatment), disruption of hydrogen bonds released ~25% of the PA bound in the normal starch-PA complex. A similar amount (~31%) was released from 50E waxy starch-PA complex after urea incubation (Table 7). This suggests that Hydrogen bonding may play a less dominant role in stabilizing starch-PA complexes in intact/ slightly gelatinized starch granules than the fully gelatinized starch.

By disrupting hydrophobic interactions in 30E normal starch–PA complex with 1,4-dioxane, ~67% of the PA bound in the complex was released, whereas in the 30E waxy starch-PA complex, ~93% of PA was released from the complex (Table 7). The significant amounts of PA released from the complex after incubation of 30E starch-PA complexes in dioxane suggest that hydrophobic interactions also contribute to the stabilization of the 30E starch-PA complex. Cai et al. [139] suggested that, in addition to

H-bonds, hydrophobic interactions involving a partial inclusion of one of the aromatic rings of the PA into the hydrophobic interior of amylose are likely to contribute to amylose-PA complexation. This may be true in our case for 30E normal starch – PA complex, where amylose molecules released into solution after starch gelatinization can partially include the C-ring on oligomeric PA in amylose hydrophobic helical core.

In 50E normal starch treatment, disruption of hydrophobic interactions in complex with 1,4-dioxane released ~39% of the PA bound in the complex, whereas in 50E waxy starch-PA complex, ~42% of PA was released from the complex. Considering the fact that dioxane released higher amounts of PA (36 – 42%) from starch-PA complexes than urea (25 – 31%), hydrophobic interactions may play a more significant role in stabilizing starch-PA complexes in intact starch granules compared to H-bonds.

Table 7 Amount of proanthocyanidins released from starch-proanthocyanidins complexes after incubation with urea and 1,4-dioxane.

Sample	PA bound in complex before incubation in solvent (mg PA / g of starch)	Solvent used	PA removed from complex	
			mg PA / g of starch	Percent (%)
30E Normal starch PA treatment	6.47 ± 0.62[a]	6M Urea	6.69. ± 1.42[a]	100
		15% Dioxane	4.32 ± 0.15[b]	67
50E Normal starch PA treatment	3.47 ± 0.70[b]	6M Urea	0.87 ± 0.09[d]	25
		15% Dioxane	1.34 ± 0.19[c]	39
30E Waxy starch PA treatment	5.94 ± 0.80[ab]	6M Urea	5.35. ± 0.45[a]	90
		15% Dioxane	5.52 ± 0.69[a]	93
50E Waxy starch PA treatment	3.44 ± 0.45[b]	6M Urea	1.06 ± 0.04[d]	31
		15% Dioxane	1.45 ± 0.21[c]	42

4.3.5 Involvement of hydrogen bonds in stabilizing starch-proanthocyanidins complexes in gelatinized starch

Urea has a plasticizing effect on starch [140,141], which may result in overestimation of RDS and SDS of starch after incubation. The changes in starch digestibility of urea treated PA-starch complexes were therefore corrected for using the *in-vitro* digestion data of corresponding non-PA treated controls.

Incubation of 30E normal starch-PA complexes with 6 M urea resulted in a significant reduction in SDS (from 293 to 185 mg/g) and RS (from 375 – 227 mg/g), with a concomitant increase in RDS (from 293 – 593 mg/g) (Figure 8). Thus, the less digestible 30E normal starch- PA complex became readily digestible (RDS increased from 29.3% to 59.3%) after urea treatment. This suggests that H-bonds are involved in stabilizing 30E normal starch-PA complexes. Considering the fact that the starch granules in this treatment swelled and were near fully gelatinized, interaction between the starch and PA likely occurred in the internal structure of the granule where the availability of hydroxyl groups on both molecules (starch and PA) favored the formation of H-bonds. Like other carbohydrates, the steric 'compatibility' of the linear amylose chains with the polymeric PA allowed for H-bond interactions between starch and PA via the abundant –OH groups in close proximity [75,103].

By disrupting the H-bonds in 30E waxy starch-PA complexes, small but significant changes in RDS (increased from 48.6% to 56%) and RS (reduced from 36% to 22.1%) were observed. The mismatch in the large amount of PA released (~90%)

from waxy starch-PA complex and the corresponding minimal changes in starch digestibility suggest that H-bonding may have played a minor role in stabilizing 30E waxy starch-PA complexes. The interaction mechanism may have largely comprised a physical entrapment of the PA in the highly branched starch polymer matrix (of waxy starch) stabilized by H-bonding via the –OH groups on amylopectin and PA in regions where PA was in close proximity with long linear portions of the amylopectin (chain A). Barros et al. [15,16] has previously suggested that amylopectin has a poor binding affinity to PA. Waxy starch-PA interactions in gelatinized starch may therefore not involve extensive H-bonding.

In deuterated 30E PA-treated normal starch where H-bonding was restricted during the starch-PA complex formation, the starch formed significantly less RS (34% less) and SDS (57% less) compared to non-deuterated controls (Figure 9).

In a corresponding 30E treatment in which pure amylose was used (Figure 10), deuterated solvent treatment decreased RS by 25% (compared to non-deuterated controls), with a concomitant 3-fold increase in SDS. The consistent decrease in RS in both treatments suggests that restricting H-bond formation significantly reduces the extent of starch-PA complex formation. It seems that RS formation in amylose rich matrices, as well as in gelatinized normal starch, is significantly driven by H-bond formation. The availability of amylose that can engage in H-bonding with PA via the hydroxyl groups on both polymers is key to stabilizing starch-PA complexes in gelatinized starch.

Restricting hydrogen bond formation in 30E waxy starch treatment with deuterated solvents, resulted in 78% decrease in SDS, with corresponding increase in RDS. RS was not affected (Figure 9 B). Similarly, deuterated 30E amylopectin treatment showed 45% decrease in SDS, while RS decreased slightly (by 9%) (Figure 10 B). The fact that restriction of hydrogen bond formation between waxy starch and PA, as well as amylopectin and PA had insignificant effect on RS further confirms that hydrogen bonds are not the dominant interactions that stabilize waxy starch-PA complexes.

Evidence generally suggests that strong H-bonding occurs between amylose and PA to increase RS, whereas H-bonding occurring between amylopectin and PA are weak and result in the formation of SDS.

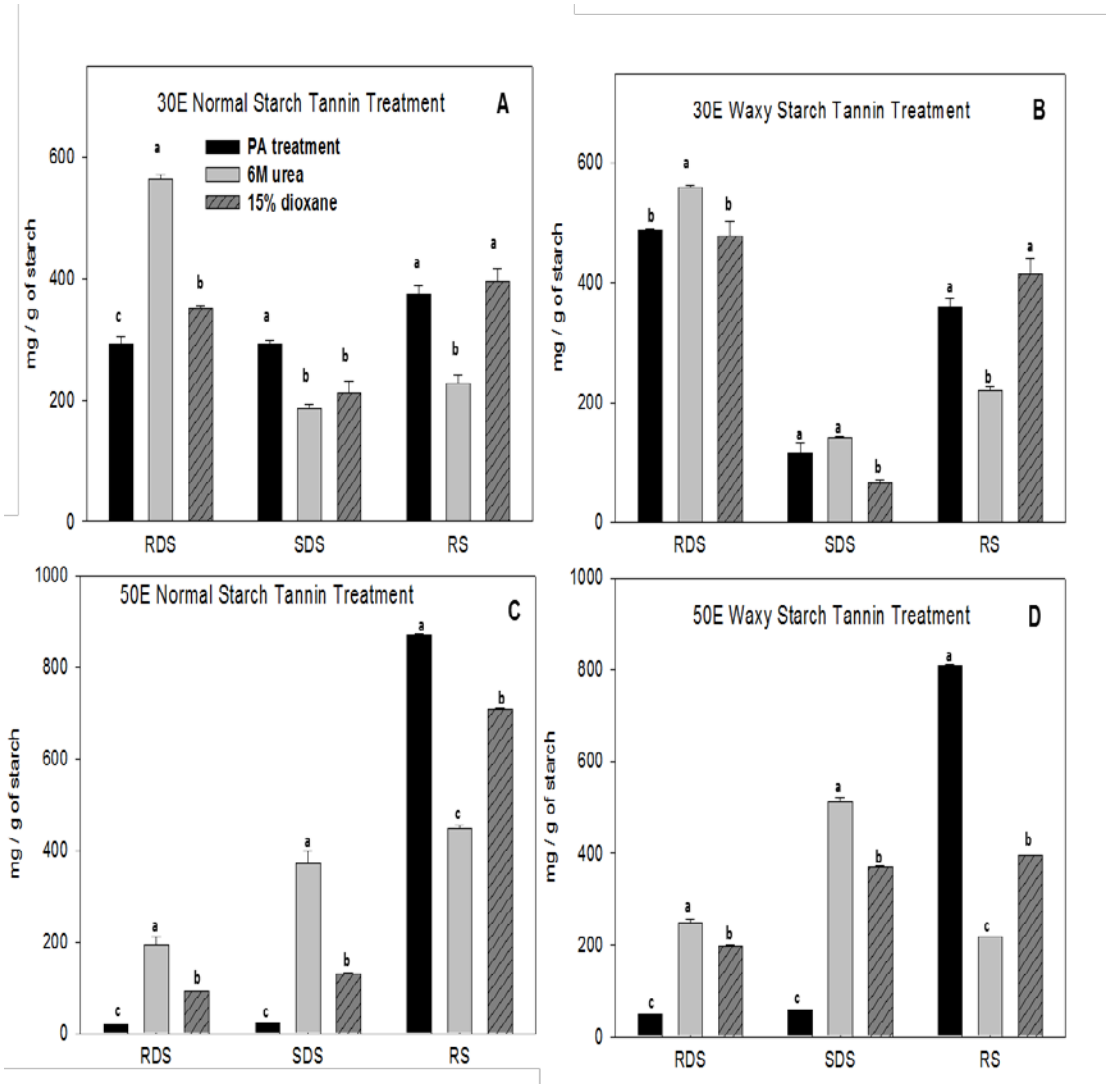

Figure 8 Effect of incubation of starch-proanthocyanidins complexes with 6 M urea and 15% 1,4-dioxane (24 °C / 30 min) on *in-vitro* starch digestibility. Complexes were previously formed by incubation of normal and waxy starch separately with proanthocyanidins in 30% (30E) and 50% (50E) aqueous ethanol solution. RDS, SDS, and RS represent rapidly digesting, slow digesting, and resistant starch, respectively. Error bars indicate ± standard deviation. Same alphabet within starch digestibility types are not significantly different ($P \leq 0.05$).

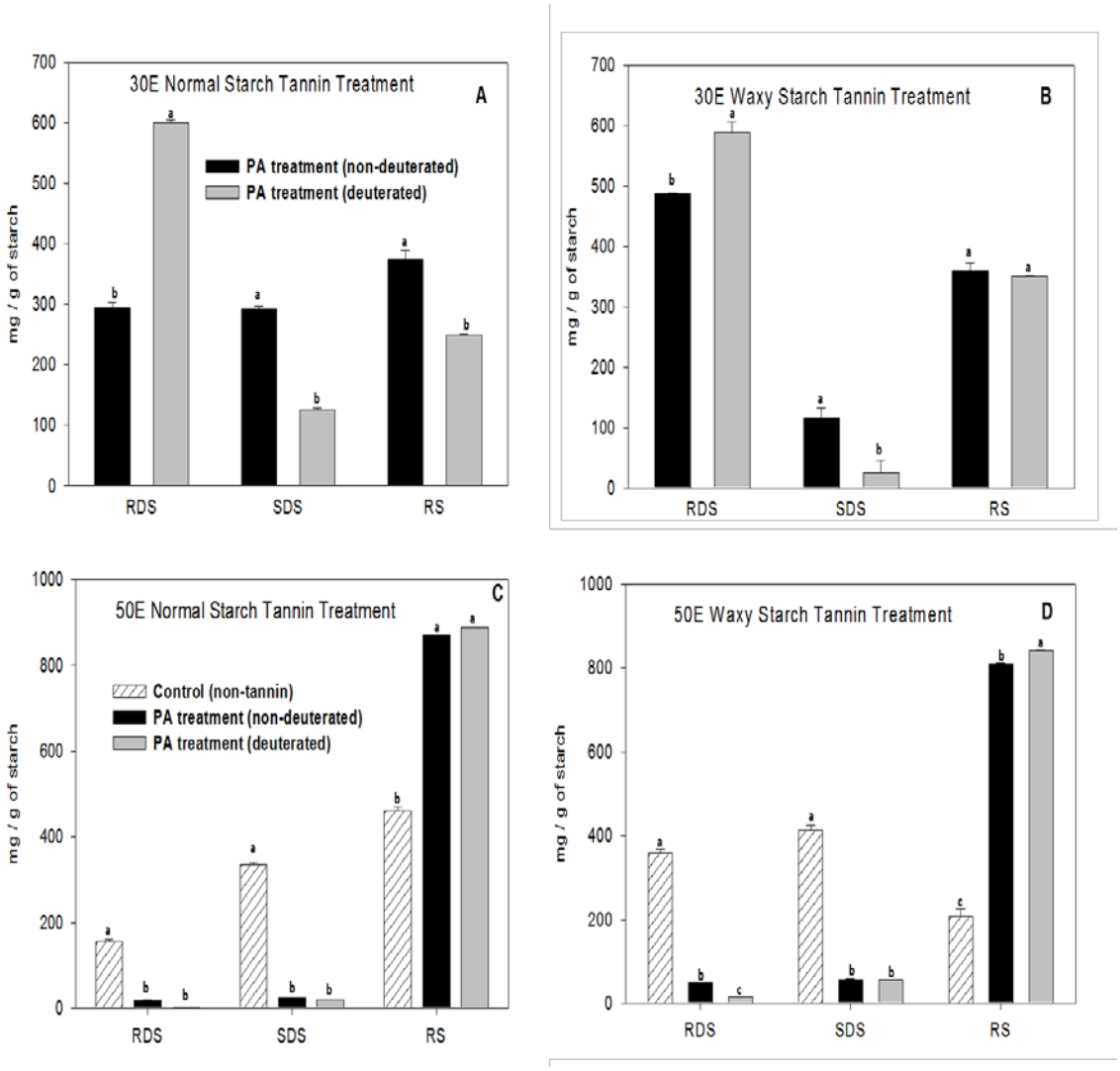

Figure 9 Effect of deuterated solvents on the *in-vitro* digestibility of partially gelatinized normal and waxy maize starch-proanthocyanidins complexes. Complexes were prepared by incubation of starch with proanthocyanidins extract in 30% (30E) and 50% (50E) deuterated ethanol/water solutions at 70 °C / 20 min. RDS, SDS, and RS represent rapidly digesting, slow digesting, and resistant starch, respectively. Controls represent corresponding treatment in which PA is replaced with cellulose. Error bars indicate ± standard deviation. Same alphabet within starch digestibility types are not significantly different ($P \leq 0.05$).

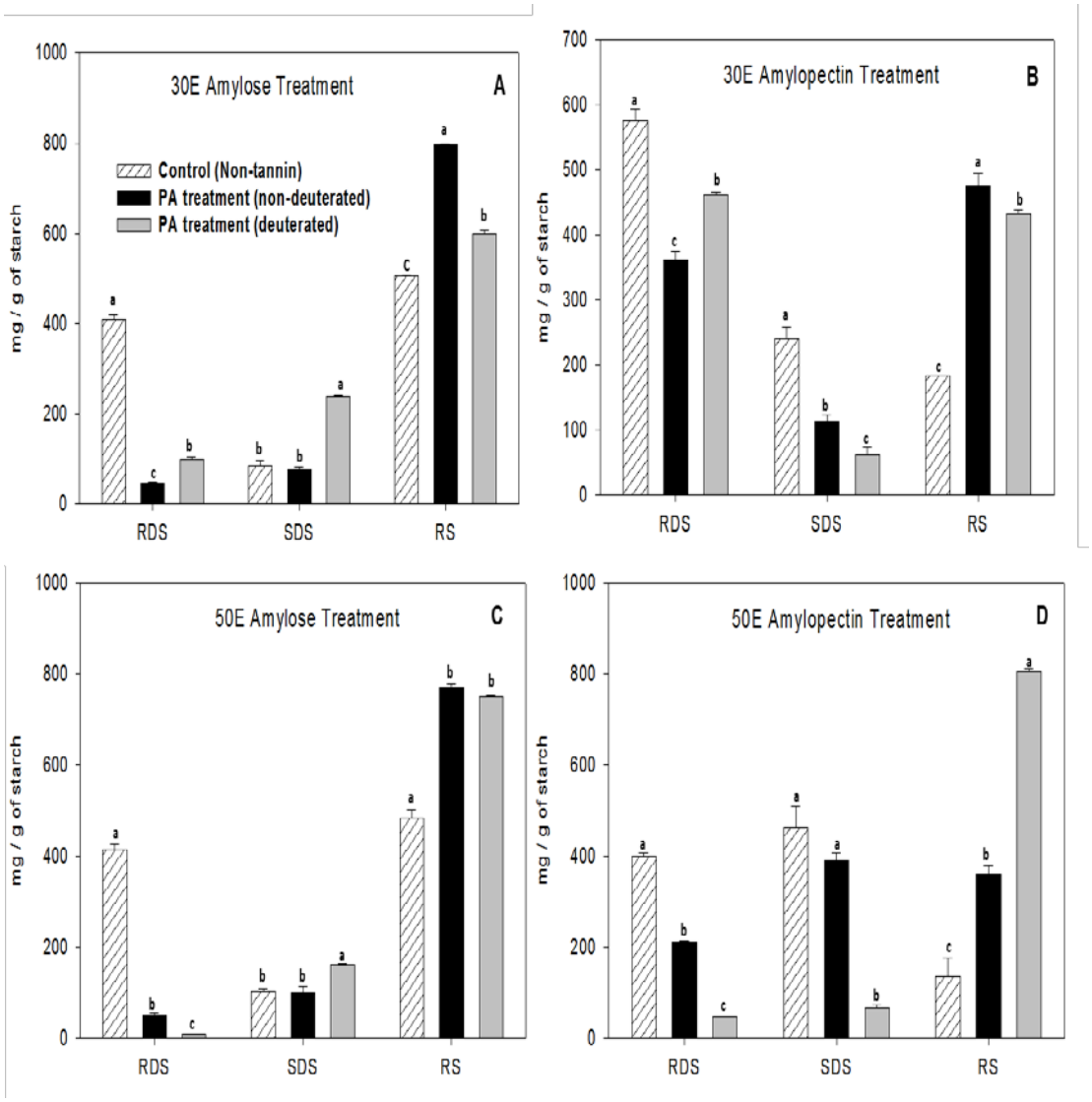

Figure 10 Effect of deuterated solvents on the *in-vitro* digestibility of proanthocyanidins complexed amylose and amylopectin. Complexes were prepared by incubation of corn amylopectin and potato amylose separately with purified proanthocyanidins extract in 30% (30E) and 50% (50E) deuterated ethanol solutions at 70 °C / 20 min. RDS, SDS, and RS represent rapidly digesting, slow digesting, and resistant starch, respectively. Controls represent corresponding treatment without PA. Error bars indicate ± standard deviation. Same alphabet within starch digestibility types are not significantly different ($P \leq 0.05$).

4.3.6 Involvement of hydrogen bonds in stabilizing starch-proanthocyanidins complexes in minimally gelatinized starch

Unlike 30E treatments, 50E treatments underwent minimal starch swelling / gelatinization, with most of their starch granules remaining intact (Figure 4 and Figure 5); hence interaction mechanisms between the intact granules and PA were expected to be different. Disruption of H-bonds between 50E normal starch and PA reduced RS by ~49% with an increase in SDS (15.5 fold) and RDS (10 fold) (Figure 8). A similar trend was observed in 50E waxy treatment; RS decreased by 75% and SDS and RDS increased 21-fold and 13-fold, respectively. These drastic changes in digestibility profile suggest H-bonds play an important role in stabilizing starch-PA complexes in intact starch granules.

Considering the fact that intact or minimally gelatinized starch granules have majority of their amylose and amylopectin polymers packed into a tight ordered structure, the –OH groups on the starch polymers may be unavailable to engage in significant H-bonding with the PA in its environment. More so, the digestion pattern observed in FE-SEM images (Figure 5) seem to suggest that starch-PA interactions in intact granules (50E treatments) block enzyme access to the granule pores, where enzyme action on intact granules is initiated. This made the digestion of the PA-starch complexes similar to raw tuber starches (such as potato starch) that lack surface pores (Figure 3). Most likely, H-bonding offered additional stabilization to starch-PA complexes by utilizing the abundance of -OH groups in close proximity on the PA structure and the few –OH groups on the starch granule surface.

It is important to note that, deuterated solvents did not result in considerable changes in the RDS, SDS and RS proportions of the 50E treatments (Figure 9 C and D). In both 50E waxy and normal starch treatments, it was apparent that reducing their H-bond bonding with PA did not affect (at least not significantly) their starch digestibility. These observations further support the fact that H-bonds may not be the dominant interactions that stabilize PA-starch complex in intact / ungelatinized starch granules.

4.3.7 Involvement of hydrophobic interactions in stabilizing starch-proanthocyanidins complexes in gelatinized starch

Using dioxane to disrupt hydrophobic interactions in 30E normal starch-PA complexes resulted in significant decrease in SDS from 293 to 212 mg / g of starch (Figure 8 A); and increase in RDS from 293 to 351, while RS was not affected. Similar to 30E normal starch, disrupting the hydrophobic interactions in 30E waxy starch-PA complex had no effect on RS, while SDS decreased from 116 to 65 mg / g of starch (Figure 8 B). This observed decrease in SDS (28 - 44%) and insignificant effect on RS in 30E treatments (both waxy and normal starch) after incubation in 1,4-dioxane may suggest that hydrophobic interactions play a minor role in fully gelatinized starch compared to H-bonding.

4.3.8 Involvement of hydrophobic interactions in stabilizing starch-proanthocyanidins complexes in minimally gelatinized starch

In 50E normal starch treatment, disruption of hydrophobic interactions with 1,4-dioxane resulted in ~19% decrease in RS with a corresponding increase in SDS (5.5 fold) and RDS (4.8 fold) (Figure 8 C). In 50E waxy starch treatment (Figure 8 D), a similar trend but more drastic changes in digestibility profile was observed; RS decreased by 55%, whereas SDS and RDS increased 15.5-fold and 10-fold respectively. The more drastic changes in RS and RDS of waxy starch than normal starch may suggest that hydrophobic interactions play a more important role in stabilizing waxy starch-PA complex than normal starch-PA complex in intact starch granules.

Compared to dioxane-treated 50E samples, incubation of 50E starch-PA complexes with urea resulted in much higher decrease in RS and increase in RDS. The more drastic changes in digestibility profile of urea incubated starches than dioxane treated starches does not necessarily suggest H-bonding is more dominant in stabilizing starch-PA complexes of intact granules compared to hydrophobic interactions. Indeed, the fact that there was no effect on starch digestibility profile when H-bond formation between starch and PA was restricted in intact starch granules (Figure 9 C and D) suggests hydrogen bonding may not be dominant. More so, disruption of hydrophobic interactions in the 50E starch-PA complex released more PA into solution (39 – 42%) than H-bonds disruption (25 – 31%). These observations clearly point to a more dominant role of hydrophobic interactions than hydrogen bonding in stabilizing starch-PA complexes of intact starch granules.

Given that in 50E treatments the starch granules were intact, and the amylose and amylopectin polymers remained ordered in the semi-crystalline structure, the starch granules are generally more hydrophobic. Such hydrophobic nature of granules is likely to favor the formation of hydrophobic interactions with PA than H-bonding.

The apparent dominant role of hydrophobic interactions in stabilizing starch-PA complexes in less gelatinized starch systems has practical implications for starch based food matrices in which the starch is partially gelatinized. In food products in which the starch is minimally gelatinized (eg. crackers and cookies), PA treated starch may be successfully substituted into their formulations without losing the non-digestible property of the complex, since hydrophobic interactions, which stabilize starch and PA in the complex are relatively stable at high temperatures (baking temperature) [142,143]. This application can be crucial to reducing the caloric value of partially gelatinized starch based food products.

4.3.9 Crystallinity, thermal, and iodine binding properties of starch-proanthocyanidins complexes

Amylose treated with PA (in non-deuterated 50E and 30E solutions), showed a prominent new peak at $2\Theta \approx 19.8°$ (Figure 11). This peak was not observed in corresponding deuterated samples or controls. Reflection at $2\Theta \approx 19.8°$ indicates the presence of V-type polymorphs, which arise from the complexation of single amylose helices with endogenous components such as lipids [48,144]. It is evident that, the interaction of PA with amylose resulted in the formation of complexes which gave the

characteristic V-complex signature peak. The fact that amylopectin-PA samples did not show this characteristic peak at $2\Theta \approx 19.8°$ (Figure 12), suggests that V-type complexes were specifically formed between amylose and PA.

More so, considering the fact that amylose samples treated with PA in deuterated solutions did not show the characteristic peak at $2\Theta \approx 19.8°$ seen in non-deuterated amylose samples suggest that restricting hydrogen bonding between amylose and PA prevented the formation of these V-type complexes. It seems clear that these V-type complexes formed as a result of PA-amylose interactions involve hydrogen bonding.

The estimated percent crystallinity for samples PA treated in non-deuterated ethanol solutions were much higher (30.2 – 58.9%) than corresponding deuterated samples (17.4 – 41.6%) (Table 8). Thus, allowing H-bonding between PA and starch polymers seems to allow the complexes to pack into a crystallite, which tends to increase % crystallinity [145].

Generally, PA treated amylose had higher % crystallinity than their controls and corresponding amylopectin treatment. Though amylose is less crystalline than amylopectin in native state, amylose association with ligands (PA in this case) produces crystalline structures *in-vitro* [146]. The high peak at $2\Theta \approx 19.8°$ (Figure 11) in V-type structure of PA treated amylose contributes significant crystallinity to the amylose [147,148], which explains why PA treated amylose had much higher crystallinity (55.4 – 58.9%) than corresponding amylopectin treatments (30.2 – 39.1%) and amylose controls (18.9 – 27.3%) (Table 8).

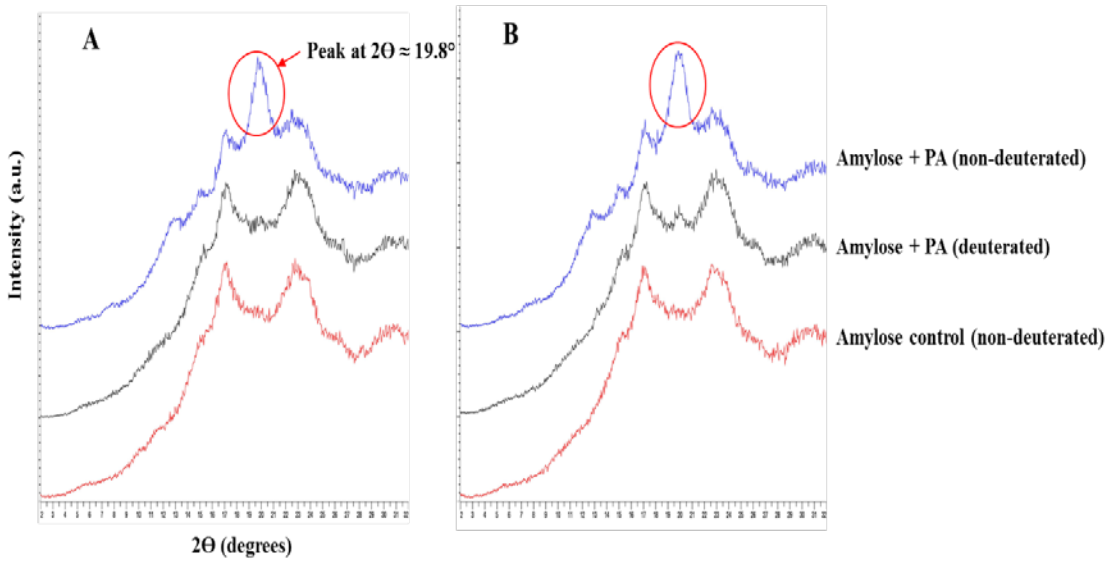

Figure 11 X-Ray diffraction patterns of amylose treated with proanthocyanidins in (A) 30% and (B) 50% deuterated and non-deuterated ethanol solutions.

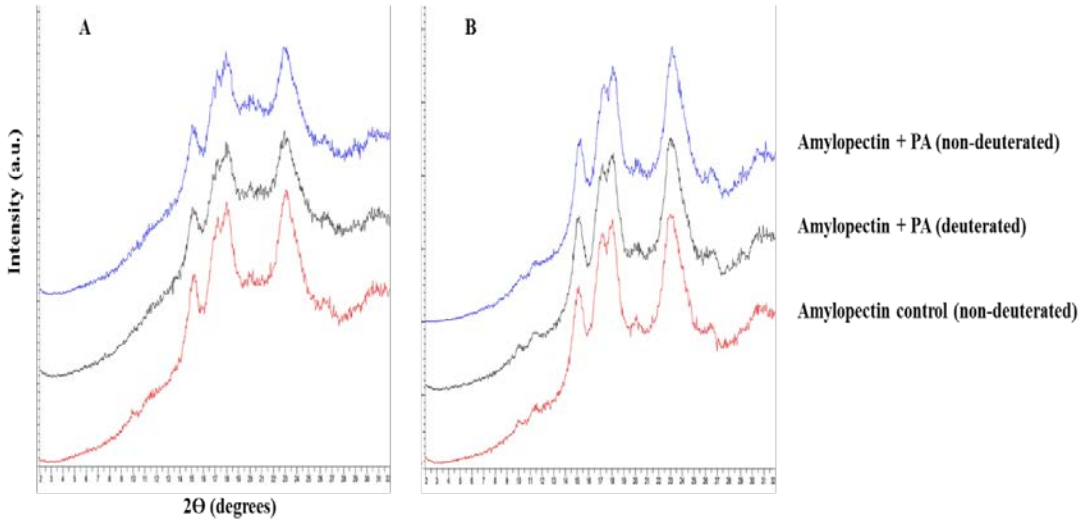

Figure 12 X-Ray diffraction patterns of amylopectin treated with proanthocyanidins in (A) 30% and (B) 50% deuterated and non-deuterated ethanol solutions.

Table 8 X-Ray diffraction crystallinity of amylose– and amylopectin–proanthocyanidins complexes.

Starch treatment	% Crystallinity (A-, B-, V- Type polymorph)[a]	
	Non-deuterated ethanol solution	Deuterated ethanol solution
30% treatment		
Amylose + PA extract	58.91 ± 0.15[a]	29.28 ± 0.53[b]
Amylose control	18.90 ± 0.55[c]	-
Amylopectin + PA extract	30.18 ± 1.65[c]	23.72 ± 1.32[c]
Amylopectin control	39.14 ± 0.82[b]	-
50% treatment		
Amylose + PA extract	55.35 ± 0.83[a]	17.44 ± 0.08[d]
Amylose control	27.26 ± 1.30[c]	-
Amylopectin + PA extract	39.10 ± 0.99[b]	41.62 ± 1.66[a]
Amylopectin control	36.68 ± 0.29[b]	-

Starch treatments were heated at 70°C/20 min in specified solutions, rinsed and dried before analysis. [a]Percent crystallinity was calculated using DIFFRAC^{plus} TOPAS software following recommendations by Lopez-Rubio et al. [48]. Means followed by the same letter within column are not significantly different ($P \leq 0.05$).

Figure 13 and Table 9 describe the thermal properties of PA-treated amylose starch. DSC thermograms (Figure 13) of amylose treated with PA (in non-deuterated 50E and 30E solutions), showed a characteristic Type II V-amylose complex melting peak at ~121 °C [149,150]. Native amylose and control samples however did not show this characteristic peak at ~121 °C (Table 9). Melting peaks of native amylose and control samples were observed at >135 °C (Table 9); characteristic of amylose melting [151,152]. These observations confirm the fact that V-complexes were indeed formed between amylose and PA. Since amylose samples treated with PA in deuterated

solutions did not show the V-amylose melting peak (at ~121 °C), it further confirms that H-bonding is involved in V-type amylose complex formation with PA.

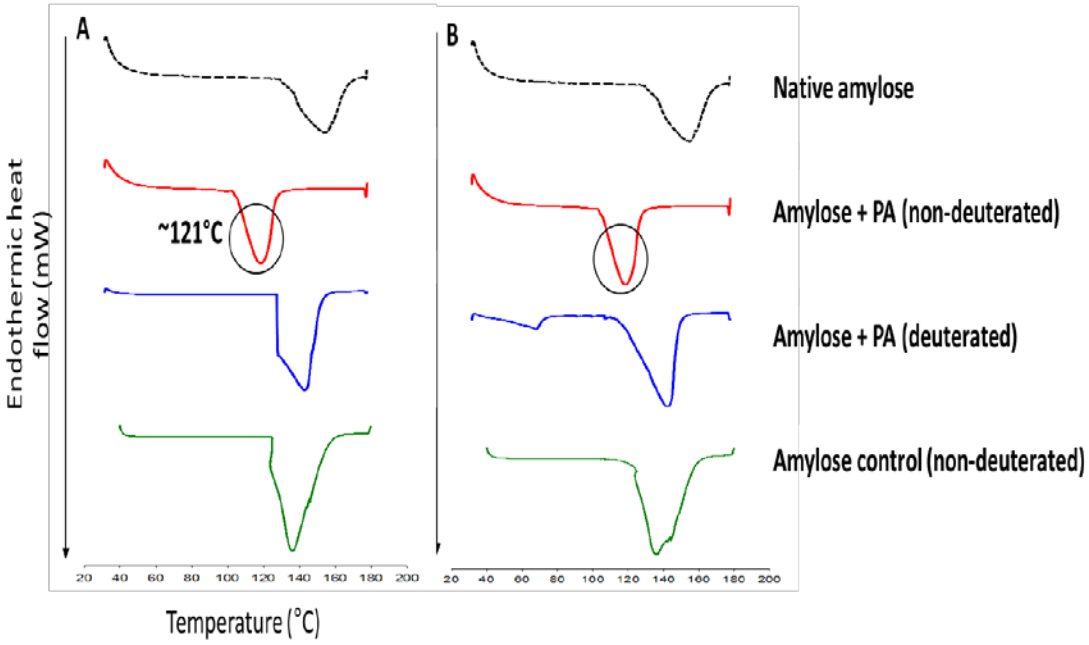

Figure 13 Differential Scanning Calorimetry thermograms of amylose samples treated with proanthocyanidins in (A) 30% and (B) 50% deuterated and non-deuterated ethanol solutions.

Table 9 Thermal properties of proanthocyanidins-treated amylose.

Starch treatment	T_o °C	T_p (°C)	T_c (°C)	ΔH (J/g dry starch)
Amylose[A]	134.1[a]	139.9[c]	163.6[a]	1713.5[a]
30% ethanol treatment				
Amylose + PA extract (non-deuterated)	109.8[d]	121.2[f]	134.1[d]	133.0[g]
Amylose + PA extract (deuterated)	131.6[b]	140.0[b]	159.3[b]	795.2[e]
Amylose control (non-deuterated)	124.8[c]	136.1[e]	158.9[b]	1360.5[c]
50% ethanol treatment				
Amylose + PA extract (non-deuterated)	105.5[e]	114.0[a]	135.1[d]	1581.0[b]
Amylose + PA extract (deuterated)	125.4[c]	144.1[a]	155.0[c]	281.1[f]
Amylose control (non-deuterated)	124.4[c]	138.2[d]	161.1[ab]	1265.0[d]

Starch treatments were heated at 70 °C/20 min in specified solutions, rinsed and dried before analysis. [A]Amylose was not subjected to the thermal treatment. T_o, onset temperature; T_p, peak temperature; T_c, Conclusion temperature; ΔH, melting enthalpy change. Means followed by the same letter within column are not significantly different ($P \leq 0.05$).

A set of PA-treated amylose samples were complexed with iodine and their peak maxima at 625 nm observed. The key question studied here was if PA is included within the hydrophobic helical core of amylose-V complex. Iodine forms inclusion complexes with free amylose; by observing the change in absorbance at peak maxima of the UV-VIS spectra of iodine treated amylose samples, the level of helix occupation by PA was estimated.

The UV-VIS spectra of iodine-amylose complexes formed by reacting PA-treated amylose samples with iodine are shown in Figure 14.

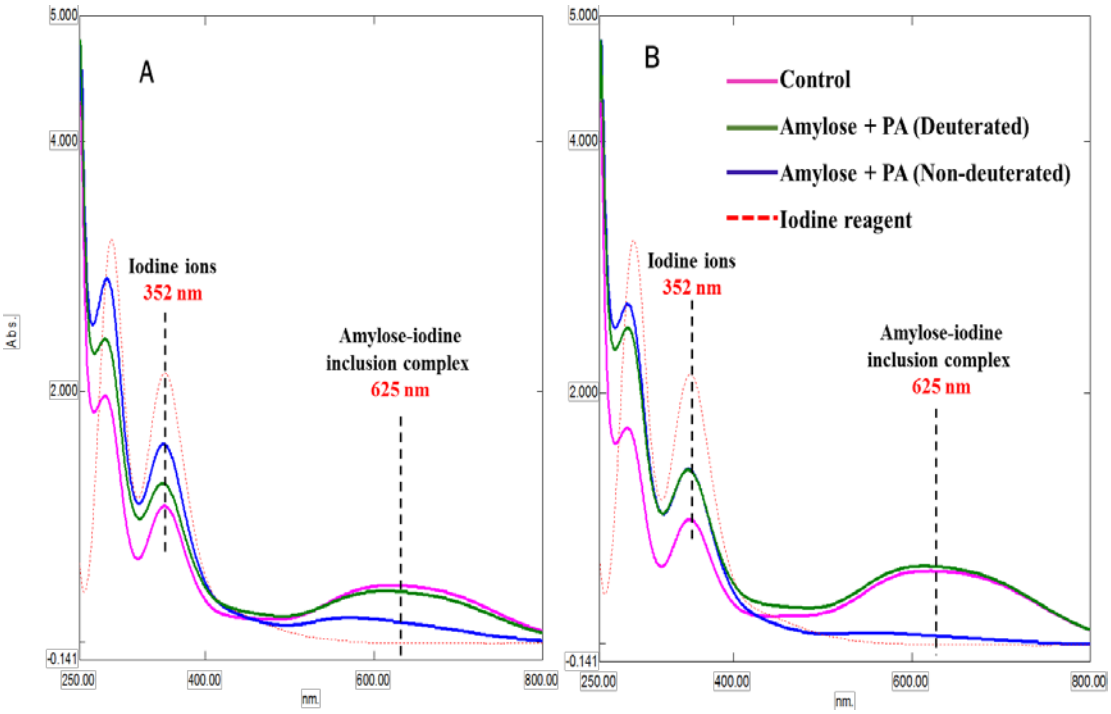

Figure 14 Ultraviolet spectra of amylose-iodine complexes in amylose samples treated with Proanthocyanidins in (A) 30% and (B) 50% deuterated and non-deuterated ethanol solutions.

Table 10 Absorbance of amylose-proanthocyanidins complexes at 352 nm and 625 nm after treatment with iodine.

Starch treatment	Absorbance at 352 nm (a.u)*	Absorbance at 625 nm (a.u)*
30% treatment		
Amylose + PA extract (non-deuterated)	1.57[a]	0.16[c]
Amylose + PA extract (deuterated)	1.24[c]	0.41[b]
Amylose control (non-deuterated)	1.09[d]	0.45[b]
50% treatment		
Amylose + PA extract (non-deuterated)	1.39[b]	0.07[d]
Amylose + PA extract (deuterated)	1.36[b]	0.62[a]
Amylose control (non-deuterated)	0.99[e]	0.59[a]

Starch treatments were heated at 70°C/20 min in specified solutions, rinsed and dried before analysis. Means followed by the same letter within column are not significantly different ($P \leq 0.05$). *a.u = absorbance units.

In PA-treated amylose prepared in 50E non-deuterated ethanol solution, no peak (absorbance = 0.59 a.u) was observed at 625 nm after reacting the sample with iodine (Figure 14 B, Table 10). Corresponding control sample (with no PA treatment) however showed a distinctive peak at 625 nm (absorbance = 0.59 a.u) after reaction with iodine (Figure 14 B, Table 10). This suggests that after amylose treatment with PA, the amylose helical core was occupied or blocked by PA which then limited the inclusion of iodine in the helix. The above observation confirms that PA was likely included within the amylose helical core during amylose-PA complexation.

Observations made in amylose-PA complexes prepared in 30E non-deuterated ethanol solution, were similar to corresponding 50E treatment above (Figure 14 A). PA-treated amylose (in non-deuterated 30E) showed a low absorbance (0.16 a.u) at ~625 nm compared to controls (0.45 a.u); which suggest little or no amylose-iodine inclusion complexes were formed because of lack of free space in the amylose helical core.

It is interesting to note that, amylose treated with PA in 30E deuterated ethanol solution showed UV-VIS spectra and absorbance (0.41 a.u) similar to controls (0.45 a.u) that were not treated with PA. Amylose treated with PA in 50E deuterated ethanol also showed similar absorbance at 625 nm (0.62 a.u) compared to control (0.59 a.u) (Table 10). Thus, by limiting H-bonding between PA and amylose, inclusion of PA within the amylose helix was limited, and consequently allowed for iodine inclusion in the helix. This observation suggests that, the inclusion of PA within the helical core of amylose

requires H-bonding. It is evident that, PA form inclusion complexes with amylose, which are stabilized by H-bonding between the amylose and PA molecules.

In a V-amylose helix, the inner surface is lined with methylene groups and glycosidic linkages that make the inner core hydrophobic, while the hydrophilic glycosyl hydroxyl groups are located on the outer surface of the helix [153]. The mechanism of V-amylose complex formation involves the inclusion of a complexing agent in the hydrophobic helical channel of single amylose strands, stabilized by hydrogen-to-hydrogen van der Waals forces between the C3 and C5 of glucose molecules of amylose with the H from the aliphatic chain of complexing agent [146,154]. Most complexes have a six glucose residue helix repeat, but bulkier complexing agents / ligands are thought to cause an expansion of the helix to seven or eight glucose units [154] to accommodate inclusion of the complexing agent [145,154].

Indeed, given that purified PA extract is dominated by polymeric PA forms (DP > 10) that are sterically bulky, it is likely that the hydrophobic core of an amylose coil would include PA partially. A likely interaction mechanism would involve the transfer of PA (via hydrophobic forces) into close proximity to the hydrophobic environment within the amylose helix cavity, and then further stabilization via hydrogen bonding between PA and amylose involving the –OH groups of C3 and C5 of amylose glucose units and the -OH groups on the B and A rings of the PA molecule. A weak partial inclusion of the B-ring of the principal catechin unit on the PA polymer into the amylose core is likely to occur. In that case, hydrogen-to-hydrogen van der Waals forces between

the H of C3 and C5 on the amylose glucose units and the H of C4’ and C5’ of the principal catechin unit are likely to dominate.

The ability of PA to form V-type structures by interacting with amylose has practical implications for starch-based products. Modification of amylose via complexation with monoacyl lipids to form V-amylose, is commonly practiced to control development of firmness in baked products, solubility and cooking loss of cereals, surface stickiness of pasta and processed rice, and texture of a wide range of starch-based products [155,156]. Formation of V-amylose with PA in starch based foods may be a useful tool for improving functionality as achieved with monoacyl lipids.

4.3.10 Starch pasting properties

Generally, there were no significant differences in peak time (min), breakdown and peak viscosity between starch samples treated in deuterated ethanol solutions and those treated in non-deuterated solutions (Table 11).

Table 11 Pasting properties of maize starches treated in deuterated ethanol solutions with sorghum proanthocyanidins extract.

Treatment	Pasting properties				
	Peak time (min)	Pasting temp. (°C)	Peak viscosity (cP)	Final viscosity (cP)	Breakdown (cP)
30% Non-deuterated ethanol solution					
Normal starch + PA extract	9.6^{b}	84.8^{b}	3220^{d}	4032^{c}	884^{e}
Waxy starch + PA extract	6.0^{d}	68.9^{d}	5571^{a}	1772^{f}	4034^{a}
30% Deuterated ethanol solution					
Normal starch + PA extract	10.0^{a}	89.7^{a}	3226^{d}	5191^{a}	590^{e}
Waxy starch + PA extract	5.9^{d}	50.1^{e}	4029^{c}	1841^{ef}	2669^{c}
50% Non-deuterated ethanol solution					
Normal starch + PA extract	8.7^{c}	74.0^{c}	4300^{c}	4150^{c}	1833^{d}
Waxy starch + PA extract	5.8^{d}	70.1^{d}	5157^{b}	2078de	3504^{b}
50% Deuterated ethanol solution					
Normal starch + PA extract	9.0^{c}	83.0^{b}	4203^{c}	4498^{b}	1651^{d}
Waxy starch + PA extract	5.8^{d}	70.3^{d}	5066^{b}	2189^{d}	3236^{b}

Starch treatments were heated at 70ºC/20 min in specified solutions, rinsed and dried before analysis. Means followed by the same letter within column and starch type are not significantly different ($P \leq 0.05$).

Pasting temperature of 30E normal starch-PA complexes prepared in deuterated ethanol solution was much higher than corresponding treatment in non-deuterated ethanol solution. This was also observed in 50E normal starch-PA complexes. Pasting temperature is related to the stability of the starch crystalline structure; the more stable the crystalline structure, the higher the temperature required to initiate starch pasting / swelling. H-bonds play an important role in stabilizing normal starch-PA complexes, and they contribute to strengthening starch crystalline structure [111]. Since H-bonds are less stable to heat [157], RVA heating / cooking of starch-PA complexes tends to weaken the interactions between normal starch-PA in a complex, and results in lower temperature required for pasting. This weakening of H-bonds in starch-PA complexes is likely responsible for the relatively lower pasting temperature of non-deuterated starch-PA complexes (since the complexes are largely stabilized by H bonds) compared to complexes prepared in deuterated ethanol solutions in which there is significantly less H-bonds between starch and PA.

The effect described above was not observed in corresponding waxy starch treatment, likely due to the dominant role H-bonds play in stabilizing waxy starch-PA complexes.

In deuterated treatments, reduction in H-bonding between starch and PA resulted in higher final viscosity after RVA cooking, compared to corresponding starch treatments in non-deuterated solutions. Final viscosity is generally driven by the extent of re-association (via H-bonding) of starch molecules (retrogradation) during the cooling stage of RVA cycle; thus, greater re-association of starch molecules results in higher

final viscosity. Reducing H-bonding between starch and PA (in deuterated treatments) left more unbound amylose and available –OH groups on starch polymers to re-associate during RVA cooling, hence the higher final viscosity. In non-deuterated treatments, however, the uninhibited interaction of starch with PA, allowed H-bonding between starch and PA, hence there were fewer available starch molecules and –OH groups to re-associate during RVA cooling, hence the lower final viscosity.

4.3.11 Starch swelling properties

Starch swelling involves the interaction of starch polymers with water via H-bonding. Generally, the presence and availability of hydroxyl groups on the starch polymer allows it to interact with water molecules, which opens up the starch structure and results in swelling.

In non-deuterated treatments, as expected, waxy starch and amylopectin swelled more than corresponding normal starch and amylose treatments (Table 12 and Table 13). Waxy starch (~99% amylopectin) and amylopectin polymers have the ability to imbibe and hold on to water by forming H-bonds with water molecules by utilizing the hydroxyl groups on their highly branched chain structure.

Generally, normal and waxy starches treated in deuterated ethanol solutions had higher swelling power than corresponding treatments in non-deuterated solutions. Amylose treatments also followed a similar trend, but not amylopectin. Deuterated solutions reduced H-bonding between PA and starch molecules, leaving hydroxyl groups

on the starch polymer uninvolved in any interaction in its environment. These free hydroxyl groups were likely responsible for interacting with water to cause starch swelling. On the other hand, PA was able to interact (and form H-bonds) with starch (via their hydroxyl groups) in non-deuterated ethanol solutions, hence the starch polymers had fewer of their hydroxyl groups available to interact with water.

Table 12 Swelling properties of maize starches treated with sorghum proanthocyanidins in deuterated and non-deuterated ethanol solutions.

Starch treatment	Non-deuterated ethanol solution		Deuterated ethanol solution	
	Solubility (%)	Swelling power (%)	Solubility (%)	Swelling power (%)
30E treatment				
Normal starch + PA extract	0.31 ± 0.01^{d}	4.09 ± 0.06^{c}	1.39 ± 0.12^{b}	5.05 ± 0.35^{b}
Waxy starch + PA extract	3.01 ± 0.06^{a}	4.21 ± 0.01^{c}	2.98 ± 0.10^{a}	6.67 ± 0.02^{a}
50E treatment				
Normal starch + PA extract	0.89 ± 0.18^{c}	2.10 ± 0.01^{d}	1.01 ± 0.07^{c}	2.09 ± 0.02^{d}
Waxy starch + PA extract	1.24 ± 0.00^{bc}	2.18 ± 0.00^{d}	1.14 ± 0.10^{bc}	2.33 ± 0.10^{d}

Starch treatments were heated at 70°C/20 min in specified solutions, rinsed and dried before analysis. Means followed by the same letter within column are not significantly different ($P \leq 0.05$).

Table 13 Swelling properties of amylose and amylopectin treated with purified proanthocyanidins in deuterated and non-deuterated ethanol solutions

Starch treatment	Non-deuterated ethanol solution		Deuterated ethanol solution	
	Solubility (%)	Swelling power (%)	Solubility (%)	Swelling power (%)
30E treatment				
Amylose + PA extract	2.02 ± 0.11^{b}	2.59 ± 0.82^{b}	1.28 ± 0.06^{c}	4.21 ± 0.03^{a}
Amylose control	0.99 ± 0.01^{cd}	4.10 ± 0.06^{a}	-	-
Amylopectin + PA extract	4.19 ± 0.03^{a}	4.35 ± 0.51^{a}	4.34 ± 0.08^{a}	3.95 ± 0.01^{a}
Amylopectin control	2.19 ± 0.27^{b}	3.29 ± 0.04^{ab}	-	-
50E treatment				
Amylose + PA extract	2.25 ± 0.03^{b}	3.22 ± 0.35^{ab}	1.22 ± 0.04^{c}	3.85 ± 0.01^{a}
Amylose control	1.03 ± 0.03^{cd}	3.80 ± 0.02^{a}	-	-
Amylopectin + PA extract	0.92 ± 0.09^{cd}	2.38 ± 0.03^{b}	0.67 ± 0.07^{d}	2.42 ± 0.03^{b}
Amylopectin control	0.71 ± 0.01^{d}	2.22 ± 0.01^{b}	-	-

Starch polymers were heated at 70°C/20 min in specified solutions, rinsed and dried before analysis. Means followed by the same letter within column are not significantly different ($P \leq 0.05$).

4.4 Conclusion

Our findings clearly demonstrate that PA interact with starch via hydrogen bonding and hydrophobic interactions. Indeed, H-bonding dominates starch-PA interactions in amylose-rich starch and gelatinized starch. Hydrophobic interactions on the other hand dominate starch-PA interactions in intact or minimally gelatinized starch granules. The levels of SDS and RS formed as a result of starch-PA complexation is also influenced by the dominant interactions (whether H-bonds or hydrophobic interactions) that stabilize the complex. Amylose forms V-complexes with PA, which are largely stabilized by H-bonds. This study provides evidence on the effect of degree of starch swelling and granule integrity on the type of interactions that stabilize starch-PA complexes. This is important given that the extent of starch gelatinization varies widely among food products, and this information is beneficial to designing novel applications of natural high molecular weight PA in starch based foods to reduce caloric density. Future work can focus on investigating the fate of starch–PA complexes on glucose release *in-vivo*. The interaction of gut microbiota and colon epithelial cells with starch-PA complexes will be highly relevant as well.

5. INTRAGRANULAR CROSSLINKING OF STARCH WITH PROANTHOCYANIDINS

5.1 Introduction

Cross-linking is one of the most common starch-modification methods utilized to improve starch functionality [56]. Cross-linking of starch is achieved by utilizing multifunctional reagents such as phosphorous oxychloride ($POCl_3$) [57] and sodium trimetaphosphate (STMP) [58], to form intermolecular bridges with hydroxyl groups of starch. The covalently linked network makes cross-linked starch swell less and become more resistant to shear, high temperature and low pH compared to its parent starch [56].

The process of making cross-linked starches involves mixing native starch granules in an alkaline aqueous system (pH ≈ 9-11.5) with phosphorylation reagents capable of forming intermolecular bridges with at least two hydroxyl groups of the starch [56]. Phosphorous oxychloride ($POCl_3$) [57] and sodium trimetaphosphate (STMP) [58] are the common reagents used to form distarch phosphates (DSP) / crosslinks. Low concentrations of cross-linking reagent result in minimal cross-linking, and therefore a high ratio of monostarch phosphate (MSP) to DSP formed [52,64]. Higher concentrations in the range of > 1% (w/w of starch), however form a high proportion of DSP. DSP / cross-linked starch is more resistant to acid, heat, and shearing than native starch, which makes it suitable for applications as thickeners, stabilizers, and texture improvers [61,62]. Monostarch phosphate on the other hand exhibit increased paste clarity, viscosity and water binding capacity [24,63].

In chapter 3, section 3.3.3, we showed that treatment of partially gelatinized normal starch with high MW sorghum PA increased the pasting temperature and peak viscosity of the starch during RVA cooking. Such increase in pasting temperature and peak viscosity is typical of minimally cross-linked starch (high proportion of MSP:DSP). With this background, we hypothesize that the use of PA alone, or in combination with cross-linking reagents may be a successful tool to form cross-linked starches with cleaner label and unique properties. PA may also offer added health benefits when applied to cross-linked starches, considering its well-researched health implications in human diet. The objective of this study is to investigate the potential covalent cross-linking action of PA with starch.

5.2 Materials and methods

5.2.1 Proanthocyanidin extract and characterization

Proanthocyanidin extract from high tannin sorghum was obtained and characterized, as described previously in section 4.2.1.

5.2.2 Starch and reagents

Normal (amylose content = 23.9%) was obtained from Ingredion Incorporated (Westchester, IL). All solvents (analytical grade) and reagents were obtained from Sigma (St. Louis, MO).

5.2.3 Preparation of cross-linked starches

Cross-linked starch was prepared using a method previously described by Felton and Schopmeyer [158] with some modifications. Three different treatments of cross-linked starch were prepared using $POCl_3$ only, $POCl_3$ and PA extract, and PA extract only.

In treatment utilizing $POCl_3$ only, normal maize starch (20 g, db) was mixed with water (30 mL) and stirred for 10 min at 25 °C. Sodium hydroxide (1.0 M) solution was slowly added to the slurry to obtain a final solution pH of ~11.5. $POCl_3$ solution (0.001% w/w of starch) was added dropwise to the starch slurry over a 30 min period, with continuous mixing, while maintaining the pH of the starch slurry at ~ 11.5. After the addition of the $POCl_3$, the slurry was mixed for 1 h, while maintaining pH at ~9 - 11.5. After mixing, the solution pH was adjusted to ~ 6 – 7 with 1M HCl. The starch was recovered by centrifugation (15,000 x *g*, 10 min) and the sediments were collected. The sediments were rinsed with water (50 mL, 3x), and oven-dried at 40 °C overnight. The dry starch recovered was stored at – 20 °C until use. Other $POCl_3$ concentrations used were 0.1%, 0.34%, 0.50%, and 0.75% (w/w of starch, db).

In the treatment which utilized both PA extract and $POCl_3$, the starch was premixed with PA extract (5% w/w of starch) and then slurried in 30 mL of water. The rest of the procedure was followed as above. $POCl_3$ concentrations used were 0.1%, 0.34%, 0.50% and 0.75% (w/w of starch, db).

Starches cross-linked with PA (extract) only were prepared as above with the following PA concentrations: 1.0%, 2.5%, 5.0% and 10% (w/w of starch basis, db).

5.2.4 Pasting properties

Rapid Visco Analyzer (RVA) was utilized to measure starch pasting properties using a method by Barros et al. [15] described earlier (section 3.2.8).

5.2.5 Statistical analysis

Data was analyzed using a one-way analysis of variance (ANOVA) to determine significant differences among treatments. Tukey's HSD ($P \leq 0.05$) was used to separate means. The statistical software SAS version 9.4 for windows was used. All tests were replicated at least twice.

5.3 Results and discussion

5.3.1 Pasting properties of starch cross-linked with phosphorous oxychloride only

As expected, the viscosity behavior of crosslinked starch was different from native starch, and the different levels of $POCl_3$ addition resulted in distinct pasting properties (Table 14). Starch cross-linking involves the formation of intermolecular bridges (covalent bonds) by cross-linking agent ($POCl_3$) with at least two of the hydroxyl groups of starch (Figure 15). Low levels of $POCl_3$ addition (0.1%, 0.34% and 0.5%) resulted in increased peak viscosity and reduced breakdown viscosity. This is typical of minimally cross-linked starches, where the low levels of $POCl_3$ addition results in the formation of few distarch phosphates [159]. The few covalently bonded starch molecules increase mechanical strength of the granule and keep the swollen starch granules intact,

which prevents loss of viscosity and provide resistance to mechanical shear [159]. This explains why starch cross-linked with low levels of $POCl_3$ (0.1%, 0.34% and 0.5%) possess higher peak viscosity and low breakdown properties.

Table 14 Pasting properties of maize starches cross-linked with phosphorous oxychloride.

Treatment	Pasting properties				
	Peak time (min)	Pasting temp. (°C)	Peak viscosity (cP)	Final viscosity (cP)	Breakdown (cP)
Normal starch (Control)	8.2[a]	72.8[b]	4269[d]	4012[d]	2026[ab]
$POCl_3$ treatments					
0.1%	7.7[a]	73.9[a]	6696[a]	7154[b]	2348[a]
0.34%	8.5[a]	72.5[b]	6144[b]	9038[a]	1720[b]
0.5%	9.0[a]	73.7[a]	5249[c]	5940[c]	1125[c]
0.75%	6.6[a]	nr	227[e]	223[e]	13.5[d]

Starch was mixed with $POCl_3$ and incubated at room temperature at pH ~ 11.5, while mixing for 1 h. Sediments collected were rinsed and dried before analysis. Means followed by the same letter within a column are not significantly different ($P \leq 0.05$). nr = not recorded.

Starch treated with 0.75% $POCl_3$ on the other hand, underwent higher level of cross-linking, which is typically characterized by a low peak viscosity compared to native starch and starch with low level of crosslinking. Highly cross-linked starch has a high density of distarch phosphate (DSP); such high levels of DSP completely prevent the starch granule from swelling and gelatinization [61,62].

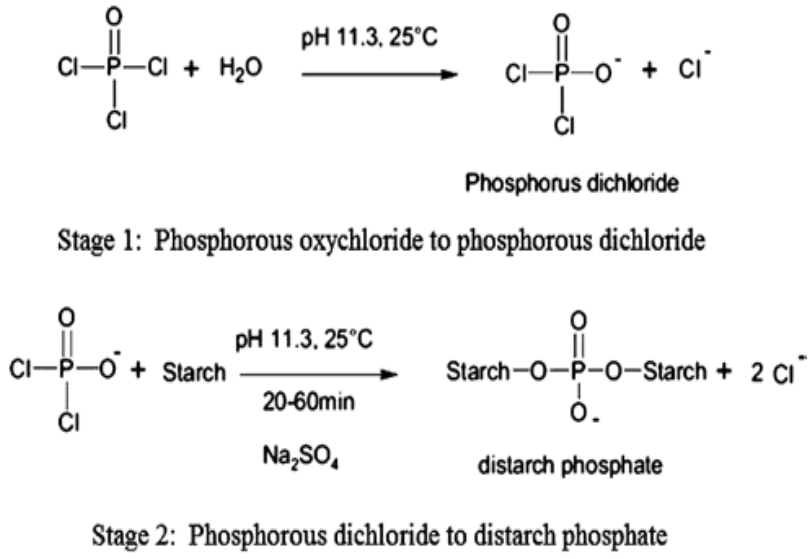

Figure 15 Mechanism of cross-linking of starch with phosphorous oxychloride. Adapted from Shah et al. [159].

5.3.2 Pasting properties of starch 'cross-linked' with proanthocyanidins only

Treatment of normal starch with PA at high pH had marked effects on the pasting characteristics of the starch (Table 15). PA treated starch generally increased in peak and final viscosity compared to native starch. At high pH, the starch molecules carry a negative charge due to ionization of the hydroxyl groups, which results in repulsion of

the starch polymers in the starch granule [160,161]. This repulsion disrupts the amorphous region in the starch granule, which reduces the restraining effect of amylose, thereby allowing starch granules to swell more freely [160]. The swelling of the starch allows the entry of PA into the granule interior to interact with amylose molecules to form amylose-PA complexes. Starch-PA complex formation in the starch interior gave the starch more stability to shear and heat, compared to native starch, hence the higher peak viscosity [111]. This increase in peak viscosity is characteristic of monostarch phosphate (MSP) or minimally cross-linked starch [24,63].

Final viscosity is highly correlated with the degree of starch polymer reassociation or polymerization (via H-bonding) after starch gelatinization. The higher final viscosity of PA treated starch compared to native starch suggests that PA may be involved in facilitating the reassociation of starch molecules by forming H-bond bridges between the starch polymers (via their –OH) groups. Starch-PA complexes formed may have also self-associated via H-bonding to increase final viscosity.

Table 15 Pasting properties of maize starches 'cross-linked' with proathocyanidins extract.

Treatment	Pasting properties				
	Peak time (min)	Pasting temp. (°C)	Peak viscosity (cP)	Final viscosity (cP)	Breakdown (cP)
Normal starch (Control)	8.2[b]	72.8[b]	4269[c]	4012[f]	2026[c]
Proanthocyanidins (PA) extract treatments					
0.5%	6.7[c]	70.4[c]	5056[b]	4724[d]	2520[b]
1.0%	6.3[c]	70.4[c]	5154[b]	4377[e]	2838[ab]
2.5%	7.8[b]	72.7[b]	5672[a]	6738[a]	2535[b]
5.0%	7.8[b]	72.5[b]	5693[a]	5452[c]	3209[a]
10%	9.0[a]	83.8[a]	4481[c]	6525[b]	1620[c]

Starch – PA extract mixtures were incubated at room temperature at pH ~ 11.5, while mixing for 1 h. Sediments collected were rinsed and dried before analysis. Means followed by the same letter within a column are not significantly different ($P \leq 0.05$).

Normal starch treated with 10% PA extract showed a distinctively higher peak time (9 min) and pasting temperature (83.8 °C) compared to other treatments and native starch. This delayed pasting and high pasting temperature is a likely due to the fact that, the excess amount of PA (from the high level of PA extract added) was involved in extensive interaction with starch polymers, which led to the formation of crystalline regions in the starch granule that strengthened the granule structure and made it more resistant to heat (high pasting temperature) [111]. It is interesting to note that, though PA

addition levels of 0.5% - 5% resulted in increased peak viscosity (in comparison to native starch), 10% PA addition resulted in no change in peak viscosity. It seems that increasing the levels of PA gives starch pasting behavior similar to that of starch cross-linked with $POCl_3$, where increasing the levels of $POCl_3$ results in a steady decline in peak viscosity [159] (as observed in Table 14), as a result of increased levels of cross-linked starch formed. With increased level of cross-linking, starch typically shows less breakdown in the RVA curve, a phenomenon also observed in the 10% PA treated starch. Indeed, these observations may be indicative of some cross-linking action of the PA with starch polymers at high levels of PA addition.

5.3.3 Pasting properties of starch cross-linked with phosphorous oxychloride and proanthocyanidins extract

The combined use of $POCl_3$ and PA was aimed at investigating a possible synergistic action by these two molecules to form cross-linked starch. Considering the potential cross-linking action of PA observed above when starch was treated with PA extract alone, we entertain a possible synergistic mode of action if PA is used together with $POCl_3$.

Table 16 Pasting properties of maize starches 'cross-linked' with a combination of proanthocyanidins extract and phosphorous oxychloride.

Treatment	Pasting properties				
	Peak time (min)	Pasting temp. (°C)	Peak viscosity (cP)	Final viscosity (cP)	Breakdown (cP)
Normal starch (Control)	8.2^{c}	72.8^{b}	4269^{c}	4012^{c}	2026^{d}
Proanthocyandins extract + $POCl_3$ treatments					
5% PA extract + 0.001% $POCl_3$	6.7^{e}	73.0^{ab}	5660^{b}	4372^{f}	3456^{a}
5% PA extract + 0.01% $POCl_3$	7.7^{d}	73.6^{ab}	5573^{b}	4977^{b}	3079^{b}
5% PA extract + 0.1% $POCl_3$	7.9^{d}	73.8^{a}	6460^{a}	6944^{a}	2353^{c}
5% PA extract + 0.34% $POCl_3$	13^{a}	nr	690^{d}	587^{d}	180^{e}
5% PA extract + 0.5% $POCl_3$	12.5^{b}	nr	305^{e}	245^{d}	21^{e}

Starch was mixed with 5% PA extract (w/w of starch) and $POCl_3$ and incubated at room temperature at pH ~ 11.5, while mixing for 1 h. Sediments collected were rinsed and dried before analysis. Means followed by the same letter within a column are not significantly different ($P \leq 0.05$). nr = not recorded.

Cross-linked starch formed from the addition of 0.34% $POCl_3$ and 5% PA extract produced limited swelling and much lower viscosities compared to starch treated with only $POCl_3$ at similar (0.34%) and even higher (0.5%) concentrations (Table 16, Figure 16). This observation clearly suggests that $POCl_3$ and PA are likely acting synergistically to form a covalent bond network in the starch structure, which made the starch more resistant to shear and heat.

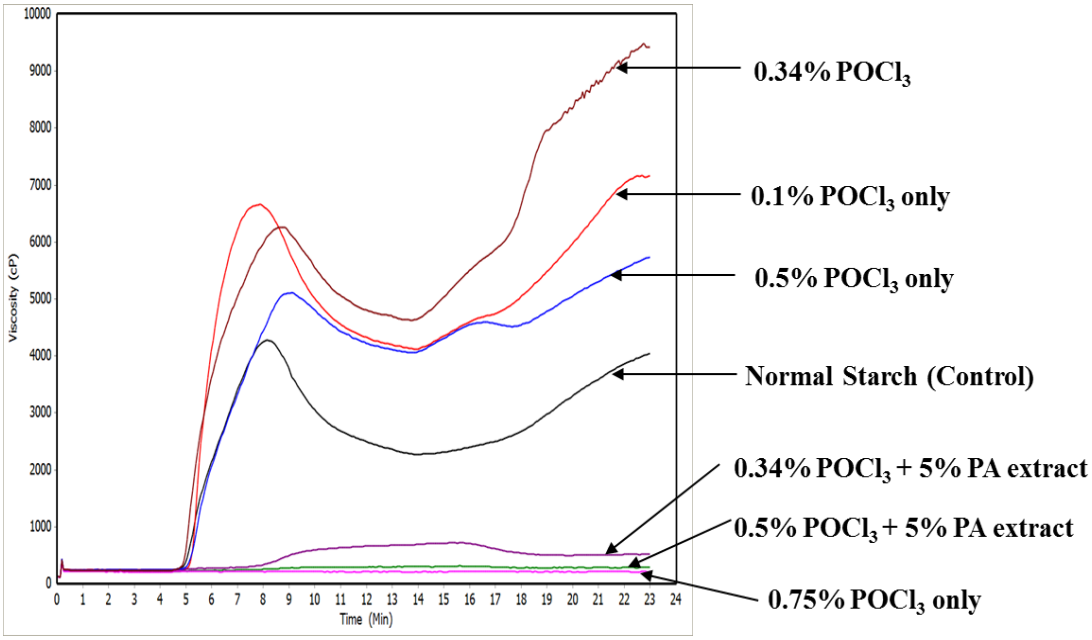

Figure 16 Rapid visco analyzer (RVA) curves of normal starch cross-linked with different levels of phosphorous oxychloride and proanthocyanidins extract.

The mode of synergistic action may likely involve an initial esterification of the starch molecule to phosphorus oxychloride to form a monostarch phosphate intermediate. PA then acts as a bridge by linking two monostarch phosphate molecules to form a Starch–P–PA–Starch polymer (Figure 17 A). PA may also link a monostarch phosphate molecule to a starch molecule to form a Starch–P–PA– P–Starch molecule (Figure 17 B). These large polymer esters formed may further interact with each other in a complex covalent network.

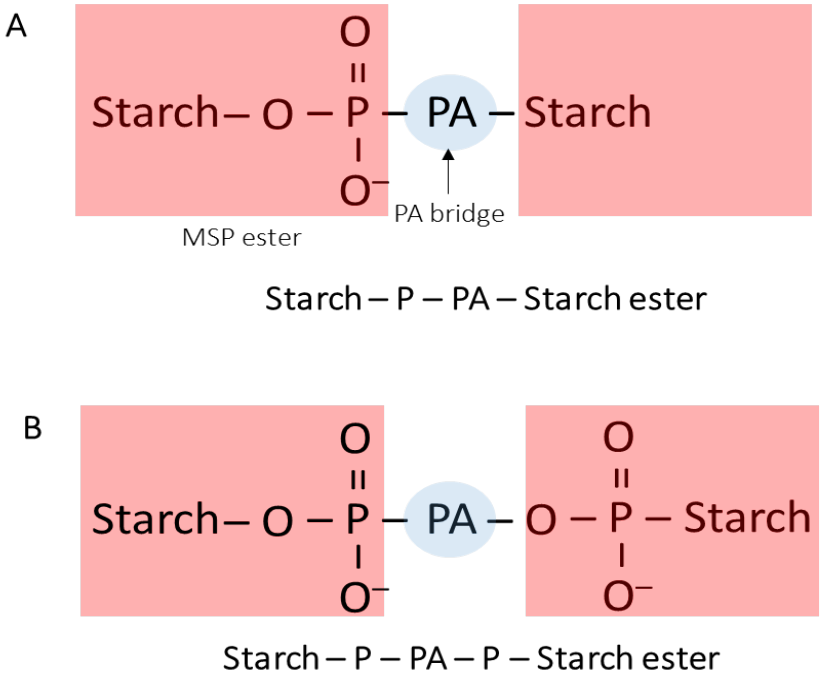

Figure 17 Predicted structures of esters formed by the synergistic cross-linking action of proanthocyanidins and phosphorous oxychloride with starch.

5.4 Conclusion

Our findings demonstrate that PA form intramolecular cross-links with normal starch that impact starch pasting properties; PA extract at inclusion levels as low as 0.5% (w/w of starch) caused significant increase in the peak viscosity of normal starch. The combined use of PA and cross-linking agent ($POCl_3$) shows potential synergistic mode of action to form cross-links in starch that drastically reduce starch swelling and increase resistance to shear and gelatinization. Their synergistic action likely forms a final product comprising a complex network of covalent and hydrogen bonds between starch, PA and phosphate molecules. This study provides evidence for the potential application of high molecular weight PA as new ingredients to produce cross-linked starches with cleaner label and added health benefits. Investigation of the mechanism of formation of starch cross-links with PA and the conditions that enhance the cross-linking action of PA on starch will be of key interest. Measurement of starch physicochemical properties such as thermal characteristics, phosphorus content, degree of crosslinking, types and proportion of starch-phosphate esters formed, phosphorus chemical shifts (using nuclear magnetic resonance (NMR) analysis), and starch swelling / solubility properties will be crucial to better understanding the nature and formation of these PA– and P cross-linked starches. The interaction of PA-containing cross-linked starches with gut microbiota is of particular interest as well.

6. SUMMARY AND CONCLUSIONS

6.1 Summary

This study demonstrates that proanthocyanidins, even at relatively low levels, interact with starch in a way that alter starch properties, and dramatically affect starch digestibility profile. The degree of granule swelling and gelatinization affects starch-PA interactions. PA interact with starch via hydrogen bonding and hydrophobic interactions. H-bonding dominates starch-PA interactions in amylose-rich starch and gelatinized starch, while hydrophobic interactions play a dominant role in stabilizing starch-PA complexes in intact or minimally gelatinized starch granules. Amylose forms V-complexes with PA, which are stabilized by H-bonds. PA form intramolecular cross-links with normal starch that impact starch pasting properties. The combined use of PA and cross-linking agent ($POCl_3$) shows potential synergistic mode of action to form cross-links in starch.

This study provides evidence for the potential of natural high molecular weight polyphenols as new ingredients to produce nutritionally beneficial starches. It also demonstrates that the degree of starch swelling and granule integrity impacts the type of interactions that stabilize starch-PA complexes, which is beneficial to designing novel applications of high molecular weight PA in starch based foods to reduce caloric density. Evidence from this study suggests that there is a potential application of PA as new ingredients to produce cross-linked starches with cleaner label and added health benefits.

This study did not describe the structure / nature of the V-amylose complexes formed between PA and amylose. The mechanism for inter-molecular cross-linking of starch with PA was also not fully elucidated.

6.2 Recommendations for further research

Further studies are needed to demonstrate the successful application of PA treated starches in food products and their potential health benefits. Follow up studies could focus on:

1. The fate of the starch–PA complexes on glucose release *in-vivo.*
2. The interaction of the starch–PA complexes with gut microbiota and colonic epithelia.
3. The application of PA treated starches in model food products, and how they impact nutritional quality.

REFERENCES

1. Awika JM: Major cereal grains production and use around the world. In *Advances in cereal science: implications to food processing and health promotion*. Edited by: ACS Publications; 2011:1-13.
2. Awika J, Piironen V, Bean S: *Advances in Cereal Science: Implications to Food Processing and Health Promotion*: OUP USA; 2012.
3. Englyst HN, Kingman SM, Cummings JH: Classification and Measurement of Nutritionally Important Starch Fractions. *European Journal of Clinical Nutrition* 1992, 46:S33-S50.
4. Englyst KN, Hudson GJ, Englyst HN: Starch analysis in food. *Encyclopedia of analytical chemistry* 2000.
5. Aller EEJG, Abete I, Astrup A, Martinez JA, van Baak MA: Starches, Sugars and Obesity. *Nutrients* 2011, 3:341-369.
6. Zhang GY, Hamaker BR: Slowly Digestible Starch: Concept, Mechanism, and Proposed Extended Glycemic Index. *Critical Reviews in Food Science and Nutrition* 2009, 49:852-867.
7. Bennett RN, Wallsgrove RM: Secondary metabolites in plant defence mechanisms. *New phytologist* 1994, 127:617-633.
8. Pandey KB, Rizvi SI: Plant polyphenols as dietary antioxidants in human health and disease. *Oxidative medicine and cellular longevity* 2009, 2:270-278.

9. Zhu F: Interactions between starch and phenolic compound. *Trends in Food Science & Technology* 2015, 43:129-143.

10. Hanhineva K, Torronen R, Bondia-Pons I, Pekkinen J, Kolehmainen M, Mykkanan H, Poutanen K: Impact of Dietary Polyphenols on Carbohydrate Metabolism. *International Journal of Molecular Sciences* 2010, 11:1365-1402.

11. Barrett A, Ndou T, Hughey CA, Straut C, Howell A, Dai ZF, Kaletunc G: Inhibition of alpha-Amylase and Glucoamylase by Tannins Extracted from Cocoa, Pomegranates, Cranberries, and Grapes. *Journal of Agricultural and Food Chemistry* 2013, 61:1477-1486.

12. Goncalves R, Mateus N, de Freitas V: Inhibition of alpha-amylase activity by condensed tannins. *Food Chemistry* 2011, 125:665-672.

13. Grussu D, Stewart D, McDougall GJ: Berry Polyphenols Inhibit alpha-Amylase in Vitro: Identifying Active Components in Rowanberry and Raspberry. *Journal of Agricultural and Food Chemistry* 2011, 59:2324-2331.

14. Hargrove JL, Greenspan P, Hartle DK, Dowd C: Inhibition of Aromatase and alpha-Amylase by Flavonoids and Proanthocyanidins from Sorghum bicolor Bran Extracts. *Journal of Medicinal Food* 2011, 14:799-807.

15. Barros F, Awika J, Rooney LW: Interaction of Tannins and Other Sorghum Phenolic Compounds with Starch and Effects on in Vitro Starch Digestibility. *Journal of Agricultural and Food Chemistry* 2012, 60:11609-11617.

16. Barros F, Awika J, Rooney LW: Effect of molecular weight profile of sorghum proanthocyanidins on resistant starch formation. *Journal of the Science of Food and Agriculture* 2014, 94:1212-1217.

17. Lemlioglu-Austin D, Turner ND, McDonough CM, Rooney LW: Effects of Sorghum [Sorghum bicolor (L.) Moench] Crude Extracts on Starch Digestibility, Estimated Glycemic Index (EGI), and Resistant Starch (RS) Contents of Porridges. *Molecules* 2012, 17:11124-11138.

18. Mkandawire NL, Kaufman RC, Bean SR, Weller CL, Jackson DS, Rose DJ: Effects of Sorghum (Sorghum bicolor (L.) Moench) Tannins on alpha-Amylase Activity and in Vitro Digestibility of Starch in Raw and Processed Flours. *Journal of Agricultural and Food Chemistry* 2013, 61:4448-4454.

19. Dunn KL, Yang LY, Girard A, Bean S, Awika JM: Interaction of Sorghum Tannins with Wheat Proteins and Effect on in Vitro Starch and Protein Digestibility in a Baked Product Matrix. *Journal of Agricultural and Food Chemistry* 2015, 63:1234-1241.

20. Varriano-Marston E, Ke V, Huang G: Comparison of methods to determine starch gelatinization in bakery foods. *Cereal Chem* 1980, 57:242-248.

21. Wootton M, Chaudhry MA: Gelatinization and Invitro Digestibility of Starch in Baked Products. *Journal of Food Science* 1980, 45:1783-1784.

22. Soares S, Mateus N, de Freitas V: Carbohydrates inhibit salivary proteins precipitation by condensed tannins. *Journal of agricultural and food chemistry* 2012, 60:3966-3972.

23. Le Bourvellec C, Renard C: Non-covalent interaction between procyanidins and apple cell wall material. Part II: Quantification and impact of cell wall drying. *Biochimica et Biophysica Acta (BBA)-General Subjects* 2005, 1725:1-9.

24. Lim S, Seib P: Preparation and pasting properties of wheat and corn starch phosphates. *Cereal chemistry* 1993, 70:137-137.

25. Gupta N, Goel K, Shah P, Misra A: Childhood obesity in developing countries: epidemiology, determinants, and prevention. *Endocrine reviews* 2012, 33:48-70.

26. Ferriero AM, Specchia ML: Obesity and Diabetes. In *A Systematic Review of Key Issues in Public Health*. Edited by: Springer; 2015:89-108.

27. Ogden CL, Carroll MD, Kit BK, Flegal KM: Prevalence of obesity in the United States, 2009-2010. *NCHS Data Brief* 2012:1-8.

28. Wild S, Roglic G, Green A, Sicree R, King H: Global prevalence of diabetes estimates for the year 2000 and projections for 2030. *Diabetes care* 2004, 27:1047-1053.

29. Cawley J, Meyerhoefer C: The medical care costs of obesity: an instrumental variables approach. *Journal of health economics* 2012, 31:219-230.

30. Finkelstein EA, Trogdon JG, Cohen JW, Dietz W: Annual medical spending attributable to obesity: payer-and service-specific estimates. *Health affairs* 2009, 28:w822-w831.

31. Fazel M, Pendergrass M: Individualizing treatment of hyperglycemia in type 2 diabetes. *J Clin Outcomes Manage* 2017, 24:23-38.

32. Lawlor DA, Chaturvedi N: Treatment and prevention of obesity—are there critical periods for intervention? *International journal of epidemiology* 2006, 35:3-9.

33. Ba S, JC S, WPT J: Diet, nutrition and the prevention of excess weight gain and obesity. *Public health nutrition* 2004, 7:123-146.

34. Hu FB, Manson JE, Stampfer MJ, Colditz G, Liu S, Solomon CG, Willett WC: Diet, lifestyle, and the risk of type 2 diabetes mellitus in women. *New England Journal of Medicine* 2001, 345:790-797.

35. Risérus U, Willett WC, Hu FB: Dietary fats and prevention of type 2 diabetes. *Progress in lipid research* 2009, 48:44-51.

36. Schulze MB, Manson JE, Ludwig DS, Colditz GA, Stampfer MJ, Willett WC, Hu FB: Sugar-sweetened beverages, weight gain, and incidence of type 2 diabetes in young and middle-aged women. *Jama* 2004, 292:927-934.

37. AlEssa H, Bhupathiraju S, Malik V, Wedick N, Campos H, Rosner B, Willett W, Hu FB: Carbohydrate Quality, Measured Using Multiple Carbohydrate Quality Metrics, is Negatively Associated with Risk of Type 2 Diabetes in US Women. *Circulation* 2015, 131:A20-A20.

38. Bachman KH: Obesity, weight management, and health care costs: a primer. *Disease Management* 2007, 10:129-137.

39. Robinson JR, Niswender KD: What are the risks and the benefits of current and emerging weight-loss medications? *Current diabetes reports* 2009, 9:368-375.

40. Izydorczyk M: Understanding the Chemistry of Food Carbohydrates. In *Food carbohydrates : chemistry, physical properties, and applications*. Edited by Cui SW: CRC Press; 2005:418 p.

41. Kumar V, Sinha AK, Makkar HP, de Boeck G, Becker K: Dietary roles of non-starch polysachharides in human nutrition: A review. *Critical reviews in food science and nutrition* 2012, 52:899-935.

42. Mishra S, Hardacre A, Monro J: Food Structure and Carbohydrate Digestibility In *Carbohydrates—Comprehensive Studies on Glycobiology and Glycotechnology* Edited by Chang C-F: InTech; 2012:558 p.

43. Wilcox G: Insulin and insulin resistance. *Clinical biochemist reviews* 2005, 26:19.

44. Arbelaez AM, Xing D, Cryer PE, Kollman C, Beck RW, Sherr J, Ruedy KJ, Tamborlane WV, Mauras N, Tsalikian E: Blunted glucagon but not epinephrine responses to hypoglycemia occurs in youth with less than 1 yr duration of type 1 diabetes mellitus. *Pediatric diabetes* 2014, 15:127-134.

45. Bello-Perez LA, Paredes-Lopez O, Roger P, Colonna P: Molecular characterization of some amylopectins. *Cereal Chemistry* 1996, 73:12-17.

46. Buléon A, Colonna P, Planchot V, Ball S: Starch granules: structure and biosynthesis. *International journal of biological macromolecules* 1998, 23:85-112.

47. Tester RF, Karkalas J, Qi X: Starch—composition, fine structure and architecture. *Journal of Cereal Science* 2004, 39:151-165.

48. Lopez-Rubio A, Flanagan BM, Gilbert EP, Gidley MJ: A novel approach for calculating starch crystallinity and its correlation with double helix content: A combined XRD and NMR study. *Biopolymers* 2008, 89:761-768.

49. Ratnayake WS, Jackson DS: Starch gelatinization. *Advances in food and nutrition research* 2008, 55:221-268.

50. Sajilata M, Singhal RS, Kulkarni PR: Resistant starch–a review. *Comprehensive reviews in food science and food safety* 2006, 5:1-17.

51. Eerlingen R, Crombez M, Delcour J: Enzyme-Resistant Starch. 1. Quantitative and Qualitative Influence of Incubation-Time and Temperature of Autoclaved Starch on Resistant Starch Formation. *Cereal Chemistry* 1993, 70:339-344.

52. Hirsch JB, Kokini JL: Understanding the mechanism of cross-linking agents (POCl3, STMP, and EPI) through swelling behavior and pasting properties of cross-linked waxy maize starches. *Cereal Chemistry* 2002, 79:102-107.

53. Abbas K, Khalil SK, Hussin ASM: Modified starches and their usages in selected food products: a review study. *Journal of Agricultural Science* 2010, 2:90.

54. Singh J, Kaur L, McCarthy O: Factors influencing the physico-chemical, morphological, thermal and rheological properties of some chemically modified starches for food applications—A review. *Food hydrocolloids* 2007, 21:1-22.

55. Koo SH, Lee KY, Lee HG: Effect of cross-linking on the physicochemical and physiological properties of corn starch. *Food Hydrocolloids* 2010, 24:619-625.

56. Chung H-J, Woo K-S, Lim S-T: Glass transition and enthalpy relaxation of cross-linked corn starches. *Carbohydrate Polymers* 2004, 55:9-15.

57. Carmona-Garcia R, Sanchez-Rivera MM, Méndez-Montealvo G, Garza-Montoya B, Bello-Pérez LA: Effect of the cross-linked reagent type on some morphological, physicochemical and functional characteristics of banana starch (Musa paradisiaca). *Carbohydrate Polymers* 2009, 76:117-122.

58. Ratnayake WS, Jackson DS: Phase transition of cross-linked and hydroxypropylated corn (Zea mays L.) starches. *LWT-Food science and technology* 2008, 41:346-358.

59. Meng Y, Rao M: Rheological and structural properties of cold-water-swelling and heated cross-linked waxy maize starch dispersions prepared in apple juice and water. *Carbohydrate polymers* 2005, 60:291-300.

60. Kaur L, Singh J, Singh N: Effect of cross-linking on some properties of potato (Solanum tuberosum L.) starches. *Journal of the Science of Food and Agriculture* 2006, 86:1945-1954.

61. Choi SG, Kerr WL: Swelling characteristics of native and chemically modified wheat starches as a function of heating temperature and time. *Starch-Stärke* 2004, 56:181-189.

62. Liu H, Ramsden L, Corke H: Physical Properties of Cross-linked and Acetylated Normal and Waxy Rice Starch. *Starch-Stärke* 1999, 51:249-252.

63. Muhammad K, Hussin F, Man Y, Ghazali H, Kennedy J: Effect of pH on phosphorylation of sago starch. *Carbohydrate Polymers* 2000, 42:85-90.

64. Polnaya F, Marseno D, Cahyanto M: Effects of phosphorylation and cross-linking on the pasting properties and molecular structure of sago starch. *International Food Research Journal* 2013, 20.

65. Manach C, Scalbert A, Morand C, Remesy C, Jimenez L: Polyphenols: food sources and bioavailability. *American Journal of Clinical Nutrition* 2004, 79:727-747.

66. Scalbert A, Johnson IT, Saltmarsh M: Polyphenols: antioxidants and beyond. *American Journal of Clinical Nutrition* 2005, 81:215s-217s.

67. Scalbert A, Williamson G: Dietary intake and bioavailability of polyphenols. *Journal of Nutrition* 2000, 130:2073s-2085s.

68. Cheynier V, Prieur C, Guyot S, Rigaud J, Moutounet M: The Structures of Tannins in Grapes and Wines and Their Interactions with Proteins. In *Wine*. Edited by: American Chemical Society; 1997:81-93. ACS Symposium Series, vol 661.]

69. Haslam E: Natural polyphenols (vegetable tannins) as drugs: possible modes of action. *Journal of Natural Products* 1996, 59:205.

70. Hagerman AE, Robbins CT, Weerasuriya Y, Wilson TC, Mcarthur C: Tannin Chemistry in Relation to Digestion. *Journal of Range Management* 1992, 45:57-62.

71. Davis AB, Hoseney RC: Grain-Sorghum Condensed Tannins .1. Isolation, Estimation, and Selective Adsorption by Starch. *Cereal Chemistry* 1979, 56:310-314.

72. Awika JM, Rooney LW: Sorghum phytochemicals and their potential impact on human health. *Phytochemistry* 2004, 65:1199-1221.

73. Acuie-Beghin V, Sausse P, Meudec E, Cheynier V, Douillard R: Polyphenol-beta-Casein Complexes at the Air/Water Interface and in Solution: Effects of Polyphenol Structure. *Journal of Agricultural and Food Chemistry* 2008, 56:9600-9611.

74. Riihimaki LH, Vainio MJ, Heikura JMS, Valkonen KH, Virtanen VT, Vuorela PM: Binding of phenolic compounds and their derivatives to bovine and reindeer beta-lactoglobulin. *Journal of Agricultural and Food Chemistry* 2008, 56:7721-7729.

75. Le Bourvellec C, Renard CMGC: Interactions between Polyphenols and Macromolecules: Quantification Methods and Mechanisms. *Critical Reviews in Food Science and Nutrition* 2012, 52:213-248.

76. Bordenave N, Hamaker BR, Ferruzzi MG: Nature and consequences of non-covalent interactions between flavonoids and macronutrients in foods. *Food & Function* 2014, 5:18-34.

77. Jakobek L: Interactions of polyphenols with carbohydrates, lipids and proteins. *Food Chemistry* 2015, 175:556-567.

78. Fernandes A, Ivanova G, Brás NF, Mateus N, Ramos MJ, Rangel M, de Freitas V: Structural characterization of inclusion complexes between cyanidin-3-O-glucoside and β-cyclodextrin. *Carbohydrate polymers* 2014, 102:269-277.

79. Palafox-Carlos H, Ayala-Zavala JF, González-Aguilar GA: The role of dietary fiber in the bioaccessibility and bioavailability of fruit and vegetable antioxidants. *Journal of food science* 2011, 76.

80. González-Aguilar GA, Blancas-Benítez FJ, Sáyago-Ayerdi SG: Polyphenols associated with dietary fibers in plant foods: Molecular interactions and bioaccessibility. *Current Opinion in Food Science* 2017.

81. D'Archivio M, Filesi C, Varì R, Scazzocchio B, Masella R: Bioavailability of the polyphenols: status and controversies. *International journal of molecular sciences* 2010, 11:1321-1342.

82. Kiokias S, Varzakas T, Oreopoulou V: In vitro activity of vitamins, flavonoids, and natural phenolic antioxidants against the oxidative deterioration of oil-based systems. *Critical reviews in food science and nutrition* 2008, 48:78-93.

83. Malheiro R, Casal S, Lamas H, Bento A, Pereira JA: Can tea extracts protect extra virgin olive oil from oxidation during microwave heating? *Food research international* 2012, 48:148-154.

84. Das N, Pereira T: Effects of flavonoids on thermal autoxidation of palm oil: structure-activity relationships. *Journal of the American Oil Chemists' Society* 1990, 67:255-258.

85. Nakahara K, Izumi R, Kodama T, Kiso Y, Tanaka T: Inhibition of Postprandial Hyperglycemia by Oolong Tea Extract (Ote). *Phytotherapy Research* 1994, 8:433-435.

86. Amoako D, Awika JM: Polyphenol interaction with food carbohydrates and consequences on availability of dietary glucose. *Current Opinion in Food Science* 2016, 8:14-18.

87. Tadera K, Minami Y, Takamatsu K, Matsuoka T: Inhibition of alpha-glucosidase and alpha-amylase by flavonoids. *J Nutr Sci Vitaminol (Tokyo)* 2006, 52:149-153.

88. Watson RR, Preedy VR, Zibadi S: *Polyphenols in Human Health and Disease*: Elsevier Science; 2013.

89. McCue PP, Shetty K: Inhibitory effects of rosmarinic acid extracts on porcine pancreatic amylase in vitro. *Asia Pacific Journal of Clinical Nutrition* 2004, 13:101-106.

90. Guzar I, Ragaee S, Seetharaman K: Mechanism of Hydrolysis of Native and Cooked Starches from Different Botanical Sources in the Presence of Tea Extracts. *Journal of Food Science* 2012, 77:C1192-C1196.

91. Liu J, Wang MZ, Peng SL, Zhang GY: Effect of Green Tea Catechins on the Postprandial Glycemic Response to Starches Differing in Amylose Content. *Journal of Agricultural and Food Chemistry* 2011, 59:4582-4588.

92. Crowe TC, Seligman SA, Copeland L: Inhibition of enzymic digestion of amylose by free fatty acids in vitro contributes to resistant starch formation. *Journal of Nutrition* 2000, 130:2006-2008.

93. Cui R, Oates CG: +The effect of amylose–lipid complex formation on enzyme susceptibility of sago starch. *Food Chemistry* 1999, 65:417-425.

94. Tufvesson F, Skrabanja V, Bjorck I, Elmstahl HL, Eliasson AC: Digestibility of starch systems containing amylose-glycerol monopalmitin complexes.

Lebensmittel-Wissenschaft Und-Technologie-Food Science and Technology 2001, 34:131-139.

95. García DE, Glasser WG, Pizzi A, Paczkowski SP, Laborie M-P: Modification of condensed tannins: from polyphenol chemistry to materials engineering. *New Journal of Chemistry* 2016, 40:36-49.

96. Gu L, Kelm MA, Hammerstone JF, Beecher G, Holden J, Haytowitz D, Gebhardt S, Prior RL: Concentrations of proanthocyanidins in common foods and estimations of normal consumption. *The Journal of nutrition* 2004, 134:613-617.

97. Chung K-T, Wong TY, Wei C-I, Huang Y-W, Lin Y: Tannins and human health: a review. *Critical reviews in food science and nutrition* 1998, 38:421-464.

98. Hagerman AE, Butler LG: The specificity of proanthocyanidin-protein interactions. *Journal of Biological Chemistry* 1981, 256:4494-4497.

99. Asquith TN, Butler LG: Interactions of condensed tannins with selected proteins. *Phytochemistry* 1986, 25:1591-1593.

100. Frazier RA, Papadopoulou A, Mueller-Harvey I, Kissoon D, Green RJ: Probing protein− tannin interactions by isothermal titration microcalorimetry. *Journal of Agricultural and Food Chemistry* 2003, 51:5189-5195.

101. Chai YW, Wang MZ, Zhang GY: Interaction between Amylose and Tea Polyphenols Modulates the Postprandial Glycemic Response to High-Amylose Maize Starch. *Journal of Agricultural and Food Chemistry* 2013, 61:8608-8615.

102. Wu Y, Chen ZX, Li XX, Li M: Effect of tea polyphenols on the retrogradation of rice starch. *Food Research International* 2009, 42:221-225.

103. Renard CM, Baron A, Guyot S, Drilleau J-F: Interactions between apple cell walls and native apple polyphenols: quantification and some consequences. *International Journal of Biological Macromolecules* 2001, 29:115-125.

104. Ya C, Gaffney S, H., Lilley T, H., Haslam E: Carbohydrate-polyphenol complexation. In *Chemistry and Significance of Condensed Tannins*. Edited by Hemingway RW, Karchesy JJ: Plenum Press; 1989:307-322.

105. Ishizu T, Kintsu K, Yamamoto H: NMR study of the solution structures of the inclusion complexes of β-cyclodextrin with (+)-catechin and (−)-epicatechin. *The Journal of Physical Chemistry B* 1999, 103:8992-8997.

106. Nugala B, Namasi A, Emmadi P, Krishna PM: Role of green tea as an antioxidant in periodontal disease: The Asian paradox. *Journal of Indian Society of Periodontology* 2012, 16:313.

107. Hogan S, Zhang L, Li JR, Sun S, Canning C, Zhou KQ: Antioxidant rich grape pomace extract suppresses postprandial hyperglycemia in diabetic mice by specifically inhibiting alpha-glucosidase. *Nutrition & Metabolism* 2010, 7.

108. Coe SA, Clegg M, Armengol M, Ryan L: The polyphenol-rich baobab fruit (Adansonia digitata L.) reduces starch digestion and glycemic response in humans. *Nutrition Research* 2013, 33:888-896.

109. Barros F, Awika JM, Rooney LW: Interaction of tannins and other sorghum phenolic compounds with starch and effects on in vitro starch digestibility. *Journal of Agricultural and Food Chemistry* 2012:11609-11617.

110. Le Bourvellec C, Bouchet B, Renard CMGC: Non-covalent interaction between procyanidins and apple cell wall material. Part III: Study on model polysaccharides. *Biochimica et Biophysica Acta (BBA) - General Subjects* 2005, 1725:10-18.

111. Amoako DB, Awika JM: Polymeric tannins significantly alter properties and in vitro digestibility of partially gelatinized intact starch granule. *Food chemistry* 2016, 208:10-17.

112. Kaluza WZ, Mcgrath RM, Roberts TC, Schroder HH: Separation of Phenolics of Sorghum-Bicolor (L) Moench Grain. *Journal of Agricultural and Food Chemistry* 1980, 28:1191-1196.

113. Awika JM, Yang LY, Browning JD, Faraj A: Comparative antioxidant, antiproliferative and phase II enzyme inducing potential of sorghum (Sorghum bicolor) varieties. *Lwt-Food Science and Technology* 2009, 42:1041-1046.

114. Langer S, Marshall LJ, Day AJ, Morgan MR: Flavanols and methylxanthines in commercially available dark chocolate: a study of the correlation with nonfat cocoa solids. *Journal of Agricultural and Food Chemistry* 2011, 59:8435-8441.

115. Ojwang LO, Yang LY, Dykes L, Awika J: Proanthocyanidin profile of cowpea (Vigna unguiculata) reveals catechin-O-glucoside as the dominant compound. *Food Chemistry* 2013, 139:35-43.

116. Baks T, Ngene IS, Van Soest JJ, Janssen AE, Boom RM: Comparison of methods to determine the degree of gelatinisation for both high and low starch concentrations. *Carbohydrate polymers* 2007, 67:481-490.

117. Mutungi C, Passauer L, Onyango C, Jaros D, Rohm H: Debranched cassava starch crystallinity determination by Raman spectroscopy: Correlation of features in Raman spectra with X-ray diffraction and C-13 CP/MAS NMR spectroscopy. *Carbohydrate Polymers* 2012, 87:598-606.

118. Englyst KN, Hudson GJ, Englyst HN: Starch analysis in food. In *Encyclopedia of Analytical Chemistry*. Edited by Meyers RA. Chichester, UK: John Wiley & Sons Ltd.; 2000:4246–4262.

119. Yang L, Allred KF, Geera B, Allred CD, Awika JM: Sorghum phenolics demonstrate estrogenic action and induce apoptosis in nonmalignant colonocytes. *Nutrition and cancer* 2012, 64:419-427.

120. Barichello V, Yada RY, Coffin RH, Stanley DW: Low-Temperature Sweetening in Susceptible and Resistant Potatoes - Starch Structure and Composition. *Journal of Food Science* 1990, 55:1054-1059.

121. Wongsagonsup R, Varavinit S, BeMiller JN: Increasing Slowly Digestible Starch Content of Normal and Waxy Maize Starches and Properties of Starch Products. *Cereal Chemistry* 2008, 85:738-745.

122. Beta T, Corke H, Rooney LW, Taylor JRN: Starch properties as affected by sorghum grain chemistry. *Journal of the Science of Food and Agriculture* 2001, 81:245-251.

123. Cohen R, Orlova Y, Kovalev M, Ungar Y, Shimoni E: Structural and Functional Properties of Amylose Complexes with Genistein. *Journal of Agricultural and Food Chemistry* 2008, 56:4212-4218.

124. Hoover R, Vasanthan T: Effect of Heat-Moisture Treatment on the Structure and Physicochemical Properties of Cereal, Legume, and Tuber Starches. *Carbohydrate Research* 1994, 252:33-53.

125. Juszczak L, Fortuna T, Krok F: Non-contact atomic force microscopy of starch granules surface. Part II. Selected cereal starches. *Starch-Starke* 2003, 55:8-16.

126. Awika JM, Dykes L, Gu LW, Rooney LW, Prior RL: Processing of sorghum (Sorghum bicolor) and sorghum products alters procyanidin oligomer and polymer distribution and content. *Journal of Agricultural and Food Chemistry* 2003, 51:5516-5521.

127. Annor GA, Marcone M, Bertoft E, Seetharaman K: Physical and molecular characterization of millet starches. *Cereal Chemistry* 2014, 91:286-292.

128. DuBois M, Gilles KA, Hamilton JK, Rebers Pt, Smith F: Colorimetric method for determination of sugars and related substances. *Analytical chemistry* 1956, 28:350-356.

129. Goldstein A, Annor G, Vamadevan V, Tetlow I, Kirkensgaard JJ, Mortensen K, Blennow A, Hebelstrup KH, Bertoft E: Influence of diurnal photosynthetic activity on the morphology, structure, and thermal properties of normal and waxy barley starch. *International Journal of Biological Macromolecules* 2017, 98:188-200.

130. Wikman J, Blennow A, Bertoft E: Effect of amylose deposition on potato tuber starch granule architecture and dynamics as studied by lintnerization. *Biopolymers* 2013, 99:73-83.

131. Koch K, Andersson R, Åman P: Quantitative analysis of amylopectin unit chains by means of high-performance anion-exchange chromatography with pulsed amperometric detection. *Journal of Chromatography A* 1998, 800:199-206.

132. Jodelet A, Rigby NM, Colquhoun IJ: Separation and NMR structural characterisation of singly branched α-dextrins which differ in the location of the branch point. *Carbohydrate research* 1998, 312:139-151.

133. Le Bourvellec C, Guyot S, Renard C: Non-covalent interaction between procyanidins and apple cell wall material: Part I. Effect of some environmental parameters. *Biochimica et Biophysica Acta (BBA)-General Subjects* 2004, 1672:192-202.

134. Oh HI, Hoff JE, Armstrong GS, Haff LA: Hydrophobic interaction in tannin-protein complexes. *Journal of Agricultural and Food Chemistry* 1980, 28:394-398.

135. Vinogradov SN, Linnell RH: *Hydrogen bonding*: Van Nostrand Reinhold New York; 1971.

136. Chaplin MF: Water's hydrogen bond strength. *Water and Life: The unique properties of H2O* 2010:69-86.

137. McQueen-Mason S, Cosgrove DJ: Disruption of hydrogen bonding between plant cell wall polymers by proteins that induce wall extension. *Proceedings of the National Academy of Sciences* 1994, 91:6574-6578.

138. Renard CM, Watrelot AA, Le Bourvellec C: Interactions between polyphenols and polysaccharides: Mechanisms and consequences in food processing and digestion. *Trends in Food Science & Technology* 2016.

139. Cai C, Lin L, Man J, Zhao L, Wang Z, Wei C: Different structural properties of high-amylose maize starch fractions varying in granule size. *Journal of agricultural and food chemistry* 2014, 62:11711-11721.

140. Wang J-l, Cheng F, Zhu P-x: Structure and properties of urea-plasticized starch films with different urea contents. *Carbohydrate polymers* 2014, 101:1109-1115.

141. Zhou XY, Cui YF, Jia DM, Xie D: Effect of a complex plasticizer on the structure and properties of the thermoplastic PVA/starch blends. *Polymer-Plastics Technology and Engineering* 2009, 48:489-495.

142. Schellman JA: Temperature, stability, and the hydrophobic interaction. *Biophysical Journal* 1997, 73:2960-2964.

143. van Dijk E, Hoogeveen A, Abeln S: The hydrophobic temperature dependence of amino acids directly calculated from protein structures. *PLoS computational biology* 2015, 11:e1004277.

144. Morrison W, Law R, Snape C: Evidence for inclusion complexes of lipids with V-amylose in maize, rice and oat starches. *Journal of Cereal Science* 1993, 18:107-109.

145. Ma UVL, Floros JD, Ziegler GR: Formation of inclusion complexes of starch with fatty acid esters of bioactive compounds. *Carbohydrate polymers* 2011, 83:1869-1878.

146. Kong L, Lee C, Kim SH, Ziegler GR: Characterization of starch polymorphic structures using vibrational sum frequency generation spectroscopy. *The Journal of Physical Chemistry B* 2014, 118:1775-1783.

147. Gelders G, Vanderstukken T, Goesaert H, Delcour J: Amylose–lipid complexation: a new fractionation method. *Carbohydrate Polymers* 2004, 56:447-458.

148. Fanta GF, Felker FC, Shogren RL, Salch JH: Preparation of spherulites from jet cooked mixtures of high amylose starch and fatty acids. Effect of preparative conditions on spherulite morphology and yield. *Carbohydrate polymers* 2008, 71:253-262.

149. Obiro WC, Ray SS, Emmambux MN: V-amylose Structural Characteristics, Methods of Preparation, Significance, and Potential Applications. *Food Reviews International* 2012, 28:412-438.

150. Karkalas J, Ma S, Morrison WR, Pethrick RA: Some factors determining the thermal properties of amylose inclusion complexes with fatty acids. *Carbohydrate Research* 1995, 268:233-247.

151. Biliaderis C, Page C, Slade L, Sirett R: Thermal behavior of amylose-lipid complexes. *Carbohydrate Polymers* 1985, 5:367-389.

152. Sievert D, Wuesch P: Amylose chain association based on differential scanning calorimetry. *Journal of food science* 1993, 58:1332-1335.

153. Immel S, Lichtenthaler FW: The hydrophobic topographies of amylose and its blue iodine. *Flexible and Rigid Non-glucose Cyclooligosaccharides: Synthesis, Structure, and Properties* 2000, 52:27.

154. Gidley MJ, Bociek SM: Carbon-13 CP/MAS NMR studies of amylose inclusion complexes, cyclodextrins, and the amorphous phase of starch granules: relationships between glycosidic linkage conformation and solid-state carbon-13 chemical shifts. *Journal of the American Chemical Society* 1988, 110:3820-3829.

155. Biliaderis CG: Chapter 8 - Structural Transitions and Related Physical Properties of Starch. In *Starch (Third Edition)*. Edited by: Academic Press; 2009:293-372.

156. Panyoo AE, Emmambux MN: Amylose–lipid complex production and potential health benefits: A mini-review. *Starch-Stärke* 2017, 69.

157. Mizan TI, Savage PE, Ziff RM: Temperature dependence of hydrogen bonding in supercritical water. *The Journal of Physical Chemistry* 1996, 100:403-408.

158. Felton GE, Schopmeyer HH: Thick-bodied starch and method of making. Edited by: US Patent 2,328,537; 1943.

159. Shah N, Mewada RK, Mehta T: Crosslinking of starch and its effect on viscosity behaviour. *Reviews in Chemical Engineering* 2016, 32:265-270.

160. Karim A, Nadiha M, Chen F, Phuah Y, Chui Y, Fazilah A: Pasting and retrogradation properties of alkali-treated sago (Metroxylon sagu) starch. *Food Hydrocolloids* 2008, 22:1044-1053.

161. Rafiq SI, Singh S, Saxena D: Effect of alkali-treatment on physicochemical, pasting, thermal, morphological and structural properties of Horse Chestnut (Aesculus indica) starch. *Journal of Food Measurement and Characterization* 2016, 10:676-684.